**Distribution Agreement**

In presenting this dissertation as a partial fulfillment of the requirements for an advanced degree from Emory University, I hereby grant to Emory University and its agents the non-exclusive license to archive, make accessible, and display my dissertation in whole or in part in all forms of media, now or hereafter known, including display on the world wide web. I understand that I may select some access restrictions as part of the online submission of this dissertation. I retain all ownership rights to the copyright of the dissertation. I also retain the right to use in future works (such as articles or books) all or part of this dissertation.

_____ _____

Tengguo Li Date

**Epigenetic Regulation and Sex Determination in the Germ Line of *Caenorhabditis elegans***

By

Tengguo Li
Doctor of Philosophy

Graduate Division of Biological and Biomedical Sciences
Genetics and Molecular Biology

_____
William G. Kelly, Ph.D.
Advisor

_____
Xiaodong Cheng, Ph.D.
Committee Member

_____
Victor G. Corces, Ph.D.
Committee Member

_____
John C. Lucchesi, Ph.D.
Committee Member

_____
Paula M. Vertino Ph.D.
Committee Member

Accepted:

_____
Lisa A. Tedesco, Ph.D.
Dean of the James T. Laney School of Graduate Studies

_____
Date

**Epigenetic Regulation and Sex Determination in the Germ Line of *Caenorhabditis elegans***

By

Tengguo Li
M.S., Shandong University, 1999
B.S., Ludong University, 1993

Advisor: William G. Kelly, Ph.D.

An abstract of
A dissertation submitted to the Faculty of the
James T. Laney School of Graduate Studies of Emory University
in partial fulfillment of the requirements for the degree of

Doctor of Philosophy

Graduate Division of Biological and Biomedical Sciences
Genetics and Molecular Biology

2011

## Abstract

Epigenetic Regulation and Sex Determination in the Germ Line of *Caenorhabditis elegans*

By Tengguo Li

Germ cells are the only cell type that contributes their genetic and epigenetic components to the next generation. They are developmentally totipotent and are protected from undergoing somatic differentiation throughout the germ line cycle. Germ cells at different developmental stages are marked with different epigenetic signatures that are correlated with their properties. The methylation of histone H3 on Lysine 4 (H3K4me) has been identified as both a mark of active transcription and a potential component of "epigenetic memory". We have demonstrated that the global maintenance of H3K4 methylation in *C. elegans* germ cells requires the homologues of components of a conserved H3K4 methyltransferase complex, the Set1/MLL complex. Interestingly, Set1/MLL component-dependent methyltransferase activity can methylate H3K4 independently of ongoing transcription in early embryonic germ line and somatic blastomeres, and also in adult germ line stem cells. A separate H3K4 methylation mechanism that operates independently of Set1/MLL component activities appears to correlate more directly with transcription. We propose that H3K4 methylation is maintained throughout the germ cell cycle by alternating transcription dependent and independent mechanisms.

WDR-5.1, one of the conserved Set1/MLL components, plays an essential role in the regulation of methyltransferase activity. Mutation of *wdr-5.1* affects both germ line stem cell population size and normal germ cell development. Notably, double mutation of *wdr-5.1* and its paralog *wdr-5.2* exhibits severe germ line sex determination defects. TRA-1, a transcriptional repressor required for oogenesis, does not localize to chromatin in the absence of both *wdr-5.1* and *wdr-5.2*. This disruption of the interaction between TRA-1 and chromatin results in the ectopic expression of *fog-3*, which subsequently causes the masculinization of the germ line (Mog). We also identified *set-9* and *set-26* as sex determination regulators that may function redundantly with WDR-5.1 and WDR-5.2. Together, these data suggest that the components of Set1/MLL complex play a critical role in mediating epigenetic and genetic networks that are essential for proper germ line stem cell maintenance and germ cell development.

**Epigenetic Regulation and Sex Determination in the Germ Line of *Caenorhabditis elegans***

By

Tengguo Li
M.S., Shandong University, 1999
B.S., Ludong University, 1993

Advisor: William G. Kelly, Ph.D.

A dissertation submitted to the Faculty of the
James T. Laney School of Graduate Studies of Emory University
in partial fulfillment of the requirements for the degree of

Doctor of Philosophy

Graduate Division of Biological and Biomedical Sciences
Genetics and Molecular Biology

2011

ACKNOWLEDGEMENTS

I would like to acknowledge my mentor and advisor Dr. William G. Kelly, who was a wonderful scientific mentor, for all of his consistent support, guidance and time. I would also like to acknowledge the members of my dissertation committee: Drs. Xiaodong Cheng, Victor Corces, John Lucchesi and Paula Vertino for their advice and support. Their time and guidance have been greatly appreciated.

I wish to acknowledge all the members of the Kelly Lab, past and present, for their helpful discussion, support, and encouragement. I enjoyed the time I spent with you. Very special thanks to the Chromatin Interest Group and the *C. elegans* community at Emory University for valuable suggestions and helpful discussions.

I want to thank my family and friends, who have given me their unconditional support and love. Finally, I am especially grateful to my wife, Liping Luo, without her faithful sacrifice, unending support, patience, encouragement, and love, this dissertation would not have been possible.

TABLE OF CONTENTS

LIST OF FIGURES

LIST OF TABLES

# Chapter 1

## Introduction

**Epigenetics: an overview**

In multi-cellular organisms the merging of the sperm and oocyte genomes yields the "totipotent" zygote; i.e., a cell capable of producing all tissue types. The zygote then undergoes proliferation and differentiation to develop into a complete organism composed of highly specialized and differentiated cells. Given that every cell has the same genome, the oldest question in developmental biology concerns how different types of cells use the same genomic content to acquire and maintain different identities, and how the cells then stably pass these novel properties to their daughter cells after cell division. Different cells have distinct profiles of gene expression, encoded by the same DNA that determines cell identity, morphology and function. The information guiding the selective gene expression and maintenance should be beyond DNA sequence, and yet be stable after cell division to ensure that the daughter cells inherit the cell-type specific gene expression pattern and retain the same cell identity. The mechanisms that underlie this inheritance of regulation that goes beyond inheritance of DNA sequence are classified as "epigenetic" mechanisms.

**DNA methylation and epigenetic regulation**

One feature of DNA that plays a role in epigenetic regulation is the methylation of cytosine. In mammals, methyl groups can be added to the C5 of cytosine of CpG dinucleotides, and this modification, 5-meC, correlates with gene repression (Bird, 1986). Non-coding, repetitive regions such as centromeric heterochromatin are highly enriched in 5-meC. Hypermethylation of so-called CpG islands located at promoter region correlates with gene silencing (Bird, 2002). DNA methylation occurs at cytosines of both

complementary CpG dinucleotides of the double strand DNA. The addition of a methyl group is catalyzed by a class of enzymes called DNA methyltransferases (Dnmts). So-called *de novo* Dnmts such as Dnmt3a and Dnmt3b can add methyl groups to CpGs in double strand DNA and can thus establish new DNA methylation patterns (Okano et al., 1999). After DNA replication, only the parental DNA strand initially has methylated cytosines, and the replicated DNA is in a hemi-methylated state. Maintenance Dnmts such as Dnmt1 recognize the hemi-methylated sites and add methyl groups to the symmetrical CpG on the other strand (Li et al., 1992). Therefore, DNA methylation is replicated faithfully and the methylation patterns can be inherited by daughter cells. Likewise, the inherited DNA methylation pattern can contribute to the gene expression profiles in daughter cells.

**Chromatin as an organizer and carrier for epigenetic information**

DNA methylation is one of many epigenetic mechanisms that have been described. Some organisms, such as *C. elegans,* do not have detectable DNA methylation yet exhibit the full range of epigenetic phenomena (Tweedie et al., 1997). In eukaryotes, DNA is packaged by proteins into a structure called chromatin. The basic building block of chromatin is the nucleosome, in which ~147 base pairs of DNA is wrapped around an octamer composed of four canonical histone proteins: H2A, H2B, H3 and H4. Each octamer consists of 4 histone heterodimers: two each of H2A-H2B and H3-H4 (Kornberg and Lorch, 1999). The two H3-H4 heterodimers pair to form a tetramer. Each H2A-H2B heterodimer binds to the H3-H4 tetramer to form a nucleosome (Luger et al., 1997; Smith and Stillman, 1991). With the help of other histones such as H1 and non-histone proteins,

the nucleosomes are further folded into more highly organized structures, which allow the relatively long chromosomal DNA strands to be packaged into the tiny nucleus. In this regard, the stable interaction between histones and DNA in the nucleosomes, and the highly ordered chromatin structure are barriers activities that require access to DNA such as DNA replication, repair and gene expression. Condensed chromatin structure must be therefore unraveled to allow accessibility at the right sites in a regulated manner. This also suggests that chromatin may function as, or contribute to an "indexing system" which ensures that the information contained in DNA can be located in a timely fashion from within its highly packaged architecture (Ruthenburg et al., 2007). From this point of view, the chromatin can thus also provide a platform through which DNA interacts with intracellular and intercellular signals. Therefore, chromatin architecture must comprise a state favoring both DNA packaging and regulated accessibility. Studies over the past decade have shown that chromatin is highly dynamic and plays a pivotal role in the regulation of DNA related activities, and in epigenetic inheritance that transmits information beyond DNA sequence but might be packaged in the chromatin between generations.

Cells have evolved a number of approaches to model and regulate their chromatin architectures. First, chromatin remodeling complexes exist that use energy from ATP hydrolysis to move, restructure or even eject nucleosomes to expose buried DNA sites (Saha et al., 2006). Eukaryotes contain at least five families of chromatin remodeling complexes: ISWI, SWI/SNF, NURD/Mi-2/CHD, INO80 and SWR (Saha et al., 2006). The components of these complexes are highly diverse but the core members are conserved (Clapier and Cairns, 2009). ISWI, which shares a conserved ATPase subunit

with SWI/SNF, plays a role in nucleosome assembly and thus might promote gene repression as this process might bury transcription factor recognizing sites on DNA. The ATPase subunit of SWI/SNF complex has a bromodomain close to the C-terminus. This domain can bind to acetylated histones. What is important is that this binding recruits the SWI/SNF complex to chromatin which disorders and reorganizes nucleosome positioning to promote the binding of transcription factors and activation (Martens and Winston, 2003; Saha et al., 2006).

Histone variant incorporation can also change the composition of nucleosomes and contribute to the establishment of distinct chromatin domains. Canonical histones are synthesized and deposited into chromatin during DNA replication, while some histone variants can be actively deposited into chromatin in a replication-independent manner (Malik and Henikoff, 2003). Changes in nucleosomal composition have important impact on chromatin structure and activities. For example, the H2A variant H2A.Z can be deposited to the nucleosomes located in promoter regions by chromatin remodeling complex SWR1 (Mizuguchi et al., 2004). The enrichment of H2A.Z subsequently guides the creation of a nucleosome free promoter region that facilitates gene expression. CENP-A, the centromere specific H3 variant, plays a central role in regulating centromeric function and chromatin segregation (Regnier et al., 2005).

Histones can also be chemically altered by post-translational modifications that include acetylation, methylation, ubiquitination, sumoylation and phosphorylation (Kouzarides, 2007). These post-translational modifications occur at specific amino acid residues such as methyaltion at Lysine 4 and Lysine 9 of H3 and phosphrylation at Ser10 of H3 (Kouzarides, 2007). Analysis of calf histones using peptide mass finger-printing

mass spectrometry revealed 13 modification sites in H2A, 12 modification sites in H2B, 21 modification sites in H3 and 14 modification sites in H4 (Zhang et al., 2003b). The most commonly modified residue is Lysine which can be acetylated, methylated or ubiquitinated. These modifications play an extensive role in the regulation of chromatin architecture (See below).

**Functions of histone modifications**

One effect of histone modifications is to change the interactions stabilizing the current chromatin structure. For example, the addition of the relative large ubiquitin moiety creates steric hindrance and hence might break existing interactions. Acetylation of lysine residues neutralizes their charge. By contrast, phosphorylation of serine residues creates a negatively charged local environment which could affect interactions within and between nucleosomes (Kouzarides, 2007). Modifications that influence the local interactions between nucleosomes can affect the higher order structure of chromatin and different transcriptional outcomes might result. Generally, acetylation is associated with transcription activation. Other marks linked to active transcription include: methylation at Lysine 4 of H3 (H3K4), Lysine 36 of H3 (H3K36) and Lysine 79 of H3 (H3K79) (Martin and Zhang, 2007). In contrast, high levels of methylation at K9 and K27 of H3 (H3K9 and H3K27, respectively), as well as methylation at lysine 20 of H4 (H4K20), are correlated with gene silencing (Cao and Zhang, 2004; Peters et al., 2003; Schotta et al., 2004). Despite these correlations, the outcomes of a certain modification might be distinct in different chromatin contexts. In fact, any given modification has the potential to facilitate either gene activation or repression. A good example is that H3K36

methylation is associated with gene activation when existing in the coding region but promotes gene repression when enriched in the promoter region (Vakoc et al., 2005). Similarly, H3K4me3, generally associated with transcription competency, was shown to associate with gene repression under acute stress (Shi et al., 2006) (see below). Furthermore, H3K4me3 is also found to be present in "bivalent domains" in Embryonic Stem (ES) cells. Genes located in these domains are mostly related to developmental programs and are expressed at very low level. H3K4me3 is preserved if the genes are activated in later developmental stages. Conversely, it will be removed if the gene is silenced (Bernstein et al., 2006; Mikkelsen et al., 2007), suggesting that H3K4me3 might participate to establish an activation-permissive state, but does not necessarily result in transcription. Therefore, it appears that the context plays a decisive role in determining the transcriptional outcomes of histone modifications.

What may also be important is the combination of histone modifications that exist on one or more histone tails, a hypothesis referred to as the "histone code" (Jenuwein and Allis, 2001; Strahl and Allis, 2000; Turner, 2000). It's hypothesized that combinations of different histone modifications can be read as a "code" by different effector proteins that result in different downstream events. Various combinations of histone modifications may contribute to create specific epigenetic signatures, which may involve the establishment of chromatin- or cell- specific contexts. For example, repetitive heterochromatic regions are highly-methylated at H3K9 and H3K27 while having low levels of acetylation and H3K4 methylation (Kouzarides, 2007). This combination of histone modification is correlated with the repressive nature of heterochromatin. Recently, a comprehensive ChIP-seq study mapped 39 different modifications in human T cells

(Wang et al., 2008). Gene ontology analysis identified a backbone of 17 modifications from 3286 promoters that seemed to be correlated with each other and associated with higher gene expression. This finding suggested that these modifications might function cooperatively to create chromatin states that facilitate transcription activation.

Interestingly, a recent study reveals a role of H3K4me3 and H3K27me3 in defining a special chromatin state called "bivalent domain" in mouse ES cells (Bernstein et al., 2006; Mikkelsen et al., 2007). These domains, which correlate with HCNE-rich (highly conserved non-coding elements) regions, contain large regions of H3K27me3 surrounding smaller regions of H3K4me3. Genes in these regions are mostly associated with embryo development programs and are expressed at low- to undetectable levels in ES cells. When differentiation commences, the pattern is changed and replaced by large regions harboring either H3K4me3 or H3K27me3 associated with active or repressive transcription, respectively. Therefore, the genes in these domains are considered to be held in a "bipotential state" with both H3K27me and H3K4me simultaneously prevent the genes from engaging in differentiation while keep them ready for activation (Bernstein et al., 2006; Mikkelsen et al., 2007).

Under some circumstance, the alternation of histone modifications can exert their effects on the whole chromatin which might affect the transcription status genome wide. In the nematode *C. elegans,* primordial germ cell specification is accompanied by what appears to be genome-wide transcriptional repression. This massive inactivation is mediated by a chromatin-based mechanism marked by global loss of active marks, including H3K4 methylation and H4K8 acetylation. In agreement with this, the DNA in the primordial germ cells appears to be more condensed (Schaner et al., 2003). These

changes in histone modification might not be sufficient for the massive repression, but may contribute to the establishment and the maintenance of this unique state of chromatin.

Modifications at histone residues can create docking sites for effector proteins. This allows histone modifications to recruit enzyme activities to chromatin that can yield biological consequences. Several protein modules that specifically recognize histone modifications have been identified. For example, acetylated lysine residues are recognized by the so-called bromodomain. Heterochromatin protein 1 (HP1) recognizes the tri-methyl group of lysine 9 of histone H3 through its chromodomain. The association of HP1 with H3K9me3 in chromatin is critical for the formation of heterochromatin (Vakoc et al., 2005). Similarly, the chromodomain of Polycomb (Pc), a component of the polycomb repressive complex, has been demonstrated to bind to H3K27me3. This binding stabilizes the complex and thus enhances repression (Ringrose and Paro, 2004). On the other hand, the active chromatin mark H3K4me3 can be recognized by certain PHD fingers. BPTF, the large subunit of nucleosome remodeling factor (NURF), binds to H3K4me3 through its PHD domain. This association tethers the ISWI ATPase to the promoter of HOX8C to activate its expression (Wysocka, 2006). Similarly, the PHD finger of ING-2 (inhibitor of growth-2) tumor-suppressor protein can bind to H3K4me3 with high affinity and specificity (Shi et al., 2006). However, the outcome is opposite to that of BPTF binding, since this interaction recruits ING-2 to highly active, proliferation-related gene promoters in response to DNA damage and stabilizes the repressive mSin3A-HDAC complex at these promoters. As a result, these genes are repressed. This unusual repression mediated by H3K4me3 is important for the rapid shut-off of

proliferation promoting genes in case of acute stress, such as DNA damage, to prevent the propagation of defective genes through cell proliferation (Shi et al., 2006).

Histone modifications also play a role in cellular memory and transgenerational epigenetic inheritance. Although the details are not clear yet, a number of recent studies have provided insights into this aspect of epigenetic regulation. Several studies suggest that histone modifications can be transmitted to daughter cells, and more importantly, that the information they bear can potentially guide the gene expression pattern in daughter cells. For example, analysis of histone modifications across the promoter and coding region of active and inducible genes revealed that the histone modifications could survive through mitosis (Valls et al., 2005). In addition, nuclear transfer experiments performed in *Xenopus laevis* suggests a role of H3K4 methylation in transcriptional memory (Ng and Gurdon, 2008). Recently, the presence of nucleosomes and histone modifications were described in mammalian sperm (Brykczynska et al., 2010; Hammoud et al., 2009) suggesting that they might play a role in transgenerational epigenetic inheritance. H3K4me2 was found to localize to promoters of certain developmental genes. Large blocks of H3K4me3 were also found in the Hox cluster regions, promoters of a subset of developmental genes and paternally expressed imprinted loci, whereas the repressive H3K27me3 is enriched in promoters of developmental genes that are repressed in early embryos. Importantly, the association of histone modification with developmental genes in sperm appears to be instructive for the regulation of developmental gene expression in embryos. Consistent with this, many bivalent regions in ES cells are also bivalent in sperm. In another study, H3K27me3 was found to be enriched in TSSs region in sperm. Correlated with the occupation of H3K27me3, genes in this region were repressed in

gametes and early embryos (Hammoud et al., 2009). These data suggest that the establishment of H3K4 and H3K27 methylation patterns in early embryos might be seeded by histones containing H3K4 and H3K27 methylation inherited from sperm.

Similarly, in *C. elegans*, a unique epigenetic status is established on the paternal X chromosome during spermatogenesis consisting of a striking depletion of H3K4me2 (Bean et al., 2004). This status is transmitted to the zygote through sperm chromatin and is then faithfully replicated in early embryos (Bean et al., 2004). On the other hand, epigenetic marks that are incompatible with the developmental potential of embryonic cells must be reset. This reprogramming process is essential for embryo development. Mutation in the *C. elegans* ortholog of the H3K4 demethylase LSD1 results in the transgenerational accumulation of H3K4me2 in sperm-expressed gene promoters and in the chromatin of primordial germ cells. This accumulation results in progressive sterility over generations (a "germ line mortal" phenotype) and increased expression of spermatogenetic genes, arguing that removal of H3K4me2 in PGCs, possibly inherited from parental germ cells, is required for germ cell immortality (Katz et al., 2009).

**Regulation and implications of H3K4 methylation**

The lysine residue of histones can be mono-, di- or tri- methylated. Methylation at Lysine 4 of Histone H3 (H3K4me), one of the mostly well-studied, plays an important role in transcription control and transgenerational epigenetic inheritance. In most cases, both H3K4me2 and me3 are correlated with transcription competence. However, their distribution on chromatin does not overlap. In budding yeast, the di-methyl modification

generally distributed within the body of active genes and the tri-methyl modification concentrated more specifically at the 5' end of active genes (Workman, 2006).

The methyl groups are added to the lysine residues of histones by enzymes called histone methyltransferases (HMTs). All the known lysine HMTs contain a SET domain (Su(var)3-9, Enhancer of Zeste [E(Z)], and trithorax) except Dot1, the H3K79 HMT (Cheng, 2005; Jones and Gelbart, 1993; Tschiersch et al., 1994). The highly conserved SET domain is composed of ~130 amino acids and harbors the catalytic activity. The budding yeast Set1 was the first identified H3K4 specific HMT. This protein is comprised of 1080 amino acids with a SET domain and a post-SET at the C-terminal. *In vivo*, Set-1 operates in a complex called COMPASS (Complex Proteins Associated with Set1). The complex is composed of conserved components including Swd1, Swd2, Swd3, Bre2, Spp1 and Sdc1 (Table 1-1). All these proteins are important for the methyltransferase activity of Set1 (Krogan et al., 2002; Roguev et al., 2001; Wood et al., 2003). Interestingly, purified Set1 protein itself is not enzymatically active, while in the context of the COMPASS, Set1 is able to mono-, di- and tri-methylate H3K4. Swd1 and Swd3 are essential for complex assembly and proper H3K4 methylation, while Bre2 and Spp1 are important for transitions to di- and tri-methylation (Shilatifard, 2008). Set1 does not contain motifs that recognize DNA sequences. Instead, the Set1/COMPASS complex is recruited to chromatin through the interaction with the elongation factor Paf1 (Polymerase II Associated Factor 1) and RNA polymerase II (Pol II). The Set1 HMT activity appears to be stimulated by H2B ubiquitination and Paf1 (Dehe and Geli, 2006; Sun and Allis, 2002). Therefore, the H3K4 methylation is thought to be strictly coupled to transcription and associated with actively transcribing genes in yeast.

A number of H3K4 HMTs have been identified in mammals. The SET domain of these proteins are either related to the yeast Set1, as in the case of Set1A, Set1B, MLL1, MLL2, MLL3 and MLL4, or unrelated, as in the case of Ash1, SET7/9, and Meisetz (Ruthenburg et al., 2007). All of the Set1 related HMTs are found to operate in COMPASS-like complexes and have been shown to have H3K4-specific HMT activities (Dou et al., 2005; Hughes et al., 2004; Milne et al., 2005). Inactivating either MLL1 or MLL2 in mouse results in embryonic lethality, suggesting that the biological functions of these HMTs are not redundant. Chromosomal translocations involving MLL1 occur in about 80% of infants with AML or acute lymphoblastic leukemia (Rowley, 1998). MLL1 is essential for axial segment identity in mouse (Yu et al., 1995). Although null mutation of MLL1 causes embryonic lethality, MLL1 knockout mice lacking the SET domain are viable and fertile, indicating that MLL1 has functions independent of H3K4 methylation. Nevertheless, the SET domain deletion mice showed skeleton defects resembling mutations in certain Hox genes. Furthermore, Chromatin Immunoprecipitation (ChIP) analysis revealed that both MLL1 and H3K4me3 were extended upstream and downstream of some Hox gene promoters (Guenther et al., 2005). These data support the idea that MLL1 stimulates Hox gene expression through the control of H3K4 methylation. Similarly, MLL3 and MLL4 are associated with the retinoic acid receptor, and mutation of MLL3 or MLL4 leads to reduced expression of retinoic acid receptor target genes (Lee et al., 2006).

MLL5 is not closely related to MLL1-4 genes. It contains a SET domain near the N-terminus and lacks some domains residing in MLLs such as an AT-hook and FYRN-FRYC motif. MLL5 seems not to be associated with Set1/COMPASS complex

components such as WDR5, Ash2L and RbBP5 (Wu et al., 2008), Nevertheless, MLL5 is associated with retinoic acid receptor α and appears to have HMT activities specific to H3K4 (Fujiki et al., 2009). Over-expression of MLL5 promotes RARα-dependent reporter gene expression. In another study, MLL5 was found to mediate repression by interacting with HDAC and NCoR, components of Set3 repression complex. In myoblasts, knockdown of MLL5 results in upregulation of MLL5 target genes (Kittler et al., 2007).

All of the six Set1 related HMTs in human (Set1A, Set1B and MLL1-4) operate in COMPASS-like complexes, with Set1A/B forming human COMPASS complexes and MLL1-4 forming human COMPASS-like complexes (Table 1-1). The components in the MLL/COMPASS like complex are diverse. Nevertheless, a core complex composed of four proteins, WDR5, RbBP5, Ash2L and DPY30, are shared by all known COMPASS like complexes (Dou et al., 2006; Mohan et al., 2010). The core components are essential for the associated HMT activities *in vitro*. Other subunits might provide an additional layer of regulation of the complex activities. *In vivo* studies have also revealed an important role for the core complex in regulating the methyltransferase activity of MLL. Knockdown of WDR5, RbBP5 or Ash2L by siRNA reduces the H3K4me3 levels at MLL target genes such as *HOXA9* and *HOXC8*, which is correlated with the down-regulation of these genes (Dou et al., 2006; Shilatifard, 2006). The MLL2/COMPASS complex, which contains additional components, Menin and HCF-1, is found to be recruited to chromatin through interaction with the elongating form of RNA Pol II; The H3K4 methylation mediated by this complex might be coupled to transcription (Hughes et al., 2004; Yokoyama et al., 2004).

Like the budding yeast Set1, isolated MLL proteins themselves have very low intrinsic HMT activities, and the enzymatic activities are highly stimulated when operating in the complex (Shilatifard, 2006). WDR5, one component of the core complex, seems to play a central role in regulating MLL activity and complex assembly, as the absence of WDR5 completely abolishes methyltransferase activity, whereas the absence of Ash2L or RbBP5 only reduces H3K4me3 (Dou et al., 2006; Shilatifard, 2006). WDR5 contains seven WD40 repeats that are organized in a structure called a beta-propeller. Protein structure studies revealed that the WD40 repeats primarily recognize H3 through interaction with the first three amino acid residues: A1, R2 and T3 (Couture et al., 2006; Han et al., 2006; Ruthenburg et al., 2006; Schuetz et al., 2006). Recently, a Win (WDR5 interaction) motif was identified in MLL1. Further studies found that the Win motif was highly conserved among metazoan Set1 and MLL family members. Crystal structure analysis revealed that the Win motif recognizes the site of WDR5 that was previous shown to interact with the H3 N-terminus (Patel et al., 2008a; Patel et al., 2008b; Song and Kingston, 2008). These findings provide a new paradigm for the interaction between WDR5 and MLLs, since it is against the previous model that WDR5 binds to the N-terminus of H3 and presents K4 to MLL. Instead, the interaction between Win motif of MLL1 and WDR5 seems to be more important for the assembly and HMT activity of the MLL1 complex.

Notably, it has been reported that the WDR5-RbBP5-Ash2 tripartite complex is associated with the nuclear receptor co-regulator-interacting factor 1(NIF-1) to promote expression of downstream targeting genes. Interestingly, no Set1 or MLL related

methyltransferase activities were identified in these complexes, suggesting that WDR5 has other functions in addition to H3K4 methylation (Garapaty et al., 2009).

Although the association of H3K4 methylation with transcription occurs in most cases, recent studies suggest that H3K4 methylation can occur in regions lacking transcriptional activity. Large-scale mapping of genomic locations of H3K4me3 in zebrafish embryos revealed that H3K4me3 is enriched on many transcriptionally inactive genes. This H3K4me3 is not directly inherited from the parental germ cells chromatin, but is established after the maternal–zygotic transition, arguing that H3K4me3 can occur without transcription (Vastenhouw et al., 2010). In mouse brain cells, unmethylated CpG islands in promoter regions are found to frequently associate with nucleosomes enriched in H3K4me3. Cfp-1, a CpG-binding protein and a member of set1/COMPASS complex, binds to unmethylated CpG sites and may possibly recruit HMT activities to the sites irrespective of the transcription status. Indeed, transgenes carrying artificial CpG clusters without promoter sequences, when integrated into the mouse genome, can accumulate H3K4me3 in a Cfp1 dependent manner (Thomson et al., 2010). These studies strongly argue that H3K4 methylation can occur in a transcription independent manner, and further can influence the genomic distribution of repressive DNA methylation.

**Implications for diseases**

As discussed above, epigenetic regulation provides an additional layer of gene regulation and contributes to the establishment and maintenance of heritable features beyond DNA sequence. These epigenetic processes can have enormous impact in the development of diseases. Studies regarding epigenetics have shed light on our understanding of disease

mechanisms and have excited new opportunities in diagnosis and treatment. A variety of diseases such as cancer, aging, immune disorders and neuropsychiatric disorders have been linked to misregulation of epigenetic components (Rodenhiser and Mann, 2006). Epigenetic signatures reflecting cellular identity are crucial for normal cellular function, and abnormal changes may cause disease states, including cancer. For example, the inappropriate inactivation of tumor suppressor genes, or inappropriate activation of a proto-oncogene, is a critical step in cancer development (Rodenhiser and Mann, 2006). Some histone methyltransferases such as MLL and trxG can become oncogenic and exert their effect through perturbing inappropriate gene expression or silencing. For example, MLL1 and MLL2 have roles in the long-term maintenance of Hox expression, probably through the maintenance of H3K4 methylation at these loci. Rearrangements of the MLL1 gene in humans are correlated to several human leukemias; the disregulation of Hox genes caused by MLL1 fusion proteins might play a role in this process (Hess, 2004). It has been found that the process of transformation from normal cells to cancer cells is accompanied by changes in global patterns of histone modification marks. In fact, the changes in global acetyl and methyl histone marks are demonstrated to be hallmarks of certain cancers (Seligson et al., 2005). Therefore, development of inhibitors targeting chromatin modifying enzymes might be a new approach for cancer therapeutics.

Environmental factors such as diet and lifestyle can also affect susceptibility to diseases. Although we do not understand the mechanisms, it is speculated that environmental factors may create “epigenetic footprints” on our genome (Dolinoy et al., 2007). These epigenetic signatures collectively form epigenomes that define the cellular contexts. Determining the epigenetic signatures associated with diseases such as diabetes

and heart diseases will help to understand the roles of epigenetic footprints in human diseases. Some studies have suggested that altered DNA methylation patterns in response to diet, alcohol consumption and hormone replacement are associated with a common polymorphism in methyleneterahydrofolate reductase (MTHFR) linked to high incidence of breast cancer (Rodenhiser and Mann, 2006).

## Overview of Germ Cells

In sexually reproducing organisms, there is a fundamental difference between germ cells and somatic cells. Germ cells give rise to gametes which contribute to the creation of next generation. The fusion of male and female gametes creates a totipotent zygote that has the capability to generate all cell types required to build a complete organism. Germ cells are the only cells that pass their genetic material to the next generation. Intriguingly, although germ cells are highly specialized and differentiated, their fusion forms a zygote with totipotency, suggesting that germ cells might be totipotent or in a "pre-totipotent" state that can be quickly transformed to a state of totipotency. Studies in many model organisms have suggested that the germ cells never undergo somatic differentiation and maintain the properties of totipotency throughout the germline cycle.

## *C. elegans* as a model system for germ cell biology

The nematode *Caenorhabditis elegans* is a tiny soil roundworm that has been used as a genetic model system since the 1970s. The adult is about 1mm in length and contains an invariant number of somatic cells. The life of *C. elegans* starts from a fertilized egg

which undergoes embryogenesis and eventually hatches to become a larva. There are four larval stages, L1-L4, before the final molt to adult stage. As a popular model system, it has a number of advantages. It is transparent at all stages, which allows investigators to track development at the cellular level under the microscope. *C. elegans* has a short life cycle and high reproductive capacity, so investigators are able to get enough animals and generations for various experiments in a relatively short period of time. The genome of *C. elegans* was the first metazoan to be sequenced, which makes it an even more appealing system to study. More importantly, since *C. elegans* has many features of development, physiology and behavior that are also found in other organisms such as mouse and human, studies of the worms can help elucidate the conserved development pathways and gene functions (Kaletta and Hengartner, 2006).

The development of the germline in *C. elegans* seems to be straightforward (Figure 1-1). The two primordial germ cells—Z2 and Z3—are specified during embryogenesis from germ cell precursors, the P-blastomere. P1-P3 undergoes asymmetrical division to produce another P-cell and a cell that undergoes somatic differentiation. Z2 and Z3 are generated by symmetrical division of P4 (Figure 1-1 A and B). Z2/Z3 and P cells are maintained in a (largely) transcriptionally inert state (Figure 1-1B). Z2/Z3 is arrested until hatching. After hatching, the two PGCs begin to proliferate to form a population of so-called germline stem cells (GSCs). The proliferating GSCs form a pool and are eventually settled in the distal region of gonad under the direction of distal tip cells (DTCs) (Figure 1-1A). The DTCs serves as a stem cell niche that maintains the proliferation and self-renewal of the GSCs through the GLP-1/Notch signaling pathway (Kimble and Crittenden, 2007). The cells that reside further from the DTCs receive less

GLP/Notch signals, exit mitosis, and enter into meiosis, whereas the cells that are close to the DTCs receive stronger signals and remain proliferative to provide a continuous supply of gametes. In the adult germline, the mitotic GSCs reside in the distal region of each gonad and the maturing germ cells reside in the more proximal region (Kimble and Crittenden, 2007). Between the mitotic and meiotic regions lies the so-called "transition zone", which contains cells that are leaving mitotic cycle or entering the leptotene and zygotene stages of meiotic prophase. Further proximally, germ cells proceed through pachytene, diplotene and diakinesis and eventually undergo gametogenesis (Figure 1-1A). There is a delicate balance between GSC self-renewal and meiotic entry which maintains the mitotic length at around 20 cell diameters in wild type hermaphrodites at 20°C (Lamont et al., 2004).

*C. elegans* has two sexes: XO worms develop as males and XX worms develop as hermaphrodites. Hermaphrodites have strictly female somatic structure, but produce both sperm and oocytes. The germ cells first generate sperm during the L3 larval stage followed by a switch to oogenesis in late L4. The primary signal controlling this sexual fate is the ratio of X chromosomes to autosomes (X:A). The X:A ratio determines the expression of the master regulator, *xol-1,* in males. *xol-1* expression leads through a series of negatively regulated genetic interactions to *tra-1*, a global sex determination transcriptional regulator (Figure 1-1C) (Ellis and Schedl, 2007). Active TRA-1 promotes oogenesis by repressing male-specific pathways in the germ line. Without *tra-1*, hermaphrodites do not switch to oogenesis and only produce sperm. The *tra-1* gene encodes several TRA-1 proteins. The largest protein contains five Zinc fingers and is called TRA-1A. Its zinc-finger is related to the members of invertebrate Gli family and

*Drosophila cubitus interuptus* (Ci) (Zarkower and Hodgkin, 1992, 1993). Moreover, the binding sites of TRA-1 resemble the ones recognized by Gli proteins. There are several known direct targets for TRA-1A, including *egl-1, mab-3* and *fog-3.* In all the three cases, TRA-1 serves as transcriptional repressor (Chen and Ellis, 2000; Conradt and Horvitz, 1998; Yi et al., 2000). TRA-1 levels are regulated by an ubiquitin ligase complex containing the three FEM proteins (Starostina et al., 2007). TRA-1 seems to control sex fate through regulating the expression of two terminal modulators: *fog-1* and *fog-3*. Active FOG-1 and FOG-3 promote sperm formation and inhibit oogenesis (Kimble and Crittenden, 2007). The molecular mechanism underlying this process is not yet known.

**Gene repression is a common feature during germ cell specification**

As mentioned above, germ cells maintain totipotency throughout the germline cycle. This unique property might be seeded during germ cell specification, which occurs in early embryogenesis in many organisms. Many years of studies suggest that the primordial germ cells (PGCs) and their precursors are specified from "pluripotent stem cells" during the early stage of embryogenesis (Seydoux and Braun, 2006). Once specified, they are well protected from undergoing somatic differentiation. In fact, the genes involved in somatic programs are inhibited throughout the germline cycle in several model organisms such as *C. elegans* and mouse. From this point of view, the totipotent state seems to be maintained in all stages of germ cell development.

Various strategies are taken to prevent these special cells from responding to signals that trigger programs for somatic differentiation. In some invertebrates such as *C. elegans* and *Drosophila*, transcription is generally repressed in PGCs and their precursors

(Blackwell, 2004). This is achieved through a combination of the regulation of transcription machinery and generating a repressive chromatin state. At the beginning of transcription, a pre-initiation complex forms at the promoter. Subsequent elongation requires the phosphorylation at serine 5 and serine 2 (P-Ser5 and P-Ser2) of the YSPTSPS repeat of the C-terminal domain (CTD) of the catalytic subunit of RNA polymerase II (RNA Pol II) (Blackwell, 2004). In early embryos of *C. elegans*, the elongating form of RNA Pol II, marked by P-Ser5 and P-Ser2, is present in all somatic cell nuclei. However, P-Ser5 is reduced and P-Ser2 is undetectable in the germline lineages before gastrulation. The lack of P-Ser-2 in worm PGCs suggests that transcription is blocked at a step between initiation and elongation (Blackwell, 2004). A protein called PIE-1(pharynx and Intestine in Excess), a CCCH Zinc finger protein, has been suggested to play a role in this repression. It is maternally loaded into embryo cells and is asymmetrically partitioned into the posterior cell (also called P-blastomeres) at each cell division. The anterior somatic cells that do not inherit PIE-1 quickly initiate zygotic gene expression, whereas the germ cell precursors that retain PIE-1 are maintained in a transcriptionally quiescent state. The loss of *pie-1* results in somatic gene expression in germ cell lineage (Seydoux and Dunn, 1997; Zhang et al., 2003a). These findings indicate that transcription is somehow initiated but is blocked at the stage of elongation in a PIE-1 dependent manner. The phosphorylation of RNA Pol II Ser-2 is catalyzed by *cdk-9*, a component of positive transcription elongation factor b (P-TEFb) complex. One model is that PIE-1 contains a domain that is similar as the RNA Pol II CTD domain, thus can compete with *cdk-9* to inhibit Pol II Ser-2 phosphorylation. As a result, transcription elongation is blocked (Zhang et al., 2003a).

There are no *pie-1* homologues in *Drosophila melanogaster*. Instead, genome-wide transcriptional repression seems to be mediated by *gcl (germ cell less)* and *pgc (polar granule component)* (Blackwell, 2004; Hanyu-Nakamura et al., 2008). The mechanism is similar as that in worms. *pgc* is required to repress P-Ser2 in pole cells, the germ cell precursors. Zygotic transcripts accumulate in PGCs in the absence of *gcl* or *pgc*. Ectopic expression of *pgc* or *gcl* in somatic cells inhibits P-Ser-2 accumulation. Notably, *pgc* interacts with P-TEFb, the Ser-2 kinase complex, and prevents it from being recruited to transcription sites (Hanyu-Nakamura et al., 2008). Although PIE-1 and *pgc* have no homology, their functions and roles in regulating Pol II repression in the embryonic germ are strikingly similar.

In mouse, somatic programs are also repressed in PGCs. Single cell gene expression profiling experiments show that Hox gene transcripts are down-regulated in PGCs while actively transcribed in the neighboring somatic cells. Down-regulation of Hox genes is dependent on a transcriptional repressor called Blimp-1. Mutants lacking Blimp-1 exhibited a reduced number of PGCs and elevated Hox gene repression (Ohinata et al., 2005). Blimp1 contains a SET-PR domain and interacts with Prmt5, an arginine specific histone methyltransferase. The co-localization of Blimp1 and Prmt5 in nuclei of PGCs is correlated with high levels of symmetrical di-methylation of arginine 3 on H2A and H4 tails (H2A/H4R3me2s). Blimp1-Prmt5 seems to function as a transcription repressor, since Dhx, one of their target genes, is upregulated in the absence of Blimp1 (Ancelin et al., 2006). These data suggest that repression of genes associated with somatic differentiation is an important aspect of germline specification in mouse.

**Two modes of germ cell specification**

Although repression of somatic programs seems to be one common feature during germ cell specification, different modes exist to accomplish the goal of germ cell specification. In invertebrates such as *C. elegans, Drosophila and Xenopus*, the germ cell lineage is associated with the presence of "germplasm", a specialized cytoplasm enriched in large, electron dense and RNA-rich organelles that are continuously associated with germ cells throughout the germ cell cycle (Seydoux and Braun, 2006). In *Drosophila*, the germplasm exists in the posterior region where the pole cells (germ cell precursors) reside. Ectopic transplant of germplasm to the anterior pole results in germ cell formation in the anterior. In *C. elegans*, the germplasm is enriched in structures called P-granules (Saffman and Lasko, 1999). They are initially localized at the posterior of early embryo and are sequentially inherited by germline blastomeres. Mutations of P-granule components such as PGL-1 impair germ cell development (Strome, 2005). Germplasm is synthesized in adult germ cells and maternally loaded into oocytes. These RNA-rich organelles are thought to store mRNAs necessary for germline development and regulate their translation. In agreement with this, mRNAs coding for essential germline factors such as *glh, the Drosophilia vasa homologue,* and *nos* have been identified in P-granules of *C. elegans* and many of the protein components of germplasm are implicated in various aspects of mRNA regulation (Strome, 2005).

A different mode of germ cell specification occurs in mouse. A group of cells in the proximal epiblast are induced to form PGCs by signals emanating from the extra-embryonic tissue around E6.25. Proximal epiblast cells lose the ability to produce PGCs if transplanted to the distal region, indicating a role for the surrounding ectoderm in PGC

induction. Several studies suggest that BMP4 (Bone Morphogenetic Protein 4) and BMP8b play critical roles in the induction. First, BMP4 and BMP8b are expressed in the extra-embryonic ectoderm. Inactivation of either gene leads to a failure to form PGCs (Ying and Zhao, 2001). Second, epiblast cells can form PGCs when cultured on COS-7 cells expressing both BMP4 and BMP8b, but not on COS-7 cells expressing either BMP4 or BMP8b (Ying et al., 2001). Once the PGC-like cell cluster is established, PGC specific genes such as Blimp1, Stella and Fragillis, are activated (Ohinata et al., 2005). In addition, pluripotent genes such as Oct4, Nanog and Sox2 are also activated to maintain the pluripotency of PGCs, and somatic programs such as Hox gene expression are repressed (Ohinata et al., 2005). Notably, epigenetic reprogramming occurs and new epigenetic signatures are established to guide germ cell development.

**Epigenetic regulation of germ cells specification and development**

After specification, germ cells continue to proliferate and migrate to the gonadal primordium, where they enter into meiosis and undergo gametogenesis to form mature gametes with highly differentiated, specialized cell morphology. Nevertheless, germ cells retain totipotency. As the only cells contributing to the next generation, they have evolved particular mechanisms to maintain this characteristic. One of the mechanisms involves in epigenetic regulation. The epigenetic signatures in germ cells are unique and fundamentally different from those of somatic cells. These signatures are established during specification, meiosis and gametogenesis and are distinct in oocyte and sperm. Therefore, when a sperm and an oocyte join together to form a zygote, their chromosomes arrive with different epigenetic patterns that reflect their different

developmental histories. These epigenetic patterns must be reprogrammed to a state compatible with totipotency (Morgan et al., 2005; Surani et al., 2007). As the differentiation occurs during embryogenesis, new epigenetic signatures corresponding to each cell type are established in each lineage, but these patterns are repressed in the germ line.

In mouse, a wave of epigenetic reprogramming including DNA demethylation occurs during early stage of embryogenesis (Figure 1-2). PGCs are specified from a group of pluripotent stem cells around E6.5. The levels of DNA methylation, H3K9me2 and H3K27me3 are similar in the newly established PGCs and surrounding somatic cells. As they become distinct and start to migrate, H3K9me2 levels decrease and DNA methylation is reduced, while H3K27me3 is increased (Seki et al., 2007). We still don't know the meanings of these changes. One possible explanation is that the upregulation of H3K27me3 compensates for the reduction of DNA methylation and H3K9me2 to maintain a proper repressive state (Sasaki and Matsui, 2008). In addition, Blimp1 interacts with the arginine methyltransferase Prmt5 to maintain the symmetric di-methylation of arginine 3 of H2A (H2AR3) and H3 (H3R3), which seem to be important for the maintenance of somatic repression (Ancelin et al., 2006). Further epigenetic reprogramming occurs in PGC chromatin when they arrive at the genital ridge around E11.5 (Figure 1-2). Among the reprogramming events, one important aspect is the erasure of parental genomic imprints, marked by the removal of DNA methylation at imprinting control regions (Figure 1-2). The inactive X chromosome in female is also reactivated during this period. Re-establishment of genomic imprints does not occur until after sex determination of the germ cells (Reik and Walter, 2001). In male germline,

imprinted DNA methylation requires the *de novo* cytosine methyltransferase DNA methyltransferase 3A (Dnmt3A), and the imprint is established between E14.5 and the new born stage. In female germ cells, DNA methylation imprinting is initiated after birth. Both DNMT3A and DNMT3L are required for this process (Sasaki and Matsui, 2008). The established imprints are maintained throughout the remaining stages of germ cell development and are further transmitted to next generation.

Epigenetic alterations are also observed during meiosis. For example, specific histone variants such as H3.3 are incorporated into nucleosomes before prophase I. This euchromatin associated variant might contribute to the massive transcription in spermatocytes (Kimmins and Sassone-Corsi, 2005). Histones H3 and H4 are generally acetylated at prophase I but are deacetylated at metaphase I by histone deacetylases (HDACs). Inhibition of HDACs causes defects in chromosome alignment at the metaphase plate, which subsequently increase the frequency of aneuploidy. Interestingly, significant retention of histone acetylation has been observed in the oocytes of older mice. This has significant implications for some human aneuploidies, such as trisomy of chromosome 21, since high incidence of aneuploidy in older pregnancies might be related to inadequate deacetylation (Akiyama et al., 2006).

Several histone methyltransferases have been demonstrated to play a role in meiosis. For example, meiosis is arrested at the pachytene stage in spermatocytes lacking the H3K9 methyltransferases *suv39h1* and *suv39h2* (Peters et al., 2001). Pericentric heterochromatin, marked by condensed DNA and enrichment in H3K9me3, is lost in these cells before and during early meiotic prophase. Further investigation revealed that these mutant germ cells show non-homologous chromosomal interactions and delayed

synapsis, suggesting that *suv39* mediated H3K9me3 might be required for the proper progression of meiotic prophase (Peters et al., 2001). Meisetz, a germ cell specific H3K4 trimethyltransferase, is also required for early meiotic prophase progression. H3K4me3 is reduced and meiotic gene transcription is changed in Meisetz mutant testis. Meisetz knockout mice are sterile due to severe defects in the double strand break repair pathway (Hayashi et al., 2005). Taken together, these studies strongly argue that the epigenetic status of chromatin plays an important role in proper meiotic progression.

In *C. elegans*, the PGC precursor cells called P-blastomeres (P1-P3) also give rise to somatic lineages. Therefore the epigenetic state of these cells is not restricted to a germ cell identity. As detailed above, transcription in P cells is maintained in a state of repression by a mechanism dependent on PIE-1 (Mello et al., 1996). However, histone modifications associated with transcription competency such as H3K4me are present in these cells, and the levels of these marks are not reduced as the cells divide (Schaner et al., 2003). This suggests that H3K4 methylation can occur independently of ongoing transcription. The last P cell, P4, divides symmetrically to produce the two PGCs--Z2 and Z3. Upon the birth of Z2 and Z3, PIE-1 is degraded, and specific histone modifications, notably H3K4me2/3 and acetylation at K8 of H4, are globally depleted from the chromatin in Z2/Z3. These marks, however, are actively maintained in surrounding somatic cells (Schaner et al., 2003). This leads to a presumably inert chromatin architecture, as evidenced by the observation that the DNA in Z2/Z3 is more condensed than in surrounding somatic nuclei. This germ cell specific chromatin reorganization succeeds PIE-1-mediated repression, and is maintained until hatching (Schaner et al., 2003). After hatching, Z2 and Z3 accumulate H3K4me2 and H3K4me3 and begin to

proliferate to form a cluster of germline stem cells (GSCs). From this point on the genome is highly active and expresses genes necessary for germ cell development. Maternal gene expression appears to ramp up in later stages when meiosis commences. Active histone modification marks including H3K4me2 and H3K4me3 are present in the germline chromatin throughout these stages. However, the X-chromosome is one exception to this pattern (Schaner and Kelly, 2006).

In *C. elegans*, multiple lines of evidence suggest that the X chromosome is transcriptionally inactive in the early germline stages of both males and hermaphrodites in *C. elegans*. First, the X chromosome lacks most active marks including H3K4 methylation, H3S10 phosphorylation, and H4 acetylation at K5, K8, K12 and K16. These marks, however, are actively maintained on the autosomes. Second, the repressive mark H3K9 methylation is enriched at the X chromosome in males. Third, genome wide microarray analyses suggest that genes on X chromosome are under-represented among genes expressed in germ cells (Schaner and Kelly, 2006). Components that participate in X chromosome repression include the *C. elegans* maternal effect sterile (*mes*) protein MES-4 and three polycomb group proteins: MES-2, -3 and -6. MES proteins are expressed in the adult germ cells of hermaphrodites and can be maternally loaded into embryos. Interestingly, MES proteins become restricted to the PGCs in later stages. Mutations in *mes* genes cause aberrant accumulation of active histone modifications on the X chromosome during meiosis (Fong et al., 2002). As is the case with strict maternal effect sterility genes, *mes/mes* homozygotes produced by heterozygous parents are fertile but give rise to sterile offspring. All the four *mes* genes exhibit similar phenotypes, but they operate in different complexes. MES-2, -3 and -6 are in a repressor complex with

H3K27-specific HMT activities. MES-2 and MES-6 are the *C. elegans* homologues of *Drosophila* Extra Sex Combs and Enhancer of Zeste, respectively (Strome, 2005). Extra Sex Combs and Enhancer of Zeste are members of the *Drosophila* Polycomb group, which play important roles in promoting and maintaining repressed chromatin states during development. MES-4 is a SET domain containing protein and has HMT activity specific for H3K36. MES-4 is associated selectively with autosomes and is thought to somehow indirectly exclude the repressive MES-2, -3, -6 complex from the autosomes. Taken together, these data support a model that MES-4 and MES-2/3/6 bind to chromatin in a mutually exclusive manner. The MES-2/3/6 complex is associated with the X chromosome and contributes to a repressed state by promoting K27 methylation, while MES-4 methylated H3K36 help maintain the active states of autosomes (Strome, 2005).

**Scope of the dissertation**

Germ cells have unique epigenetic signatures that define their fate and properties. Different epigenetic states are associated with different stages of germ line development such as specification, germ line stem cell (GSC) self-renewal, mitosis/meiosis determination, sex determination and gametogenesis. It has been proposed that epigenetic marks are "written" into chromatin by modification enzymes during various chromatin based activities such as transcription and replication. These marks are then "read" or "recognized" by certain modules of effector proteins which recruit other factors to chromatin that might change or maintain the current states (Ruthenburg et al., 2007). Through such a strategy, the epigenetic marks written by upstream activities are translated into various downstream biological outcomes, with each step subject to

regulation (Kouzarides, 2007). More importantly, these marks can also be passed to daughter cells. For example, fertilized eggs contain epigenetic marks inherited from the parental gametes (Brykczynska et al., 2010; Hammoud et al., 2009). As the zygote proliferates and development proceeds, some of the marks might be kept to direct the establishment of new marks, while those marks that are not required for current cell activities are erased for new epigenetic modifications. Eventually the epigenetic status is reprogrammed to a state that is compatible with the activities of cells of different developmental stages. The normal regulation of this epigenetic cycle is essential for cells to respond appropriately to specific surrounding signals. Within the epigenetic cycle, the establishment and the maintenance of epigenetic signatures are of particular of interest, because this is the first step to build an epigenetic blueprint on chromatin that will define the properties and functions of the cell.

We aim to understand how germ cells establish and maintain H3K4 methylation, an epigenetic mark that is correlated with transcription competency. This mark is present in PGC precursor cells in the P-lineage in the early *C. elegans* embryo. H3K4me is actively and specifically depleted from the germ cell chromatin upon the birth of the two primordial germ cells, Z2 and Z3 (Figure 1-3). After hatching, however, H3K4 methylation returns to the nuclei of Z2 and Z3 and is actively maintained throughout the remaining stages of germ cell development (Figure 1-3). Although the global H3K4 methylation on chromatin reflected by immunostaining seems to be consistent, it is highly possible that the methylation status of individual genes and specific chromatin domains have been changed dramatically as the transcription programs change in different stages of development. I hypothesize that the histone methyltransferases (HMTs)

play a primary role in the establishment and maintenance of H3K4 methylation pattern during the normal development of germ cells. The HMTs might cooperate either with transcriptional machinery, or with other complexes independently of transcription, to initiate new methylation and/or propagate existing patterns (Figure 1-4). Mutation of the HMTs involved with these processes will cause aberrant methylation patterns for H3K4, and are predicted to disrupt the epigenetic cycle and consequently interfere with the normal developmental programs of germ cells.

During the experiments described in this dissertation, I identified a number of components that contribute to normal global H3K4me2 and H3K4me3 maintenance. These components are homologues of the subunits of the yeast Set1/COMPASS complex. Different components appear to be required in different developmental stages and tissues. Two components, WDR-5.1 and RBBP-5, are required at all stages. Furthermore, H3K4me3 and H3K4me2 are regulated by different HMTs. I demonstrated that the WDR-5.1/RBBP-5 mediated H3K4 methylation is capable of operating independently of transcription, and that H3K4 methylation levels in GSC chromatin primarily depends on this mechanism. In meiotic cells, H3K4 methylation is largely mediated by a transcription coupled mechanism(s), but some levels show dependence on the WDR-5.1-based, transcription independent mode. Mutation of either *wdr-5.1* or *rbbp-5* results in a reduction in GSC population and various germ cell developmental defects.

Investigation of the functions of *wdr-5* in germ cell development has also identified a unique role for this MLL complex component in sex determination. I show that *wdr-5.1* and *wdr-5.2* are both required for initiation of oogenesis in hermaphrodites. I provide evidence that the failure of initiating oogenesis is largely caused by the ectopic

expression of *fog-3*, a gene promoting spermatogenesis. TRA-1, a transcription repressor of *fog-3*, is depleted from nuclei of adult germ cells in absence of *wdr-5.1* and *wdr-5.2*. We propose that *wdr-5.1* and *wdr-5.2* function as sex determination regulators that promote the inhibition of *fog-3* by regulating TRA-1. This role seems to be independent of H3K4 methylation, but might be incorporated into other epigenetic pathways.

Taken together, the study in this dissertation contributes to our understanding how germ cells establish and maintain H3K4 methylation on their chromatin. This research provides significant implications for the epigenetic mechanisms that govern germ cell development. Given the possibility that the epigenetic mechanism could be evolutionary conserved, investigating these processes in *C. elegans* will shed light on the mechanisms employed in human cells.

**Table 1-1. Subunit composition for yeast Set1/COMPASS complex and its human homologues.** Human SET1 (SET1A/B) and MLL1-4 are found in COMPASS and COMPASS-like complexes. Blue boxes mark the common subunits shared by all complexes.

| Yeast Set1-Compass | Human SET1-COMPASS | | Human MLL COMPASS-like | | | |
|---|---|---|---|---|---|---|
| Set-1 | SET-1A | SET1B | MLL1 | MLL2 | MLL3 | MLL4 |
| Swd3 | WDR5 | WDR5 | WDR5 | WDR5 | WDR5 | WDR5 |
| Swd1 | RbBP5 | RbBP5 | RbBP5 | RbBP5 | RbBP5 | RbBP5 |
| Bre2 | Ash2L | Ash2L | Ash2L | Ash2L | Ash2L | Ash2L |
| Sdc1 | DPY30 | DPY30 | DPY30 | DPY30 | DPY30 | DPY30 |
| Spp1 | CFP1 | CFP1 | HCF1 | HCF1 | UTX | UTX |
| Swd2 | WDR82 | WDR82 | Menin | Menin | NcoA6 | NcoA6 |
| | HCF1 | HCF1 | | | PA1 | PA1 |
| | | | | | PTIP | PTIP |

**Figure 1-1. The Germ line Cycle of *C. elegans***

(A) The germ line in *C. elegans* is specified from P-lineage during early stages of embryogenesis. The primordial germ cells, Z2 and Z3, are generated by symmetrical division of P4. Z2 and Z3 are arrested until hatching. After hatching, Z2/Z3 starts proliferation to form a cluster of germ cells during larval stages. The germ cells are finally settled in the gonad in adult stage. The germline stem cells reside in the distal region of gonad and undergo mitotic division (black). The cells that are leaving mitotic cycle or entering into meiosis reside in the transition zone (light blue). More proximal regions harbor meiotic cells (dark blue). In hermaphrodites, the germ cells first make sperm for a short period of time during larval stages and switch to oogenesis. The oocytes are fertilized when they pass the spermatheca where the sperm are stored. Orange marks the primordial germ cells and their precursors: the P cells.

(B) A line diagram showing embryonic lineage. P-lineage is shown in red and somatic cells are in green. P1-P3 undergoes asymmetrical division and produces another P cell and a cell that undergoes somatic differentiation. P4 divides symmetrically to produce Z2 and Z3. The transcription is maintained in an inactive state in P cells and Z2/Z3.

(C) The Sex determination pathway in *C. elegans*. The sex of *C. elegans* is determined by X:A ratio through a series of negative genetic interactions between a number of genes.

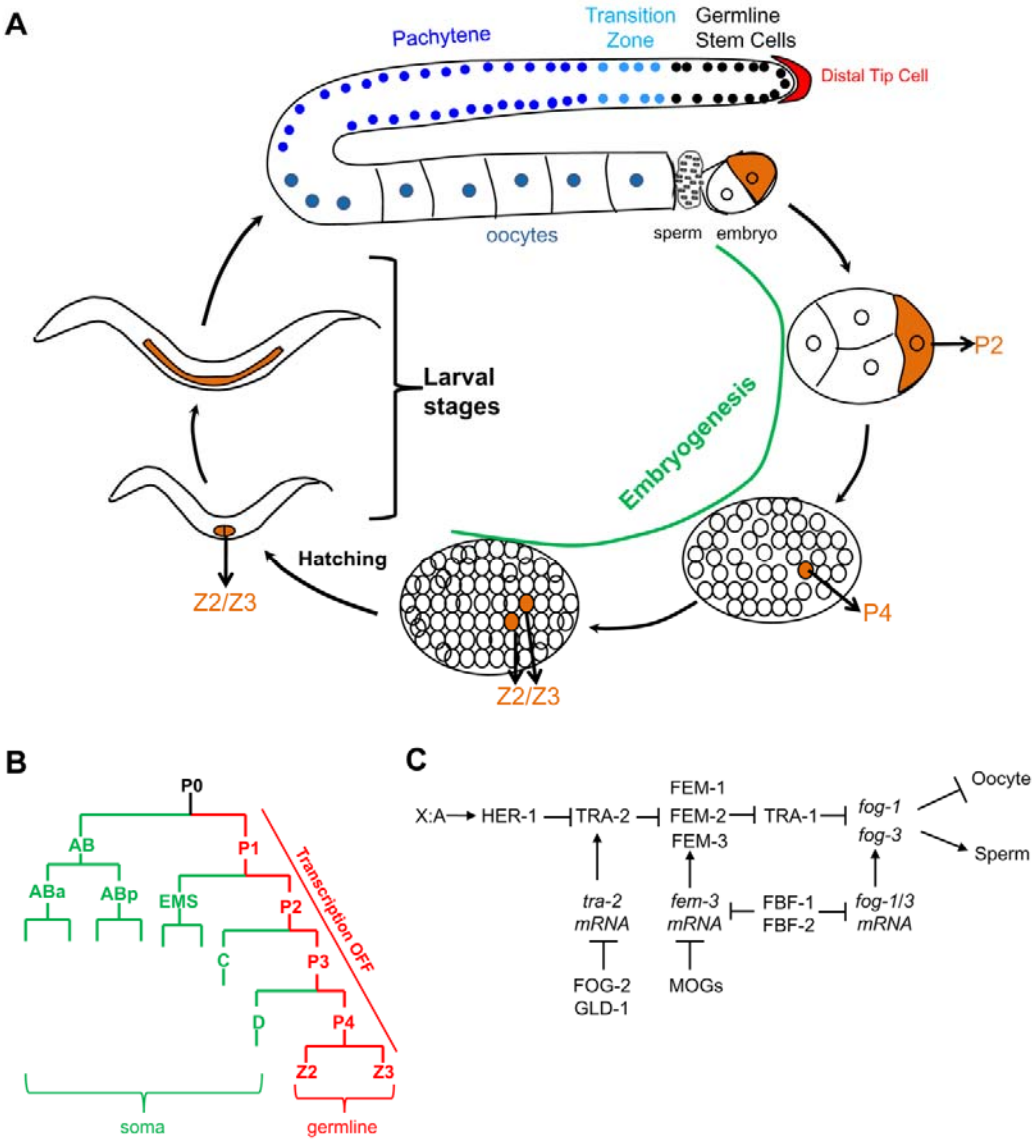
A
Pachytene
Transition Zone
Germline Stem Cells
Distal Tip Cell
oocytes
sperm
embryo
P2
Larval stages
Embryogenesis
Hatching
Z2/Z3
P4
Z2/Z3
B
P0
AB
P1
ABa
ABp
EMS
P2
C
P3
D
P4
Z2
Z3
Transcription OFF
soma
germline
C
X:A
HER-1
TRA-2
FEM-1
FEM-2
FEM-3
TRA-1
fog-1
fog-3
Oocyte
Sperm
tra-2 mRNA
fem-3 mRNA
FBF-1
FBF-2
fog-1/3 mRNA
FOG-2
GLD-1
MOGs

**Figure 1-2. The epigenetic reprogramming cycle in mouse**

The embryogenesis starts from a zygote, which is generated by the fusion of a sperm and an oocyte. Epigenetic modifications undergo reprogramming during preimplantation development and gametogenesis. During the preimplantation stages of embryogenesis, the embryo's DNA is demethylated while imprinted genes maintain their methylation through this reprogramming. A wave of de novo methylation occurs at about E3.5 when the first two lineages of the blastocyst are differentiated. Primordial germ cells **(**PGCs, shown in red) arise from epiblast between E6.5 and E7.25. Epigenetic reprogramming including DNA methylation and histone modifications occurs in PGCs as soon as they are specified and continues as the germ cells develop. Imprinted genes are demethylated in germ cells between E11.5 and E12.5. In later stages, the germ cells acquire imprints through de novo methylation on their genomes; this process continues up to E18.5 in males and in maturing oocytes before ovulation in females.

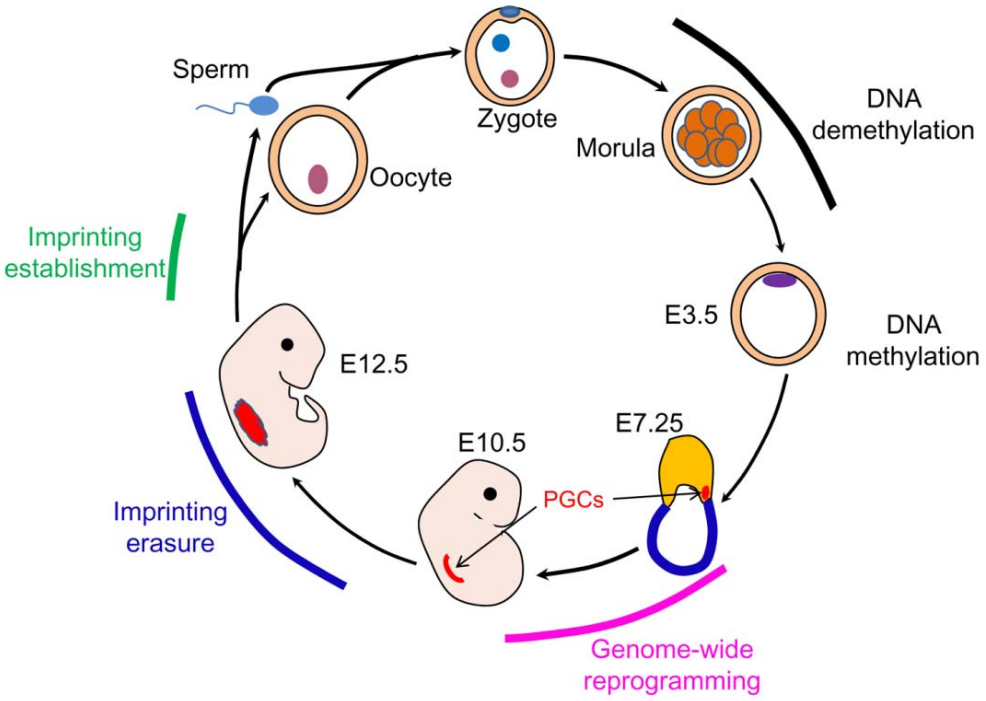
Sperm
Zygote
Morula
DNA
demethylation
Oocyte
Imprinting
establishment
E3.5
DNA
methylation
E12.5
E7.25
E10.5
PGCs
Imprinting
erasure
Genome-wide
reprogramming

**Figure 1-3. Dynamics of H3K4me2 and H3K4me3 in the germline of *C. elegans***

Samples are stained with antibodies specific to H3K4me2 or H3K4me3 (green). Anti-PGL signals (blue) mark P cells or PGCs (Z2 and Z3). DNA was counter-stained with DAPI (red). H3K4me2 is maintained in the P-cells and is depleted from nuclei of Z2 and Z3 upon their birth, while H3K4me3 begins to decrease in P4 and becomes undetectable in Z2 and Z3. The absence of H3K4me2/3 in Z2 and Z3 persists through all subsequent stages of embryogenesis. After hatching, H3K4me2/3 return to Z2 and Z3 chromatin, and the marks are then present in all germ cell nuclei throughout all subsequent stages of germline development.

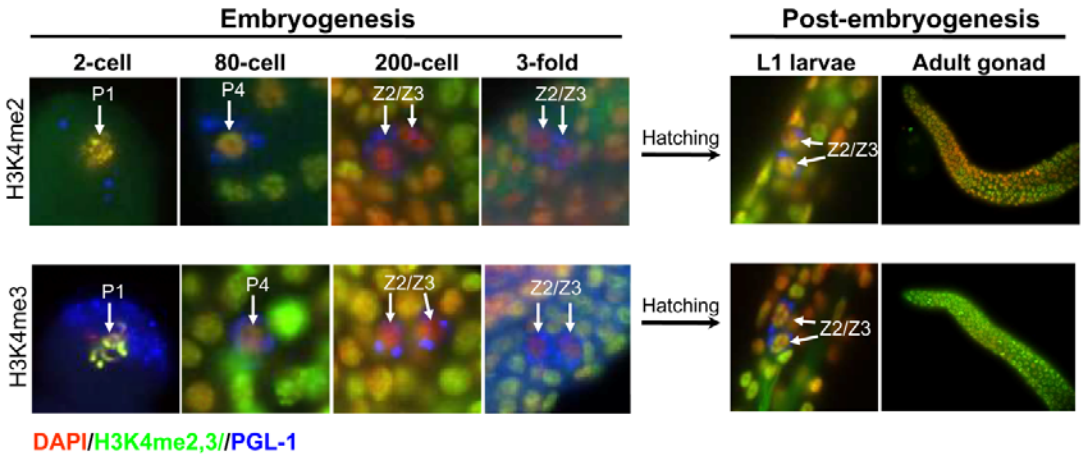
Embryogenesis
Post-embryogenesis
2-cell
80-cell
200-cell
3-fold
L1 larvae
Adult gonad
H3K4me2
H3K4me3
P1
P4
Z2/Z3
Hatching
DAPI/H3K4me2,3//PGL-1

**Figure 1-4. Potential HMTs regulating H3K4me2/3 in germ cells**

The H2K4me2 and H3K4me3 are maintained in P-cell chromatin. After hatching, H3K4me2/3 accumulates to chromatin lacking of H3K4me2/3, de novo HMTs might contribute to this process. In the adult germline, H3K4me2/3 is present in all nuclei. Both *de novo* and maintenance HMTs might be involved in the regulation of H3K4me2/3 on specific genes or chromatin domains.

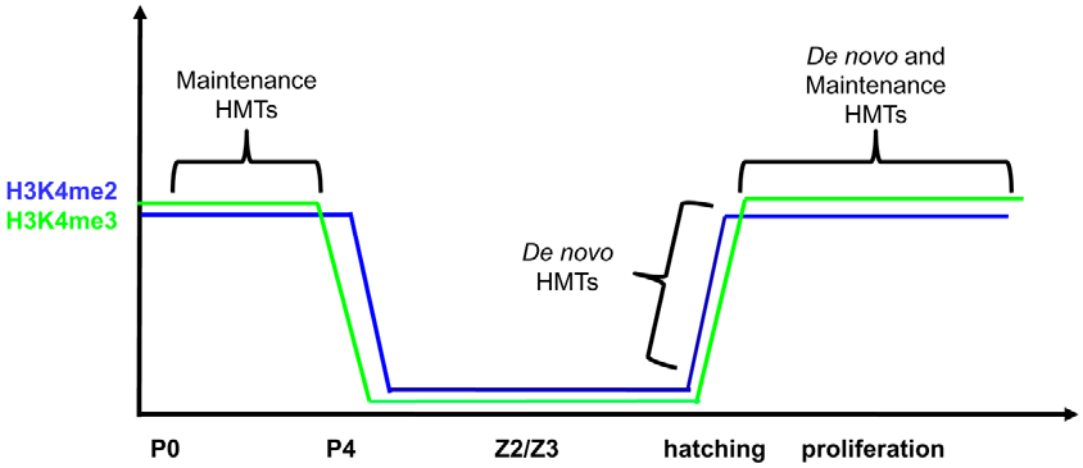
Maintenance
HMTs
De novo and
Maintenance
HMTs
H3K4me2
H3K4me3
De novo
HMTs
P0
P4
Z2/Z3
hatching
proliferation

# Chapter 2

## A Role for Set1/MLL Related Components in Epigenetic Regulation of the *Caenorhabditis elegans* Germ Line

Tengguo Li [1,2] and William G. Kelly [1]

[1]Biology Department, 1510 Clifton Road, Rollins Research Center, Emory University, Atlanta, Georgia 30322, USA

[2] Graduate Program in Genetics and Molecular Biology, Emory University, Atlanta, Georgia 300322, USA

This manuscript has been published on PLoS Genetics: Li, T and Kelly, W (2011) A role for Set1/MLL related components in epigenetic regulation of the *Caenorhabditis elegans* germ line. PLoS Genetics 7(3): e1001349

**Abstract**

The methylation of lysine 4 of Histone H3 (H3K4me) is an important component of epigenetic regulation. H3K4 methylation is a consequence of transcriptional activity, but also has been shown to contribute to "epigenetic memory"; i.e., it can provide a heritable landmark of previous transcriptional activity that may help promote or maintain such activity in subsequent cell descendants or lineages. A number of multi-protein complexes that control the addition of H3K4me have been described in several organisms. These Set1/MLL or COMPASS complexes often share a common subset of conserved proteins, with other components potentially contributing to tissue-specific or developmental regulation of the methyltransferase activity. Here we show that the normal maintenance of H3K4 di- and tri-methylation in the germ line of *C. elegans* is dependent on homologs of the Set1/MLL complex components WDR-5.1 and RBBP-5. Different methylation states that are each dependent on *wdr-5.1* and *rbbp-5* require different methyltransferases. In addition, different subsets of conserved Set1/MLL-like complex components appear to be required for H3K4 methylation in germ cells and somatic lineages at different developmental stages. In adult germ cells mutations in *wdr-5.1* or *rbbp-5* dramatically affect both germ line stem cell (GSC) population size and proper germ cell development. RNAi knockdown of RNA Polymerase II does not significantly affect the *wdr-5.1*-dependent maintenance of H3K4 methylation in either early embryos or adult GSCs, suggesting that the mechanism is not obligately coupled to transcription in these cells. A separate, *wdr-5.1*-independent mode of H3K4 methylation correlates more directly with transcription in the adult germ line and in embryos. Our results indicate that H3K4

methylation in the germline is regulated by a combination of Set1/MLL component-dependent and independent modes of epigenetic establishment and maintenance.

## Introduction

The modulation of chromatin architecture is a key level of regulation for potentially all eukaryotic DNA-based processes including gene expression, and DNA replication, repair, and recombination (Li et al., 2007). One level of chromatin modulation involves the methylation of lysines in nucleosomal histones, which can be mono-, di-, or tri-methylated. The positions of methylated lysine residues, and even the extent of methylation at any single lysine, have been associated with distinct transcriptional outcomes (Fischle et al., 2003). For example, methylation at lysine 4 of histone H3 (H3K4me) correlates with transcriptional activation, whereas methylation on lysines 9 or 27 of H3 (H3K9me/H3K27me, respectively) is most often linked to gene repression (Fischle et al., 2003; Sims and Reinberg, 2006). Methyl groups are added to the lysine residues of histones by histone methyltransferases (HMTs) (Dillon et al., 2005). In *S. cerevisae*, the sole H3K4 HMT, Set1, is recruited to chromatin by the RNA polymerase II (Pol II) elongation machinery (Krogan et al., 2003; Ng et al., 2003). The occupancy of Set1 and H3K4 methylation are highly correlated on transcribing genes, with trimethylated H3K4 (H3K4me3) enriched in the 5'-end and dimethylated H3K4 (H3K4me2) extending further into the gene body (Ng et al., 2003; Pokholok et al., 2005; Santos-Rosa et al., 2002). Set1 is the only H3K4-specific HMT identified in *S. cerevisae,* yet it is not essential for yeast survival under laboratory growth conditions (Briggs et al., 2001).

While some HMTs have detectable *in vitro* activity as isolated proteins, substantial and specific *in vitro* activities of the known H3K4-specific SET HMTs often require the addition of other components from their *in vivo* complexes (Dou et al., 2006;

Krogan et al., 2002; Shilatifard, 2006). The COMPASS complex, within which budding yeast Set1 operates, contains seven components that are important for Set1 activity (Table 2-1 and (Dehe and Geli, 2006; Miller et al., 2001; Nagy et al., 2002; Roguev et al., 2003)). Components of the COMPASS complex are highly conserved from yeast to humans, although different subsets of the subunits are distributed among different H3K4 HMT complexes in multi-cellular organisms (Dou et al., 2006; Dou et al., 2005; Wysocka et al., 2005). At least six Set1 homologs have been identified in mammalian cells: Set1A, Set1B, and four members of the Mixed-Lineage Leukemia (MLL) family: MLL1, -2, -3, and -4 (Glaser et al., 2006; Hughes et al., 2004; Milne et al., 2005; Wysocka et al., 2003; Yokoyama et al., 2004). The *S. cerevisiae* homologs of other components in the mammalian Set1/MLL complex(es) include RbBP5 (Swd1), WDR5 (Swd3), Ash2 (Bre2), Cfp1 (Spp1), and hDPY30 (Sdc1) (Table 2-1 and (Hughes et al., 2004; Lee and Skalnik, 2005; Milne et al., 2005; Wysocka et al., 2003; Yokoyama et al., 2004)). Biochemical studies suggest that WDR5/Swd3 and RbBP5/Swd1 are essential for complex stability and activity, whereas Ash2/Bre2 and Cfp1/Spp1 might play roles in the conversion from di- to tri-methylation (Dou et al., 2006; Schneider et al., 2005; Steward et al., 2006). Knockdown of WDR5 affects H3K4me1/2/3 to various degrees in mammalian cells (Wysocka et al., 2005), consistent with the idea that WDR5 plays a central role in stabilizing the complex and regulating its HMT activity (Dou et al., 2006; Steward et al., 2006).

Important developmental roles for this complex have been identified in multiple organisms. WDR5 is required for the maintenance of H3K4me3 levels at the HOXA9 and HOXC8 loci in mammalian cells and is important for the normal expression of these two

genes (Wysocka et al., 2005). In *X. laevis*, knockdown of WDR5 leads to reduction of H3K4me1 and H3K4me3 levels and a variety of developmental phenotypes including somatic and gut defects (Wysocka et al., 2005). Previous studies in *C. elegans* have also implicated the Set/MLL complex as playing important roles in growth and somatic gonad and vulva development, at least partly through attenuation of Ras signaling (Fisher et al., 2010; Simonet et al., 2007).

Although some structural studies have suggested that WDR5 recognizes the most N-terminal residues of histone H3's "tail" (Couture et al., 2006; Han et al., 2006; Ruthenburg et al., 2006; Schuetz et al., 2006), other studies have shown that H3 tail recognition by WDR5 may not require K4, as the interaction between WDR5 and the H3 tail can be independent of H3K4's methylation status. In contrast, asymmetric dimethylation of arginine 2 of H3 (H3R2me2a) abolishes binding of WDR5 to the H3 tail (Guccione et al., 2007; Hyllus et al., 2007; Kirmizis et al., 2007). Recent studies indicate that MLL interacts with WDR5 through a WDR5-interacting (Win) motif that shares homology with the N-terminus of H3, and indeed the interaction site in WDR5 is the same for both MLL and H3, suggesting that H3 and MLL might compete for the binding to WDR5 and this may be important for the regulation of H3K4 methylation status (Cosgrove and Patel, 2010; Patel et al., 2008a; Patel et al., 2009; Patel et al., 2008b; Song and Kingston, 2008). This suggests that interactions of WDR5 with H3 and MLL may be mutually exclusive. Intriguingly, *in vitro*-assembled complexes composed of WDR5, Ash2L, RbBP5 and DPY30 that lack the MLL protein still exhibit H3K4-specific HMT activity (Patel et al., 2009). This suggests that MLL is not the sole HMT activity in the MLL complex, and that WDR5 binding to H3, to the exclusion of MLL, may not

necessarily abrogate the complex's role in histone modification. In addition, histone demethylase activities are reported to copurify or otherwise interact with Set1/MLL core components, suggesting the complex may have a variety of roles in epigenetic regulation (Cho et al., 2007; Fisher et al., 2010).

These studies have provided significant insight into how H3K4 methylation may be differentially regulated by components of the HMT complex, yet the contributions of this regulation to developmental pathways are still poorly understood. Indeed, the function of the H3K4me mark itself is unclear. Although H3K4 methylation has been assigned roles in the regulation of gene activation, it is also clearly a downstream consequence of gene activity. It has been proposed that H3K4 methylation could serve as a "memory" of where transcription has occurred, which in turn may stably guide further transcriptional regulation after cell division and throughout differentiation (Muramoto et al., 2010; Petruk et al., 2001; Ringrose and Paro, 2004). Recent data support this and suggest that histone methylation can serve as a component of epigenetic memory that can even be transferred intact across multiple generations. For example, mutation of the H3K4 demethylase LSD1/KDM1 causes an inappropriate and continued accumulation of H3K4me2 in germ cell chromatin across many generations (Katz et al., 2009). This H3K4me2 accumulation correlates with a progressive, generation-dependent "germline mortality" phenotype in mutant populations, a phenotype that presumably results from the heritable accumulation of H3K4me2 that is not properly removed in the absence of LSD1 (Katz et al., 2009).

Another mark normally considered a product of ongoing transcription, H3K36me, has recently been shown by our lab and others to heritably mark, in embryos, genes that

had last been expressed in the germ cells of the preceding generation (Rechtsteiner et al., 2010). This heritable marking is by a metazoan-specific H3K36 HMT, MES-4, that in *C. elegans* can operate in a largely transcription-independent mechanism. The role of MES-4 in this mode of "maintenance histone methylation" is essential for germline viability.

Recent studies have shown that histone modifications imposed in the paternal germ cells can be transferred into subsequent generations through sperm chromatin in mammals (Hammoud et al., 2009). These include chromatin regions at genes transcribed in germ cells, but also so-called bivalent domains, regions marked by both H3K4 and H3K27 methylation, which have been observed to similarly mark inactive, developmental loci in ES cells (Azuara et al., 2006; Bernstein et al., 2006; Brykczynska et al., 2010; Hammoud et al., 2009). Indeed, there is significant overlap in the loci marked by bivalent domains in both sperm and ES cells, suggesting that H3K4me can be maintained at these unexpressed loci in both germ cells and in embryonic lineages that retain pluripotency. In *C. elegans,* transcriptional inactivity of the X chromosome during male spermatogenesis results in the X chromosome being largely depleted of H3K4me during meiosis and gametogenesis; this dearth of H3K4me persists in spermatid chromatin, and is heritably maintained through multiple cell divisions in the early embryo (Bean et al., 2004).

Although epigenetic marks, including histone modifications and DNA methylation imprints, can be inherited from parents through the gametes, there is significant erasure, or "reprogramming", of information in the zygote, and then again during germ cell specification (Hajkova et al., 2008; Schaner et al., 2003; Seki et al., 2007). The purpose of this reprogramming is unclear, but it is presumably related to the establishment and/or maintenance of epigenetic content that is compatible with

developmental pluripotency. Conversely, epigenetic information that defines the pluripotent state must be recognized and protected from erasure and/or actively maintained during this process. Many regions of the genome carrying this information may not be transcriptionally active during early embryonic stages therefore maintenance of the epigenetic content may not be obligatorily coupled to transcriptional activity. Maintenance of transcription-associated marks like H3K4me and H3K36me may therefore require mechanisms operating outside of active gene expression. Evidence is mounting that such mechanisms exist. In addition to the maintenance of bivalent silenced loci and the MES-4 system mentioned above, a recent study in zebra fish embryos revealed a class of genes in which H3K4me3 alone is present at promoters with no evidence of ongoing transcription, further uncoupling this modification from transcription (Vastenhouw et al., 2010). In addition, unmethylated CpG-rich regions of the genome can recruit H3K4 methylation independently of transcription, and this requires the Set1/MLL complex component Cfp1/CxxC1 (Thomson et al., 2010). These data indicate that H3K4 HMT complexes may play a role in the establishment and/or maintenance of H3K4me patterns in the genome independently of transcription.

RNA Polymerase II (Pol II) is normally inactivated in the early embryonic germline of *C. elegans* (Baugh et al., 2003; Edgar et al., 1994; Seydoux and Dunn, 1997). Despite the absence of Pol II activity, and cell divisions that could dilute this mark (through replication-coupled *de novo* chromatin assembly), the level of H3K4me2 in the germline precursor chromatin remains relatively stable (Schaner et al., 2003). This suggests the existence of transcription-independent mechanisms capable of maintaining this mark. In these studies, we show that conserved components of Set1/MLL-like

histone methyltransferase complexes are required for what appears to be a largely Pol II-independent mode of H3K4me maintenance in germ cells. Interestingly, this mode predominates in early embryonic somatic and germline precursors, and in larval and adult stages Set1/MLL complex component-dependent H3K4 methylation is most obvious in the germline stem cell (GSC) population. Mutations in some components show defects in germline stem cell maintenance, impair fertility and germ cell development, and exhibit a germline mortality phenotype (Simonet et al., 2007). Our results suggest that H3K4 methylation is an important component of the epigenetic regulation of germline establishment, maintenance, and function. We propose that a combination of transcription-dependent insertion, and transcription-independent maintenance, of this mark may be required to maintain a totipotent epigenome as it passes through the germ line across generations.

## Results

### Conserved Set1/MLL complex components are present in the genome of *C. elegans*

H3K4me2 and me3 are considered to be hallmarks of transcriptional activity, as these marks are generally correlated with active genes in genome-wide studies (Bernstein et al., 2005; Ng et al., 2003; Santos-Rosa et al., 2002; Schneider et al., 2004). However, significant levels of H3K4me2 are stably observed in the chromatin of early dividing blastomeres and germline precursors (P cells) of *C. elegans* embryos, which exhibit little detectable RNA Polymerase II transcription (Baugh et al., 2003; Edgar et al., 1994). This suggests that transcription-independent ways of maintaining this modification exist in these cells. We wished to identify the H3K4 methyltransferase(s) involved in the

maintenance of this epigenetic mark and the consequences of their absence. All known H3K4 specific methyltransferases share the conserved catalytic SET-domain (Martin and Zhang, 2007). *C. elegans* contains 34 genes that encode SET domain proteins; sequence analysis suggests that two of them, *set-2* and *set-16*, are most closely related to yeast Set1 and human MLL H3K4 HMT's. The SET domain of worm *set-2* shares 80.6% and 74.2% homology with the human Set1A and yeast Set1 proteins, respectively, whereas the SET-domains of worm *set-16* and human MLL3 share 66.7% homology (not shown).

*C. elegans* also contains homologs of other yeast COMPASS components (see Table1 for nomenclature). Because COMPASS is often used to refer to the specific complex found in *S. cerevesiae*, we hereafter refer to the *C. elegans* homologs of conserved components as Set1/MLL complex components to denote the metazoan complex. Note also that although homologs of most Set1/MLL complex components have been identified in *C. elegans*, the existence of a complex composed of these components can only be inferred at this time. Three homologues of *Swd3*/WDR5 (*wdr-5.1*, *wdr-5.2*, and *wdr-5.3*) are found in the *C. elegans* genome (Table 2-1 and (Fisher et al., 2010; Simonet et al., 2007)). Other homologues include: *F21H12.1* (*Swd1*/RbBP5), *Y17G7b.2* (*Bre2*/Ash2), *dpy-30* (*Sdc1*/hDPY30), *cfpl-1/F52B11.1* (*Spp1*/Cfp1), and *C33H5.6* (*Swd2*/Wdr82) (Table 2-1, and (Fisher et al., 2010; Simonet et al., 2007)). No *Shg1* homologs were identified in *C. elegans*. Previous studies have shown that a SET1/MLL complex, as in other organisms, contributes to H3K4 methylation in *C. elegans* (Fisher et al., 2010; Simonet et al., 2007). Inactivation of the Set1 homolog *set-2* resulted in a global decrease of H4K4me3 levels in mixed-staged populations, but little detectable change in H3K4me2 levels (Simonet et al., 2007). Knockdown of each of three

other worm homologs of the Set1/MLL complex components, *wdr-5.1*/WDR5, *dpy-30*/hDPY30, or *cfpl-1*/Spp1, resulted in decreases of both H3K4me2 and H3K4me3 to various degrees (Simonet et al., 2007). These experiments, while informative, did not assess stage- or tissue-specific effects of loss of these components, particularly in the germ line.

**An essential role for Set1/MLL components in embryonic H3K4me regulation**

To investigate how H3K4 methylation is regulated developmentally, we first asked if *set-2* or *set-16* was required for H3K4 methylation in early embryos. We dissected embryos from mutant strains and/or RNAi-treated animals and probed fixed whole mount specimens with antibodies specific to H3K4me2 or H3K4me3. In the RNAi protocol performed, the target mRNAs should be knocked down in both parental germ cells and embryos, thus treated animals are expected to have both maternal and zygotic supplies of the targets reduced. *set-16 (RNAi*) caused >80% embryonic lethality, with survivors growing up to be Dumpy (Dpy phenotype) and sterile adults. In contrast, homozygous embryos from animals heterozygous for the *set-16 (gk438)* deletion allele (i.e., Maternal+/Zygotic-), developed into Dpy and sterile adults, indicating substantial maternal rescue. Appreciable loss of either di- or tri- methylated H3K4 (H3K4me2/me3) in any stage or tissue examined was not observed in either RNAi-treated or (maternally rescued) mutant embryos in our immunofluorescence assays (Figure 2-1 and data not shown). This result potentially differs from a recent report showing a decrease in H3K4me3 in *set-16* (RNAi) adults detected by western blot assays (Fisher et al., 2010);

the differences in the respective results may be due to differences in the assays and experimental focus.

However, and similar to a previous report, we observed that H3K4me3 was substantially depleted from nuclei of *set-2 (tm1630)* deletion mutant embryos (Figure 2-2A; (Simonet et al., 2007)). We also confirmed that H3K4me2 was not significantly affected in *set-2* mutant embryos (Figure 2-2B; (Simonet et al., 2007)). Knockdown of *set-2* by RNAi caused similar reduction in H3K4me3 levels in embryos, also without affecting H3K4me2 (data not shown). These results indicate that SET-2 is an HMT principally responsible for H3K4me3, and that other HMTs may regulate H3K4me2. We do not know if SET-2 acts to convert H3K4me2 to H3K4me3, but we did not notice any increase in H3K4me2 in *set-2* mutants, as might be expected from a lack of such conversion (not shown).

In an attempt to identify the additional HMT(s) responsible for H3K4me2, we knocked down several additional SET domain containing H3K4 HMT candidates including: *F15E6.1 (set-9), Y51H4a.2 (set-26), K09F5.5 (set-12), Y41D4b.12 (set-23), lin-59, set-25,* and *F25D7.3* by RNAi. We did not detect changes in H3K4me2/3 by immunofluorescence in any of these experiments (data not shown). These results confirm and extend the findings of others that SET-2 is the HMT activity that is largely responsible for H3K4 trimethylation in embryos ((Simonet et al., 2007)). The dimethyl H3K4 HMT activity still remains to be identified.

To test whether the other conserved components of Set1/MLL complexes are similarly required for normal H3K4me regulation in embryos, we examined animals with either mutation in the homologous genes and/or treated with RNAi targeting those loci.

We first focused on the WDR5 homologs. Similar to *set-2(tm1630)* mutant embryos, H3K4me3 was strongly depleted from the nuclei of *wdr-5.1(ok1417)* embryos (Figure 2-2A). The *wdr-5.1(ok1417)* deletion allele is likely a null allele since an antibody against WDR-5.1 did not detect the WDR-5.1 band in western blot analyses (Figure 2-3), and *wdr-5.1(RNAi)* resulted in phenotypes similar to *ok1417* (not shown). However, unlike *set-2(tm1630)*, significant loss of H3K4me2 was also observed in *wdr-5.1* embryos, albeit not to the near background levels observed for H3K4me3 (Figure 2-2B). These defects are specific to loss of WDR-5.1 activity in the deletion mutants since both H3K4me2 and H3K4me3 defects could be rescued by a WDR-5.1::GFP transgene (Figure 2-2C). In contrast, neither mutation of *wdr-5.2,* nor knockdown of *wdr-5.3* by RNAi, the other Swd3/WDR5 homologues, noticeably affected H3K4me3 or H3K4me2 levels in embryos, nor did combinations with *wdr-5.1(ok1417)* mutants exhibit additive defects in H3K4me (data not shown). These data indicate that among the WDR5 homologs, WDR-5.1 plays the predominant role in H3K4 methylation in early embryonic stages. Protein blot analysis of H3K4me2 and H3K4me3 marks present in embryos confirmed the immunofluorescence results (Figure 2-2D). H3K4me1 levels were not detectably affected in any of the mutants tested (Figure 2-2D and data not shown).

We then examined other conserved Set1/MLL components. As with *wdr-5.1(ok1417)* mutants, both H3K4me3 and H3K4me2 were strongly reduced in the nuclei of *rbbp-5(tm3463)* mutant embryos (Figure 2-1A and B). Knockdown of *rbbp-5* by RNAi resulted in similar defects, indicating our RNAi experimental conditions were efficient (data not shown). We then targeted homologs of other Set1/MLL complex components in an RNAi hyper-sensitive strain, *eri-1(mg366).* As shown in Figure 2-1A and B, *ash-2*,

*dpy-30,* and *cfp-1* are also required for normal levels of both H3K4me3 and H3K4me2 in early embryos. RNAi of *wdr-82* showed no discernible effects on H3K4 methylation in our assays. Interestingly, H3K4 methylation was observed to become increasingly detectable in later stages of embryogenesis (>300 cells) in mutant and RNAi-treated embryos (Figure 2-4 and data not shown). This indicates that HMT activities independent of these components exist in the embryo, and that the H3K4 marks provided by these activities become increasingly evident as development progresses.

Taken together, these data show that conserved homologues of Set1/MLL components contribute to the predominant mode of H3K4me regulation in early *C. elegans* development. All of the predicted complex components, with the exception of *wdr82/swd-2*, are essential for this HMT activity. SET-2 appears to be the H3K4 HMT operating in the context of this putative complex that is specifically required for H3K4 trimethylation, whereas a separate as yet unidentified HMT activity is responsible for H3K4me2 regulation. In later embryos, H3K4 methylation becomes detectable in the absence of Set1/MLL component function; this H3K4 methylation activity may correlate with a transcription-dependent process (see below).

**WDR-5.1 binding to H3 is dependent on H3R2 methylation**

As mentioned, WDR5 is thought to play a central role in core complex assembly and HMT regulation by interacting with MLL and/or histone H3 N-terminal tails (Dou et al., 2006; Wysocka et al., 2005). Binding of WDR5 to the histone H3 N-terminus is not affected by lysine 4 methylation, but instead is strongly inhibited by asymmetric dimethylation of arginine 2 (H3R2me2a) (Guccione et al., 2007; Kirmizis et al., 2007).

To test if worm WDR-5.1, like its mammalian WDR5 counterpart, has similar interactions with the H3 tail, we incubated wild-type nuclear extract with biotinylated H3 peptides and assayed for WDR-5.1 interactions by western blot analysis of peptide-bound material using a WDR-5.1 specific antibody. As shown in Figure 2-5, WDR-5.1 showed specific interactions with unmodified (H3K4me0) and H3K4me2 peptides, but not with an H3R2me2a-modified peptide. *C. elegans* WDR-5.1 thus has similar histone H3 binding characteristics to those of mammalian WDR5. These data, in addition to the H3K4 methylation defects observed in *wdr-5.1*, *rbbp-5,* and *ash-2 (RNAi)* animals described above, strongly suggest that the these proteins probably exist in a complex that has similar attributes to other bona fide Set1/MLL complexes.

**Set1/MLL dependent H3K4 methylation maintenance in the early embryo is largely independent of transcription**

The COMPASS complex is recruited to chromatin by the RNA polymerase II (RNA Pol II) holoenzyme complex in *S. cerevisiae* (Ng et al., 2003), and thus in yeast H3K4 methylation appears to be strictly dependent on transcriptional elongation. However, as discussed earlier, there is growing evidence that H3K4 methylation in metazoans may not always be coupled to ongoing transcription.

In *C. elegans* embryonic germline precursors (P cells) there is little or no Pol II transcription (Seydoux and Dunn, 1997) yet H3K4 methylation persists through the four cell divisions in this lineage. However, some differences are observed between di- and tri-methylated forms (Figure 2-6 and (Schaner et al., 2003)). In wild type embryos, H3K4me3 is present from P1 and P2, but is decreased by 30% and by ~85% in P3 and P4,

respectively (Figure 2-6C and F), whereas H3K4me2 is maintained at comparable levels in P1 through P4 (Figure 2-6A and E). The levels of both H3K4me2/3 are essentially uniform in all somatic blastomere chromatin in all early stages. In *wdr-5.1/wdr-5* mutant embryos both H3K4me2 and H3K4me3 are initially observed in the chromatin of 1-2 cell nuclei; this is presumably inherited from the gamete chromatin, as it is also strongly retained in the polar bodies (Figure 2-6B and D; arrowheads) (Bean et al., 2004), However, the maintenance of both marks in subsequent cell divisions is severely compromised in the P cells of *wdr-5.1* embryos (Figure 2-6). The loss is presumably through replication-coupled histone replacement, or other types of histone dynamics, as the levels decrease with cell number. Notably, H3K4me2/3 in the somatic cells were also strongly reduced in the absence of *wdr-5.1* (Figure 2-6). Similar results were observed in the *rbbp-5/swd-1* mutant, as well after RNAi of *ash-2, dpy-30,* and *cfp-1* (data not shown). These data suggest that Set1/MLL component- dependent mechanisms are responsible for maintaining normal levels of H3K4me2/3 in the transcriptionally inactive P cells and early somatic blastomeres. Early development is largely driven, and cell viability largely maintained by maternal supplies in *C. elegans*, so even the early somatic blastomeres are not thought to be robustly active (Allegrucci et al., 2005). The maintenance of H3K4me in these early somatic lineages may also be largely independent of ongoing transcription

To further investigate this disconnection between Set1/MLL mediated H3K4 methylation and active transcription, we knocked down *ama-1* (the large, catalytic subunit of RNA Pol II) by RNAi in both WT and *wdr-5.1* mutants. *ama-1 (RNAi)* resulted in 100% embryonic lethality and AMA-1 protein dropped to undetectable levels by immunofluorescence in early embryos (Figure 2-7). In addition, the RNAi conditions

employed were sufficient to abolish detection of the phospho-Ser2 modification on RNA Pol II (Ser2p; recognized by the H5 monoclonal antibody), which correlates with the elongating form of the RNA Pol II holoenzyme (Figure 2-8A). The depletion of AMA-1 in wild-type embryos did not significantly impact H3K4me3/me2 levels, and this *ama-1(RNAi)* "resistant" H3K4 methylation was not observed when *wdr-5.1* was also defective (Figure 2-7). RNAi of *cdk-9,* the kinase component of the essential RNA Pol II transcription elongation factor pTEF-b, also knocked down Pol II Ser2p to undetectable levels and this also had no appreciable effect on H3K4me3/2 maintenance (Figure 2-8). We could not test if the WDR-5.1-independent H3K4 methylation we observed in later stages was depleted by either RNAi, since the embryos arrested prior to those stages (not shown). Taken together with what we observed in the P cells above, these data strongly suggest that in all early embryonic nuclei, including germline precursors, H3K4 methylation maintenance is largely Set1/MLL component-dependent, and this activity is unaffected by significant reduction of ongoing transcription.

**H3K4 methylation in adult germ cells has a unique mode of regulation**.

We next asked whether the Set1/MLL complex components are similarly required for H3K4me regulation in post-embryonic tissues. A recent report has shown that a worm MLL-like complex can attenuate Ras signaling in vulva development, but the vulva defects are only observed in a sensitized genetic background (Fisher et al., 2010). In our hands, mutants in some of the Set1/MLL component homologs, such as *wdr-5.1/wdr-5* and *rbbp-5/swd-1,* exhibited fertility defects (below), so we focused on the adult germ line. In *C. elegans*, hermaphrodite germ cells first undergo spermatogenesis in larvae

followed by a switch to oogenesis in adults. The adult germ cells are linearly and progressively arranged by developmental stage within the gonad arms, such that defects in any particular stage are easily identified. The mitotically active germ line stem cells (GSCs) reside in the most distal region of the gonads, and their entry into and progression through meiosis and gametogenesis occur sequentially as the cells move more proximally (e.g., left to right in Figure 2-9). The border between mitotic exit and meiotic entry, for example, is readily visualized by a characteristic condensation and crescent-shaped localization of all chromosomes within each nucleus in the "transition zone", comprising leptotene and zygotene. After exiting the transition zone, germ cells progress proximally into pachytene and then further on into oogenesis. H3K4me3 and H3K4me2 are normally abundant in the chromatin of all adult germ cell stages, and both are broadly distributed on all autosomes (Figure 2-9A and Figure 2-10A). These marks, however, are generally absent from the X chromosomes in all stages (with the exception of oogenesis), as these chromosomes are relatively transcriptionally inert in meiotic stages (Bean et al., 2004; Schaner and Kelly, 2006).

We first examined the role of the Set1/MLL component homologs in H3K4me3 regulation in adult germ cells. H3K4me3 was dramatically decreased in a specific population of nuclei in *set-2(tm1630), wdr-5.1(ok1417)* and *rbbp-5(tm3463)* deletion mutants. The decrease we observed was limited to chromatin in the most distal nuclei, the region within which the germline stem cell population (GSC) resides (Figure 2-9). This pattern was identical to that observed with RNAi knockdown of *set-2*, *wdr-5.1*, or *rbbp-5*, indicating that these cells are not specifically resistant to RNAi (not shown). Interestingly, and in contrast to what we observed in embryos, RNAi mediated knockdown of *ash-2*,

*dpy-30* or *cfp-1* had minimal effects on H3K4me3 levels in adult germ cell chromatin compared to the near 90% reduction observed in *set-2*, *wdr-5.1* and *rbbp-5* mutants (Figure 2-9). Consistent with our results in embryos, *wdr-82* knockdown also did not affect H3K4me3 in adult cells (data not shown). Significant H3K4me3 loss was also restricted to the GSCs in *wdr-5.1* males, showing that the requirement for *wdr-5.1* and *rbbp-5* for GSC H3K4me3 is not sex-specific (Figure 2-11A).

The absence of redundancy and the highly overlapping H3K4me3 defect patterns in these three mutants are evidence that SET-2, WDR-5.1 and RBBP-5 work together in these cells. The absence of H3K4me defects observed with RNAi of *ash-2, cfp-1,* or *dpy-30* indicates that, unlike in embryonic cells, these conserved components are not required for H3K4 methylation in the adult germline stem cells. The strong effect of RNAi targeting these loci in embryos shows these genes are susceptible to RNAi-mediated depletion. The GSCs also are not less susceptible to RNAi gene targeting, since RNAi of *set-2, wdr-5.1*, or *rbbp-5* substantially knocks down methylation of H3K4 in the GSCs and *ama-1(RNAi)* was effective in this region of the gonad. Furthermore, RNAi mediated knockdown of *ash-2, cfp-1,* and *dpy-30* all significantly affected H3K4 methylation in embryos, and the lack of effect in the adult germ cells was observed in both the parents and adult siblings of affected embryos in these experiments (details diagrammed in Figure 2-12).

As the germ cells in the *set-2, wdr-5.1,* and *rbbp-5* mutants progressed into meiosis, levels of H3K4me3 became detectable in the chromatin of pachytene stage and more proximal nuclei (Figure 2-9A'-D'). However, the levels of H3K4me3 in pachytene and diakinesis regions in *wdr-5.1* were reduced by 43% and 38%, respectively, compared

to wild type levels (Figure 2-13A-C). The *wdr-5.1/rbbp-5*-independent mechanism in meiotic germ cells may be additive to, or partially dependent on, what is placed in the chromatin by the WDR-5.1 "complex" in the GSCs. Indeed it is also possible, and we cannot rule out by these experiments, that the separate mechanisms have separate targets. The bulk of transcription in adult germ cells occurs in meiosis (Starck and Brun, 1977), so the *wdr-5.1* independent H3K4 methylation may be similar to the Set1/MLL-independent H3K4 methylation observed in late-stage embryos (Figure 2-4). These results indicate that the regulation of H3K4me3 in embryos and adult GSCs depends on an HMT activity that requires different subsets of the "panel" of Set1/MLL components. The results also indicate that an additional, Set1/MLL component independent mode of H3K4 trimethylation is predominantly active in meiosis.

We also tested for H3K4me2 changes in mutant and/or RNAi-treated adult germ cells. We found that, like H3K4me3, H3K4me2 in the GSC region was also only slightly affected by knockdown of *ash-2*, *dpy-30,* or *cfp-1* (Figure 2-10E-F). As in embryos, *set-2*, which is required for H3K4me3 maintenance, also was dispensable for H3K4me2 in adult germ cells (Figure 2-10B). In contrast, and similar to H3K4me3, H3K4me2 levels were decreased 90% and 85% in the GSC region of *wdr-5.1(ok1417)* and *rbbp-5(tm3463)* mutant gonads, respectively (Figure 2-10I). RNAi of these two genes again showed similar defects in adult germ cells (data not shown). However, as shown in Figure 2-14, H3K4me2 was reduced but not completely absent in the distal region of *wdr-5.1(ok1417)* gonads. Low levels of H3K4me2 are apparent, with longer exposure times, as dispersed foci on the chromosomes, rather than the more diffuse chromatin pattern observed in wild-type GSC nuclei (Figure 2-14C). As with H3K4me3, H3K4me2 appeared in

pachytene and diakinesis regions, and was also 50% below that of WT chromatin (Figure 2-14A and D). These defects and patterns were also observed in *wdr-5.1* males (Figure 2-11B).

Notably, we observed similar defects in H3K4me2 staining (in both adults and embryos) in the *wdr-5.1* strain using two different monoclonal antibodies from mouse (Kimura et al., 2008) and rabbit (Millipore cat# 04-790). A significant decrease was also observed using a polyclonal antibody, but to a lesser extent (Millipore cat#, 07-030). Both the mouse monoclonal and rabbit polyclonal antibody signals were efficiently reduced when competed with H3K4me2 peptides, but not with H3K4me0, H3K4me1, or H3K4me3 peptides (not shown). The reason for the increased residual signal detected by the polyclonal antibody in the mutants is not known.

These results show that WDR-5.1 and RBBP-5 are essential for normal H3K4me2 and H3K4me3 in adult GSCs, and to a lesser extent, meiotic germ cells and (as in embryos) appear to rely on different HMT activities for the differently methylated products. Furthermore, some Set1/MLL components that are essential for H3K4 methylation in embryos do not appear to be required in adult germ cells. Regulation of H3K4 methylation in *C. elegans,* as in mammals, may therefore involve distinct HMT complexes to yield a variety of different outcomes in different tissues and developmental stages. There also appears to be H3K4-specific HMT activities in *C. elegans* that can be roughly divided into those that share a requirement for at least some homologs of the Set1/MLL components, and those that do not. The H3K4 methylation we observe in meiotic chromatin and in later embryonic stages appear to fall into the latter class.

**H3K4me maintenance by WDR-5.1/ RBBP-5 dependent mechanisms in adult GSCs is largely independent of ongoing transcription**

As described earlier, H3K4me2/3 maintenance in the embryonic blastomeres and germline precursors was not appreciably affected by the significant disruption of RNA Pol II activity. We investigated whether this was also the case in adult germ cells by targeting *ama-1* with RNAi. AMA-1 protein is normally observed in all germ cell nuclei until diakinesis, which largely lack RNA Pol II associated with chromatin (Figure 2-15A-a' and c'; data not shown and (Kelly et al., 2002)). In both *ama-1(RNAi)* and *wdr-5.1;ama-1(RNAi)* animals, AMA-1 protein was depleted to undetected levels in the distal GSCs and in the more distal early- to mid-pachytene meiotic nuclei, but was still faintly detectable in more proximal nuclei (Figure 2-15A-b' and d'). This is consistent with the more proximal (older) nuclei containing AMA-1 protein that had been translated prior to mRNA depletion by RNAi treatment. These results indicate that the RNAi had efficiently knocked down AMA-1 to undetectable levels in distal- to mid-proximal germ cells in both genotypes in these experiments. Furthermore, the progression of germ cell development appeared to be crippled in these animals, as oocyte production had ceased, and 100% of all embryos produced up to the time point of analysis failed to hatch (not shown).

In parallel experiments, H3K4me3 and H3K4me2 patterns in *ama-1(RNAi)* gonads showed an interesting defect. In wild-type gonads treated with *ama-1* RNAi, H3K4me2/3 levels in the GSCs (where H3K4me is dependent on *wdr-5.1*) were not significantly affected (Figure 2-15). However, a swath of nuclei that had recently entered into and engaged in meiosis showed a 60-70% decrease in the levels of H3K4me3 and

H3K4me2 (Figure 2-15B-b', f', brackets; and C and D, red bars). Note that both the GSC and this "swath" of distal meiotic nuclei showed comparable depletion of AMA-1 protein in parallel animals, but H3K4me levels were only decreased in the meiotic nuclei (Figure 2-15A-b' and d'). Late pachytene nuclei that exhibited AMA-1 antibody staining in parallel animals still showed significant H3K4me2/3 levels (Figure 2-15C, green bars). In *wdr-5.1*; *ama-1(RNAi)* animals, H3K4me2/3 was dramatically decreased in all nuclei from the distal GSC region to the mid-meiotic nuclei; i.e., the *ama-1(RNAi*) resistant H3K4 methylation in the GSC region was not observed (Figure 2-15B; d',h', C and D). We also analyzed *ama-1(RNAi)* wild-type and *wdr-5.1(ok1417)* animals using the H5 (Pol II phospho-Ser2) antibody, and confirmed that the elongating form of RNA Pol II was depleted in the treated germ cells (Figure 2-16 A and B). H3K4me3 in GSC chromatin was again largely unaffected in wild-type *ama-1* (RNAi), whereas that in meiotic chromatin was significantly depleted (Figure 2-16C). *In wdr-5.1; ama-1(RNAi)* germ cells, both GSC and meiotic cell again showed reduced H3K4me3 in these experiments (Figure 2-16D).

Taken together, our data suggest that the H3K4 methylation in GSCs, that is largely dependent on *wdr-5.1/rbbp-5* mediated mechanisms, is also largely impervious to substantial depletion of RNA Pol II. We cannot conclude that all Pol II activity was completely eliminated in these experiments, but the lack of AMA-1 and H5 staining, and the fully penetrant embryonic lethality preceding the cessation of oogenesis, indicates substantial ablation of ongoing transcription in the treated germ cells. Importantly, a significant component of H3K4 methylation that occurs in meiotic cells is largely independent of WDR-5.1, and this methylation was dramatically affected by the *ama-*

*1(RNAi)* conditions employed. The meiosis-coupled H3K4 HMT activity is thus more closely linked to ongoing transcription. Thus WDR-5.1/RBBP-5-dependent mechanisms can maintain H3K4 methylation in both the embryonic germline and their post-embryonic germline stem cell descendants in a largely RNA Pol II independent manner. We next investigated the role of WDR-5.1 in the larval transitions that bridge these germ cell stages.

**Transitional regulation of H3K4me3/2 in proliferating larval germ cells**

The H3K4 methylation that is maintained by Set1/MLL components in the transcriptionally inert P-blastomere chromatin is dramatically erased in the primordial germ cells (PGCs), named *Z2* and *Z3* (Schaner et al., 2003). The reduction in H3K4me is maintained throughout embryogenesis, and normally does not reappear until hatching (Figure 2-17A and (Schaner et al., 2003)). The re-appearance of H3K4me2/3 usually coincides with the reappearance of the phospho-Ser2 modification of RNA Pol II, and thus presumably the re-initiation of productive transcription in these cells (Furuhashi et al., 2010). PGC proliferation in early stage larvae produces the germline stem cells that ultimately contribute to and maintain the adult germ cell population. In wild-type animals, H3K4me2/3 are present at robust levels in all germ cell nuclei at all post-embryonic stages. In *wdr-5.1(ok1417)* mutants, H3K4me3 reappearance was initially normal in the early PGCs and their progeny in L1 larvae, and remained detectable for a few cell divisions (Figure 2-17B). However, as the number of germ cells increased, H3K4me3 levels substantially decreased in the proliferating (now established) GSCs in *wdr-5.1* L2 and early L3 larvae. In later larval stages, as the *wdr-5.1(ok1417)* germ cells began to

enter meiosis, H3K4me3 was observed to again accumulate in their chromatin, as observed in *wdr-5.1* adult gonads (e.g., Figure 2-9). The H3K4me2 pattern was similarly defective in *wdr-5.1* mutants (data not shown). These results indicate that concomitant with PGC reactivation, there is a period of *wdr-5.1*-independent H3K4 methylation as the GSCs first become established. Shortly thereafter, and during all subsequent larval and adult stages, H3K4 methylation in the proliferating GSCs becomes largely dependent on the WDR-5.1 mechanism.

**WDR-5.1 and RBBP-5 are required for normal GSC maintenance**

The GSCs are the proliferative cells that support the large numbers of gametes ultimately produced by *C. elegans* adults. Mutations that affect the maintenance of this stem cell population affect the number of nuclei and thus the length of the pre-meiotic region of the gonad arms (Austin and Kimble, 1987; Crittenden et al., 2002; Lamont et al., 2004). We examined the effect of *wdr-5.1* and *rbbp-5* mutations on the length of the GSC zone in young adult gonads. The established procedure is to measure the number of cell diameters from the most distal nucleus (the distal tip cell) to the first nuclei exhibiting the crescent-shaped chromosome morphology characteristic of cells entering early prophase I of meiosis ("transition zone" nuclei; e.g. (Lamont et al., 2004)). We also assayed for SYP-1 appearance, a synaptonemal complex protein (MacQueen et al., 2002), to help identify the boundaries between the mitotic region and transition zone (Figure 2-18B, D and F). A temperature-dependent defect was observed for GSC maintenance in both *wdr-5.1* and *rbbp-5* mutants: at 25°C the mutants exhibited shorter GSC zones (average 11 cell diameters) compared to identically staged wild-type animals (average 18 cell

diameters; Figure 2-18G). Indeed, some *wdr-5.1* animals had GSC zones as short as 6 cell diameters (Figure 2-18G). The brood size of *wdr-5.1* mutants was also substantially lower than wild-type animals, even at normal temperatures (Figure 2-19A). These data suggest that the H3K4me2/3 marks in the GSC chromatin that are maintained by the WDR-5.1/RBBP-5 dependent mechanisms, or the proteins themselves, may be important for normal maintenance of this stem cell population.

**_wdr-5.1_ and _rbbp-5_ mutants display only partially overlapping somatic and germline developmental phenotypes**

We further characterized the phenotypes of *set-2, wdr-5.1* and *rbbp-5* mutants. *set-2(tm1630)* mutants do not display obvious phenotypes when grown at either 20°C or 25°C (Table 2-2), indicating that neither SET-2 or its H3K4me3 mark are overtly essential for normal development. At 20°C, *wdr-5.1* animals were fertile, but showed 12% embryo lethality (Emb) and a moderate egg laying defect (Egl) (Table 2-2 and Figure 2-20A). At 20°C, *rbbp-5(tm3465)* mutants exhibited multiple phenotypes including a Dumpy phenotype (Dpy), Egl, and significant sterility (24.4%; Table 2-2 and Figure 2-20A and B). The Dpy phenotype was not observed in *wdr-5.1(ok1417)* animals at any temperature, indicating that these factors may have non-overlapping roles in some somatic developmental pathways. The basis of the Dpy phenotype in *rbbp-5(tm3465)* animals, for which many candidate pathways exist, is unknown.

At elevated temperatures, *wdr-5.1(ok1417)* embryonic lethality rose dramatically to 29% for the 1$^{st}$ generation at 25°C, and a previously reported germline mortality phenotype in subsequent generations was also confirmed (Figure 2-19B and (Simonet et

al., 2007)). When grown at 25°C, the mutant exhibited an increased frequency of sterile progeny with each generation. By the F4 generation, 67% of the embryos developed into sterile adults. Interestingly, sterility reached a maximum by the F4 generation, although the number of offspring produced by the few fertile animals at subsequent generations was low (Figure 2-19B and not shown). When *rbbp-5* L4 larvae were shifted to 25°C, 12.1% of their F1 progeny arrested as embryos; however, most (82.9%) of the survivors developed into sterile adults (Table 2-2). The remainder appeared to be capable of producing sperm and oocytes: some embryos were observed in these animals *in utero*, yet these embryos were not laid onto the plates nor did they hatch.

In vertebrates, mutations in WDR5 and MLL cause developmental defects, presumably because of their reported roles in regulation of Hox gene expression (Byrd and Shearn, 2003; Wysocka et al., 2005). Because of the embryonic lethality we observed in *wdr-5.1* and *rbbp-5* mutants, we tested for defects in Hox gene expression. We examined the expression of the Hox loci *lin-39, ceh-13, mab-5 and egl-5* in *wdr-5.1* mutant embryos grown at 20°C by qRT-PCR. We found no significant alteration in the expression levels of these four genes in *wdr-5.1(ok1417)* compared to wild type embryos, suggesting that WDR-5.1 is not required for Hox gene expression at normal temperatures in *C. elegans* (data not shown).

### *wdr-5.1/WDR5* and *RBBP-5/RbBP5* mutants exhibit defects in germ cell development

To investigate the mechanism underlying the sterility of *wdr-5.1(ok1417)* and *rbbp-5(tm3463)* mutants, we dissected the gonads from sterile worms and stained with DAPI.

We found that 75.9% of the gonads in sterile *wdr-5.1(ok1417)* mutants grown at 25°C had endomitotic oocytes (Emo phenotype); i.e., unfertilized eggs had prematurely entered the cell cycle and engaged multiple rounds of replication in the absence of cytokinesis (Figure 2-21B and D; Class I). In addition, a small percentage of hermaphrodite gonads (5.1%) exhibited a Mog (masculinization of germline) phenotype in which only sperm were produced (Figures 2-21B and D; Class II). An additional 19% of sterile *wdr-5.1* mutant animals had germ cells with severely abnormal DNA morphology and many apparently polyploid nuclei. The cells within the gonads of these animals were disorganized; we observed what appeared to be spermatids in the mid-pachytene zone of some gonads (Figure 2-21B; Class III). Interestingly, 100% of the *rbbp-5(tm3463)* animals raised at 25°C were Emo and the other phenotypes were not observed (Figure 2-21C and D). The Emo phenotype in hermaphrodites can be caused by ovulation defects, which can result from either oocyte defects or defective sperm signaling spermatogenesis defects, leading to misregulated re-entry into the cell cycle (Harris et al., 2006). To test if the Emo phenotype in *wdr-5.1* and *rbbp-5* mutants was due to defective sperm in these animals, sterile *wdr-5.1* and *rbbp-5* animals grown at elevated temperature were mated with wild type males. We found that fertility could be at least partially rescued by WT sperm, suggesting that sperm defects contribute to the Emo phenotype in these animals (not shown).

## Discussion

Our data provide evidence that conserved Set1/MLL complex components regulate global H3K4 methylation in early embryos. We also show evidence that only a subset of

the canonical Set1/MLL components modulates H3K4 methylation in the post-embryonic germline stem cells of *C. elegans*. Assuming that, as in mammals and yeast, these components function in complexes, then there may be separate complexes that share WDR-5.1 and RBBP-5, with SET-2 as an H3K4me3-specific HMT. Interestingly, neither activity seems to be completely dependent on ongoing transcription, in contrast to the related COMPASS complex in yeast. Instead a separate, and as yet unidentified mechanism appears to provide transcription-coupled H3K4 methylation in *C. elegans*. The loss of Set1/MLL activities that require WDR-5 and RBBP-5 is detrimental to normal development, function, and generational maintenance of germ cells in *C. elegans*, illustrating the importance of this core complex in maintaining and regulating the germline cycle as it transits across generations. Furthermore, individual mutants in the different complex homologs exhibit different spectra of somatic and germline phenotypes, indicating that these proteins may also function in unique contexts in different tissues.

**H3K4 methylation is regulated by different complexes in different tissues and developmental stages.**

Set1 is the only identified H3K4 HMT in *S. cerevisiae* and is solely responsible for H3K4 methylation in this organism. The yeast Set1-associated complex (COMPASS) is composed of seven subunits: Swd1-3, Swd2, Swd1, Bre1, Sdc1, Spp1 and Shg1 (Dehe and Geli, 2006; Nagy et al., 2002; Roguev et al., 2003; Shilatifard, 2006). The Swd1 and Swd3 subunits are considered to be essential for complex stability and hence HMT activity. Sdc1 and Bre2 are required to stimulate transition from di- to trimethylation of

H3K4, while Spp1 plays a role in H3K4 trimethylation efficiency (Ng et al., 2003; Schneider et al., 2005; Steward et al., 2006).

The organization of the Set1/MLL complexes in metazoans seems to be different from that of COMPASS. There are multiple HMTs with non-redundant functions, and the different HMTs function in the context of slightly different complexes (Crawford and Hess, 2006; Dou et al., 2006; Dou et al., 2005; Hughes et al., 2004). Most, if not all, appear to share a common platform composed of WDR5, RbBP5 and ASH2L (Dou et al., 2006). This metazoan "core platform" is shared among different Set1/MLL complexes that differentially regulate H3K4 methylation in different tissues or developmental stages (Crawford and Hess, 2006; Dou et al., 2006; Ruthenburg et al., 2007).

All of the COMPASS and Set1/MLL components except Shg1 have orthologs in worms. We demonstrated that WDR-5.1, RBBP-5, ASH-2, CFP-1, and DPY-30 are all non-redundantly required for normal, global H3K4me2/3 maintenance in early embryos, strongly indicating that a complex that includes all of these factors is involved, although any individual complex could interact with either SET-2 and/or a different HMT (Figure 2-1). Interestingly, in the post-embryonic germ line only WDR-5.1/Swd3 and RBBP-5/Swd1 are essential for the normal maintenance of H3K4me2/3 in germline stem cells, while the other components appear to be dispensable.

Strikingly, we observed no significant requirement for ASH-2 for H3K4 methylation in adult germline stem cells, although ASH-2 is required in embryos and is the homolog of Ash2L, an essential member of the core complex in mammalian cells. This is inconsistent with a recent report that concluded that ASH-2 affects lifespan through regulation of H3K4 methylation in germ cells; however, a germ cell-specific

defect in H3K4me after *ash-2(RNAi)* was not directly shown in that study (Greer et al., 2010). Our results suggest that H3K4 methylation mechanism in the GSCs, if indeed it is operating within a complex, involves a complex with a unique, and potentially novel, subunit composition. Importantly, whereas H3K4me3 levels are nearly undetectable in *set-2, wdr-5.1*, and *rbbp-5* mutant GSCs, H3K4me2 loss was not as complete in the *wdr-5.1* and *rbbp-5* mutants, and unaffected in *set-2* mutants in early embryos and the adult GSCs. It is possible this represents a partial redundancy for a separate WDR5 isoform (e.g., WDR-5.2 and WDR-5.3), a more complex dynamics of the two levels of H3K4 methylation, or a role for another mechanism that is not dependent on WDR5 or RBBP-5.

Interestingly, in both embryos and post-embryonic germ cells, SET-2 is only required for H3K4me3 but not H3K4me2, while two core complex proteins, WDR-5.1 and RBBP-5, affect both modifications. This finding may indicate that H3K4me2 and H3K4me3 require distinct HMTs that rely on the same core complex containing at least WDR-5.1 and RBBP-5. Although we have not done an exhaustive combinatorial deletion/RNAi analysis of all SET protein candidates, it is interesting to note the reports showing that the core MLL complex in other species can exhibit H3K4 HMT activity in the absence of the MLL subunit (Patel et al., 2009). H3K4 dimethylation in early embryo and GSC chromatin could involve a complex that includes WDR-5.1 and RBBP-5, but may not include a SET domain protein.

Notably, WDR-5.1/RBBP-5-independent, and presumably transcription-coupled, H3K4 HMT activities are present in cells of mid-to-late stage embryos and meiotic germ cells, and at very low levels in early embryos and the GSCs. To attempt to identify the HMT involved, we also tested numerous SET domain candidates by RNAi in the *wdr-*

*5.1(ok1417)* mutant background, but did not observe any significant changes in H3K4 methylation (data not shown). A recent report concluded that SET-16 is an H3K4-specific HMT required for efficient attenuation of Ras signals in some somatic lineages, and reported a decrease in total H3K4me using Western blot analyses (Fisher et al., 2010). We did not observe significant H3K4me2/3 decreases by immunofluorescence in either early embryos or adult germ cells in *set-16(gk438)* mutants or *set-16(RNAi)*.

Notably, the transcription-dependent process and H3K4me1 levels in chromatin are both largely independent of Set1/MLL components. This could indicate that this activity is only capable of single methyl group transfers, and that the transcription-dependent H3K4me2 and H3K4me3 levels that we observe result from reiterative RNA Pol II initiation events at active loci. It will be interesting to determine what HMTs and/or complexes are responsible for WDR5/RBBP-5-independent H3K4 methylation.

**The Set1/MLL activities can operate independently of transcription in *C. elegans***

Yeast Set1 is recruited to chromatin through the RNA polymerase II elongation machinery. As a result, yeast Set1 HMT activity is dependent upon transcription activation, and H3K4 methylation is thus associated with transcribing genes (Briggs et al., 2001; Santos-Rosa et al., 2002). In contrast, our data indicate that Set1/MLL and WDR-5.1/RBBP-5 mediated H3K4 methylation may not strictly rely on active transcription in *C. elegans*. First, H3K4me2/3 is maintained by Set1/MLL components in early germline precursors, cells that have been shown to lack significant levels of active RNA Pol II transcription (Seydoux and Dunn, 1997). The H3K4me we observe in the P cell chromatin (and indeed chromatin in all blastomeres) is densely distributed throughout all

chromosomes (an exception being the paternal X (Bean et al., 2004)), and this distribution seems inconsistent with low levels of active transcription of a small number of genes. Second, although zygotic transcription of some genes can be detected in early somatic blastomeres (Seydoux and Fire, 1994), the genome appears to be also largely quiescent in these cells, and bulk zygotic genome activation is not thought to occur until later embryonic stages (Baugh et al., 2003). Indeed, H3K4 methylation in the early somatic blastomeres is also unaffected by *ama-1* and *cdk-9* RNAi indicating that the bulk of H3K4me is also maintained in a transcription-independent process in these cells. Third, whereas *ama-1* RNAi is able to deplete SET-2/WDR-5.1/RBBP-5 independent H3K4 methylation in meiotic nuclei, the H3K4 methylation in GSCs that depends on these proteins is untouched by substantial loss of AMA-1 activity. Fourth, the detection of H3K4me in chromatin is not a reliable indicator of productive transcription in *C. elegans* germ line, in which disrupted correlations between RNA Pol II activity, or signs thereof, and H3K4me regulation are apparent at multiple developmental stages. For example, the first appearance of phosphoSer2-modified RNA Pol II occurs at PGC birth, which antithetically coincides with a dramatic genome-wide erasure of H3K4me2 (Hajkova et al., 2008) .

We cannot rule out that the Set1/MLL components may also be capable of participating in transcription-coupled H3K4 methylation; indeed, there are slightly reduced H3K4me2 and H3K4me3 levels observed in meiotic germ cell chromatin in the *wdr-5.1* and *rbbp-5* mutants. This may indicate either an additional role for these proteins in transcription-dependent accumulation of these marks, or a requirement for WDR-5.1/RBBP-5 dependent marks to achieve normal levels of H3K4 methylation

during transcription (or normal transcription itself). Regardless, our evidence suggests these processes can operate independently in germ cells. A summary of the disconnected dynamics between RNA Pol II CTD phosphorylation and H3K4me3 in wild type and *wdr-5.1/rbbp-5* mutants through the germline cycle, summarizing from this study and published work, is illustrated in Figure 2-22.

In the L1 larva, there is an initial coincidence of active Pol II transcription activation and the WDR-5.1/RBBP-5/SET-2 independent mode of methylation in the expanding population of germ cells. Interestingly, once the GSC population becomes established from the founder PGCs, the mode of H3K4 methylation switches to what appears to be a largely transcription-independent or maintenance mode in the GSCs. A hypothetical reason for this switching of modes could be that the initial reactivation of transcription, and its accompanying transcription-dependent H3K4 methylation, could be used to re-establish a germ cell-specific "epigenome" that is then maintained in the GSCs by the WDR-5.1/RBBP-5 dependent mechanisms. This could be guided, in part, by other epigenetic marks, such as H3K36 and H3K27 methylation imposed by the *C. elegans* germ-cell enriched, PRC2 related MES-2/3/6 complex and the metazoan-specific H3K36 HMT MES-4, respectively (Bender et al., 2006). We have also found that H3K4me2 incorporated during post-embryonic germ cell development appears to contribute to the distribution of this mark in both gametes and subsequently in early embryos (J. Arico and W. Kelly, manuscript submitted). The overall pattern inherited by the embryo from the gametes is then maintained in a Set1/MLL component-dependent manner in early cell divisions (this study), thus completing the germline epigenome cycle.

The loss of WDR-5.1 or RBBP-5 leads to defects in germ cells that include an undetermined defect in sperm development, which contributes to the Emo phenotype. Mutations in these genes also lead to progressive germ cell defects in later generations (e.g., the observed temperature sensitive mortal germline defect). This indicates that successive passage of the genome through the compromised epigenetic environment of these mutants leads to progressive defects from successive failure, during multiple rounds of the germ cell cycle, to properly maintain the epigenome. The temperature dependence of these phenotypes is not unusual for germline processes; indeed, we have previously described a null mutation in the gene *emb-4* that yields a temperature-sensitive maternal effect embryonic lethality and that also shows defective H3K4 methylation dynamics in the PGCs (Checchi and Kelly, 2006). Importantly, we cannot rule out the functions for *wdr-5.1* and *rbbp-5* that might be independent of their role in the maintenance of H3K4 methylation, since the H3K4me defects in these mutants were present at both 20°C and 25°C while the phenotypes are far more severe at 25°C. This is an important question that we are currently addressing.

A recent report showed that mutations in *wdr-5.1, ash-2*, or *set-2* result in an increase in lifespan in *C. elegans* (Greer et al., 2010). In that study it was shown that the enhanced lifespan increase was not observed in animals that lacked GLP-1 function, a Notch receptor required to maintain the post-embryonic proliferating germline stem cell population. It was concluded that the germline function of the Set1/MLL complex contributes to its role in lifespan. Our results could imply that it is the GSC-specific role for this complex that may play a more direct role in lifespan. However, we did not observe a role for ASH-2 in either stem cell maintenance or H3K4 methylation in our

studies, whereas *ash-2* mutants were observed to have an extended lifespan. This may further indicate that these Set1/MLL components play roles that may not be tied to their function in H3K4 methylation.

It is becoming increasingly clear that epigenetic processes guide germline establishment and the trans-generational maintenance of this totipotent lineage in many, if not all, metazoans. Although there has been much focus on the role of erasure mechanisms during epigenetic reprogramming, there is also a requirement to establish and/or maintain epigenetic information that contributes to pluripotency. This is especially true in the germ line; the lineage that transports both the DNA and its epigenetic content across generations. Any changes or defects in establishment, maintenance, or selective erasure of the epigenetic content required during any stage of the germ cell cycle encounters the strong selective filter of fertility. Our results suggest that this filter acts through alternating cycles of transcription-dependent establishment and transcription-independent maintenance of histone methylation. We propose that these mechanisms help provide and maintain a germline-specific epigenome that contributes to the underlying basis of the totipotency of this lineage.

## Materials and Methods

### Worm Strains:

*C. elegans* strains were maintained using standard conditions at 20°C unless otherwise noted. N2 (Bristol) was used as the wild-type *C. elegans* strain. The following mutant strains were used in this study: *set-2(tm1630)III, wdr-5.1(ok1417)III, wdr-5.2(ok1444)X, rbbp-5(tm3463)II, set-16(gk438)III and eri-1(mg366)IV*. The *wdr-5.1::GFP* transgenic

strain was a generous gift from Dr. F. Palladino, Ecole Normale Superieure de lyon, France.

**RNAi analysis**

Double stranded RNA (dsRNA) corresponding to *set-2, wdr-5.1, rbbp-5, ash-2, dpy-30, cfp-1, wdr-82,* or *ama-1* were generated using the Ribomax Large Scale RNA production kit (Promega). L4 staged *eri-1(mg366)* or WT animals were soaked in 1ug/ul of dsRNA for 24 hours at 20°C. The worms were then transferred to feeding plates containing bacteria expressing dsRNA targeting the corresponding gene, or carrying the empty L4440 vector for control experiments. After the first 24 hours, the worms (P0) were transferred to a new set of feeding plates. The worms (P0) were dissected after 24-48 hours and stained as described below. In some experiments F1 animals and their F2 progeny were also analyzed in immunofluorescence experiments, and/or assessed for embryonic lethality and sterility. For *ama-1*, wild-type or mutant L4 larvae were picked and soaked in either 0.5ug/ul dsRNA in 1x soaking buffer, or buffer alone for 24 hours at 20°C. The worms were then transferred to feeding plates with bacteria expressing the same dsRNA. Worms were dissected, fixed and prepared for immunofluorescence analyses 50 hours post soaking.

**Immunofluorescence**

Worms were dissected and fixed in paraformaldehyde/methanol (Furuhashi et al., 2010) for H3K4me2/3, AMA-1, GFP, 8WG16 and SYP-1 staining. A methanol/acetone fixation procedure (Strome and Wood, 1983) was used for L1-L4 larvae staining. Samples were

fixed in methanol/formaldehyde for H5 staining as described (Furuhashi et al., 2010). Rabbit anti-H3K4me3 (1:1000) and anti-H3K4me1 polyclonal antibodies were purchased from Abcam (ab8580 and ab8895, respectively). Mouse monoclonal antibodies against H3K4me3 (CMA 304; 1:1000) and H3K4me2 (CMA303; 1:20) were gifts from Dr. Hiroshi Kimura (Osaka University, Japan (Kimura et al., 2008)). Mouse monoclonal antibody against GFP (MAB3580 1:500), Rabbit polyclonal (07-030 1:1000) and monoclonal (05790 1:1000) antibodies against H3K4me2 were purchased from Millipore. Monoclonal antibody OIC1D4 (1:5) and rabbit anti-PGL (1:10000**)** were gifts from Dr. S. Strome, UC Santa Cruz. The RNA polymerase II monoclonal antibodies used to detect AMA-1 protein (clone 8WG16 1:100) and phosphoserine 2 isotope of RNA Pol II (clone H5 1:50) were purchased from Covance (MMS-126R and MMS-129R, respectively). Rabbit anti-SYP-1 (1:100) was a gift of Dr. A. Villeneuve, Stanford University. All secondary antibodies were purchased from Molecular Probes and were used at 1:500 dilutions: goat anti-mouse IgG (Alexafluor 488); goat anti-rabbit IgG (Alexafluor 594), donkey anti-rabbit IgG (Alexafluor 488); donkey anti-mouse IgG (Alexafluor 594). DAPI (Sigma, 2ug/ul) was used to counter-stain DNA. Worms were mounted in anti-fade reagent (Prolong Gold, Molecular Probes). Images were collected using a Leica DMRXA fluorescence microscope and analyzed with Simple PCI software (Hamamatsu Photonics). To quantify the immunofluorescence signals, the mean fluorescence intensity was measured for middle focal plane images of each nucleus from Z-stack images collected for each sample. For all compared samples, the exposure time for each probe was set below image saturation for the brightest nucleus among the samples being compared. The antibody signals were normalized to DAPI.

**Western Blot Analysis**

Worms were washed from OP50 plates and bleached to collect embryos. To remove egg shells, the embryos were subsequently treated with 1U/ml chitinase (Sigma, C6137) in egg buffer (25mM HEPES pH7.4, 118mM NaCl, 48mM KCl, 2mM $MgSO_4$, 2mM $CaCl_2$) at 20°C for 40 min, and were boiled in 1X SDS-PAGE sample buffer. The samples were loaded and run on a 15% SDS-PAGE gel and transferred to PVDF membrane. The proteins were probed with the following antibodies: rabbit polyclonal anti-H3 at 1:10,000 (Abcam ab1791), rabbit polyclonal anti-H3K4me3 at 1:3,000 (ab8580), mouse monoclonal anti-H3K4me2 at 1:100 (gift from Dr. Hiroshi Kimura, Osaka University, Japan), rabbit polyclonal anti-H3K4me1 at 1:1000 (ab8895).

**Peptide Pulldown Assays**

Biotinylated peptides corresponding to the N-terminus of histone H3 were used for peptide affinity analyses of WDR-5.1 in worm nuclear extracts. Biotinylated H3 (unmodified) and H3 (dimethyl-Lys4) peptides were purchased from Millipore (Cat#12-403 and 12-460, respectively). Biotin conjugated H3 peptides asymmetrically dimethylated at Arg2 (H3R2me2a) were synthesized by the Keck Biotechnology Resource at Yale University. For the binding assay, mixed-stage WT worms were washed off plates with PBS, washed 3X in PBS with protease inhibitor cocktail (Roche), and the worms were frozen at -80°C. To isolate the nuclei, the worm pellet was thawed and ground by mortar and pestle in 2x volume of Nuclear Isolation Buffer (NIB; 25mM HEPES (pH7.5), 25mM KCl, 0.1mM EDTA, 0.1mM DTT, 10mM $MgCl_2$ and 0.5M

sucrose) in liquid nitrogen. The samples were then transferred to a homogenizer in NIB buffer and stroked 20 times on ice. Nuclei were collected by centrifugation. Nuclear proteins were extracted in Nuclear Extract Buffer (NEB 20 mM HEPES (pH7.5), 2mM EDTA, 25% glycerol and 0.1% NP-40) with 350mM KCl. Prior to pulldown, the nuclear extracts were diluted with NEB buffer without KCl to obtain a solution with 150mM KCl. The peptide pull down assay was performed according to Wysocka, et al (Wysocka, 2006). Briefly, the extracts were incubated with peptides pre-bound to avidin beads overnight at 4°C. After washing with HEPES buffer containing 150mM KCl for 3 times, the beads were then boiled in 1X SDS buffer and subjected to western blot analysis for WDR-5.1 detection. The WDR-5.1 rabbit polyclonal antibody was generated by immunizing with the last 15 C-terminal peptides of WDR-5.1 (Pickcell Laboratories, The Netherlands). Anti-WDR-5.1 antibodies were affinity purified on Affi-Gel 15 columns (Bio-Rad Laboratories).

**Temperature Sensitive (ts) Phenotypic Analysis**

WT and mutant L4 worms (P0) were picked and shifted to 25°C. F1 embryos were counted to score embryonic lethality. To score sterility, 100 L1 larvae of F1s grown at 25°C were picked onto separate plates pre-warmed to 25°C. Sterile adult F1 animals were counted 24 hours post L4 based on the lack of embryos in uterus. The sterile animals were dissected to extrude gonads. The samples were stained with anti-SYP-1 antibody and counter stained with DAPI. The images were collected on a Leica DMRA microscope. The length of mitotic regions (MR) were measured based on the crescent

nuclei morphology of transition zone and SYP-1 staining. The number of nuclei on one focus plane of DAPI images was used to reflect the length of mitotic zone.

**Brood Size and Mortal Germline Assay**

10 L4 worms were picked and incubate at 20°C or 25°C. F1 embryos were counted for brood size. To score sterility, 100 L1 larvae of F1 from 20°C or 25°C plates were picked onto a new set of plates and kept at the corresponding temperatures. Sterile adult F1 animals were counted based on the lack of embryos *in utero*.

**Table 2-1**
Conserved components of COMPASS complex in *C. elegans*

| *S. cerevisiae* | Human | *C. elegans* | *C. elegans** |
|---|---|---|---|
| *set1* | SET1<br>MLL1<br>MLL2<br>MLL3 | C26E6.9<br>T12D8.1 | *set-2*<br>*set-16* |
| *bre2* | Ash2L | Y17G7B.2 | *ash-2* |
| *swd1* | RbBP5 | F21H12.1 | *rbbp-5* |
| *swd3* | WDR5 | C14B1.4<br>K04G11.4<br>ZC302.2 | *wdr-5.1*<br>*wdr-5.2*<br>*wdr-5.3* |
| *spp1* | CxxC1/<br>Cfp-1 | F52B11.1 | *cfp-1* |
| *swd2* | WDR82 | C33H5.6 | *wdr-82* |
| *sdc1* | hDPY30 | ZK863.6 | *dpy-30* |
| *shg1* | | None | |

* Nomenclature used in text and figures; modified from simonet et al. 2008

**Table 2-2**
Phenotypic analysis of the HMTase core complex component mutants

| | Embryo Lethality | | Sterility | |
|---|---|---|---|---|
| | 20°C | 25°C | 20°C | 25°C |
| WT | 0.6% (n=619) | 2.7% (n=1509) | 0 (n=114) | 0.75% (n=133) |
| *set-2 (tm1630)* | 0.5% (n=871) | 11.5% (n=893) | 0.8% (n=114) | 1.9% (n=104) |
| *wdr-5.1 (ok1417)* | 12% (n=1201) | 36% (n=557) | 2.5% (n=119) | 29% (n=89) |
| *rbbp-5 (e1834)* | 3.18% (n=345) | 12.1% (n=173) | 24.4% (n=104) | 82.9% (n=88)* |

* 82.9% had no embryos; 17.1% exhibited dead embryos in *utero*.

**Figure 2-1. Knockdown of *set-16* does not affect H3K4me3 in adult germ cells**

L4 larvae of *eri-1(mg366)* were soaked in *set-16* dsRNA, or 1x soaking buffer in control samples for 24 hours at 20°C and recovered on feeding plates with HT115 expressing *set-16* dsRNA. F1 animals were continuously exposed to RNAi feeding during subsequent growth. Dissected and whole-mount fixed gonads from F1 adult animals were stained with H3K4me3 antibodies and counter-stained with DAPI. Exposure times were the same for each condition. Bars=10um. (A, B, E and F) H3K4me3 in the germ cell nuclei of distal region of gonad was not affected by knockdown of *set-16*. Gonads were displayed with the distal regions to the left. (C, D, G and H) H3K4me3 in meiotic germ cells was not significantly decreased in *set-16* RNAi knockdown. (I) Graph of anti-H3K4me3 signal from fluorescence microscopy of adult germ cell nuclei. Qualification was done as in Figure 2-9. Anti-H3K4me3 signals (arbitrary units ± SEM) were normalized to RNAi control mitotic region nuclei.

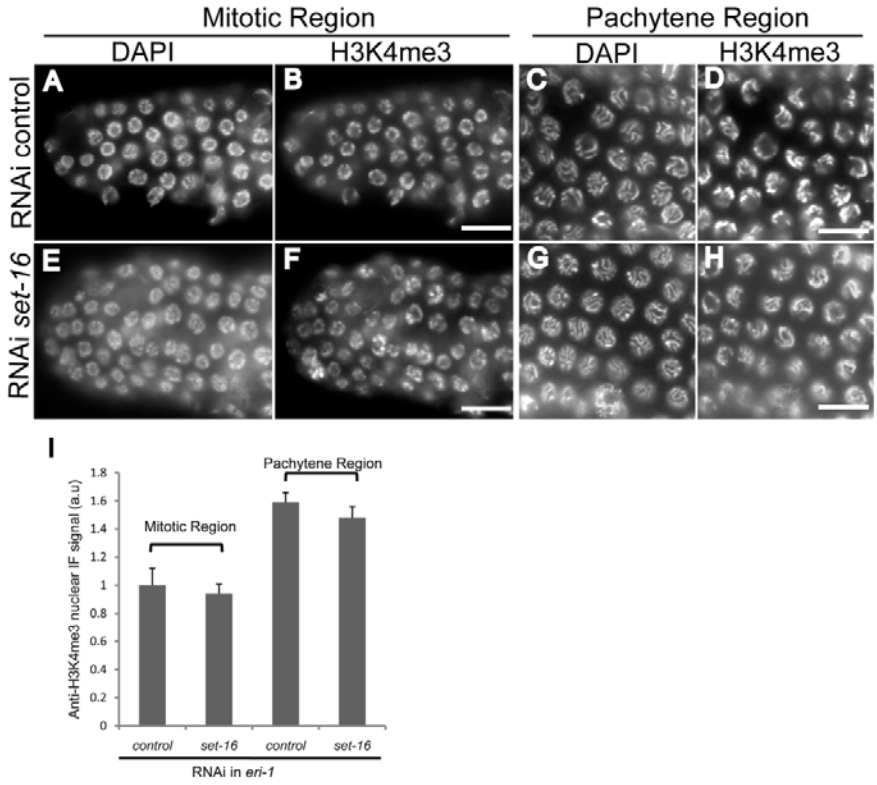
Mitotic Region
Pachytene Region
DAPI
H3K4me3
DAPI
H3K4me3
RNAi control
RNAi set-16
A
B
C
D
E
F
G
H
I
Anti-H3K4me3 nuclear IF signal (a.u.)
Mitotic Region
Pachytene Region
control
set-16
control
set-16
RNAi in eri-1

**Figure 2-2. Set1/MLL complex components are largely responsible for H3K4me2/3 in embryos**

Embryos were dissected from WT, mutant, or RNAi treated adult *eri-1* (*mg366)* enhanced RNAi animals. RNAi mediated knockdown was used for *ash-2, dpy-30, cfp-1 and wdr-82*. Embryos were probed with rabbit anti-H3K4me3 (Panels in A) or mouse anti-H3K4me2 monoclonal antibodies (Panels in B); DNA was counter-stained with DAPI. Exposure times were the same for each condition. Scale bars represent 10um. (A and B) H3K4me3 and H3K4me2 are present in chromatin of wild-type embryos, but both are dramatically decreased in chromatin of embryos from *wdr-5.1/wdr-5* and *rbbp-5/swd-1* mutants and *ash2, dpy-30, cfp-1* embryos from RNAi treated mothers. H3K4me3, but not H3K4me2, is reduced in *set-2(tm1630)* mutant embryos. RNAi mediated knockdown of *wdr-82* did not affect either H3K4me3 or H3K4me2. (C) A *wdr-5.1::GFP* transgene rescues H3K4 methylation in the *wdr-5.1(ok1417)* mutant. *wdr-5.1(ok1417);wdr-5.1::wdr-5.1-GFP* embryos were probed with antibodies against GFP and H3K4me3/2 as indicated. H3K4me3/2 were restored in the chromatin of early embryos in which WDR-5.1:GFP expression was detected. (D) Western blot of mixed stage embryo lysates from *wdr-5.1(ok1417), wdr-5.2(ok1444), wdr-5.1;wdr-5.2* double mutant, *set-1(tm1630)* mutant strains. The blots were probed with anti-histone H3, anti-H3K4me1, mouse anti-H3K4me2 or rabbit anti-H3K4me3 antibodies, as indicated. H3K4me3/2 levels were dramatically decreased in strains with the *wdr-5.1(ok1417)* allele, whereas H3K4me3 levels were more strongly depleted than H3K4me2 in *set-2(tm1630)*. H3K4me1 levels were not noticeably affected in any mutant strain tested.

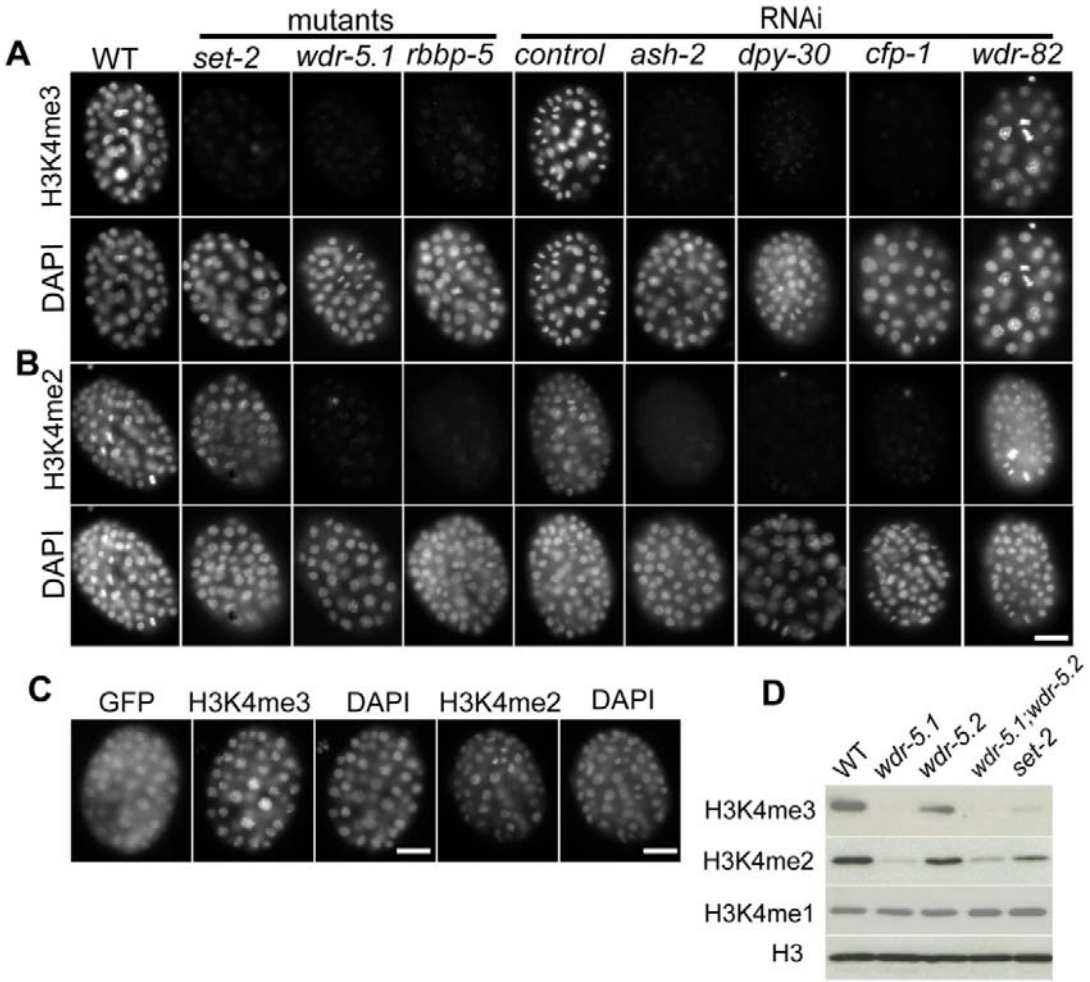
A
mutants
RNAi
WT
set-2
wdr-5.1
rbbp-5
control
ash-2
dpy-30
cfp-1
wdr-82
H3K4me3
DAPI
B
H3K4me2
DAPI
C
GFP
H3K4me3
DAPI
H3K4me2
DAPI
D
WT
wdr-5.1
wdr-5.2
wdr-5.1;wdr-5.2
set-2
H3K4me3
H3K4me2
H3K4me1
H3

**Figure 2-3. *wdr-5.1 (ok1417)* is a null mutant**

Lysates from mixed stage wild type and *wdr-5.1 (ok1417)* populations were analyzed by Western blot using an affinity-purified anti-WDR-5.1 polyclonal antibody. A band corresponding to the predicted MW of WDR-5.1 was present in wild type but absent in *wdr-5.1 (ok1417)* mutant. This antibody detected a non-specific band at about 80 kDa.

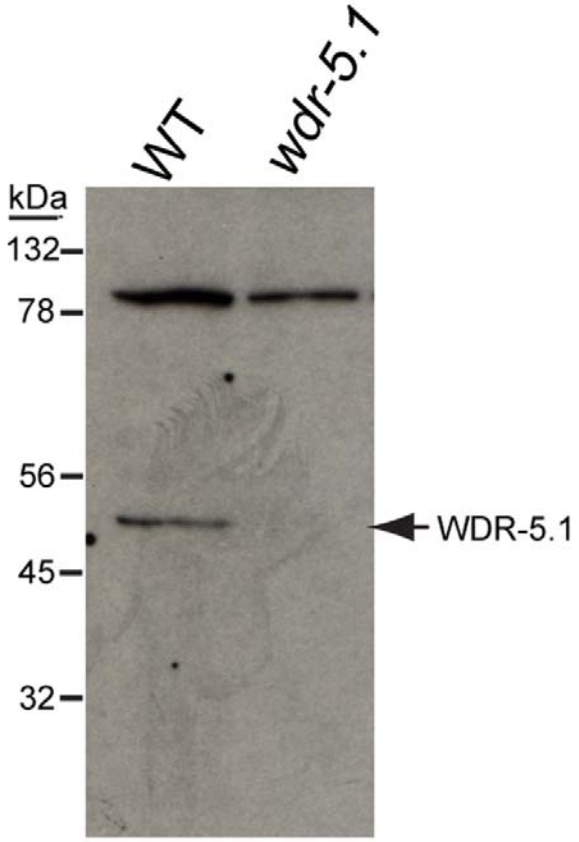
WT
wdr-5.1
kDa
132
78
56
45
32
WDR-5.1

**Figure 2-4. Set1/MLL-independent H3K4 methylation exists in later stages of embryogenesis**

Comma- stage to 1 ½-fold stage embryos from wild-type, *wdr-5.1(ok1417),* and *rbbp-5(tm3463)* animals, or *eri-1(mg366)* animals treated with either control RNAi or *ash-2(RNAi)* were fixed and stained for H3K4me2 or H3K4me3 (as indicated), and counter stained with DAPI. Arrows indicate nuclei with significant levels of H3K4me2/3 despite loss of the indicated Set1/MLL components. Scale bars = 10um.

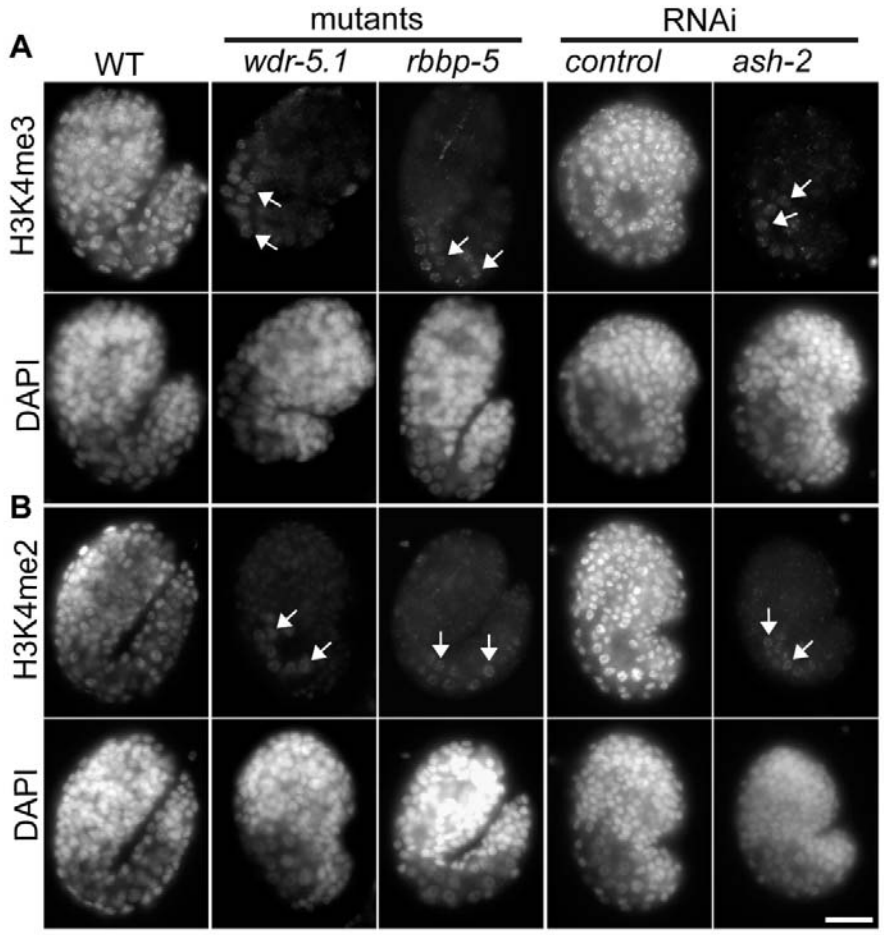
A
WT
mutants
wdr-5.1
rbbp-5
RNAi
control
ash-2
H3K4me3
DAPI
B
H3K4me2
DAPI

**Figure 2-5. WDR-5.1 interacts with H3 peptides**

Nuclear extracts from WT (N2) were incubated with biotinylated histone H3 N-terminal peptides either unmodified on K4 (H3K4me0), dimethylated on K4 (H3K4me2), or unmodified on K4 and asymmetrically dimethylated on R2 (H3R2me2a). The peptides were pulled down by avidin beads, washed, and bound proteins eluted with SDS sample buffer and then analyzed by Western blot using anti-WDR-5.1 antibodies. Total lysate (5% input) was included as control to identify WDR-5.1, which was identified as a single band with the expected mobility. This protein showed interaction with the H3K4me0 and H3K4me2 peptides, but no interaction with the H3R2me2a was observed. A control in which no peptide was added to the lysate prior to avidin bead affinity purification is also shown (Avidin lane).

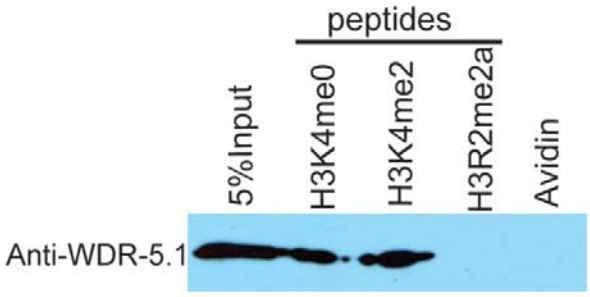
peptides
5%Input
H3K4me0
H3K4me2
H3R2me2a
Avidin
Anti-WDR-5.1

**Figure 2-6. Embryonic cells that lack RNA Pol II activity require WDR-5.1 for H3K4 methylation maintenance**

Embryos from wild-type and *wdr-5.1(ok1417)* animals were probed with mouse monoclonal antibody to H3K4me2 (A, B) or rabbit polyclonal antibody to H3K4me3 (C,D) in green, and anti-PGL-1 or mouse monoclonal antibody OIC1D4 to mark the germline precursors, P1-P4 (blue), and counterstained with DAPI (red). P-blastomeres are boxed and enlarged grayscale images are shown in insets with arrows marking chromatin stained for H3K4me2/3 as indicated. Arrowheads mark out-of-focus polar bodies, which retain oocyte chromatin and associated modifications. Images were taken of each sample with identical exposure times for each respective probe for comparison. mRNA production does not occur in wild-type germline P-blastomeres, yet H3K4me2 levels remain relatively constant in P1-P4 in these nuclei (A). H3K4me3, in contrast, significantly declines at P4 (C). All H3K4me2 and H3K4me3 methylation in both the P-blastomeres and early somatic blastomeres is dependent on WDR-5.1 function. Bar=10um. (E and F) Quantitation of anti-H3K4me2/ me3 signals in the P cell nuclei. The mean anti H3K4me2/3 IF intensity in single nucleus was measured using Simple PCI software and was normalized to DAPI. Normalized signals were compared to those of wild type P1 nuclei which were arbitrarily set to 1. 3-5 nuclei in similar states of chromatin condensation, from each P-cell stage (P1-P4), were used for measurement in each experiment. The graph represents results from 3 independent experiments. a.u.= arbitrary units. Error bars= SEM.

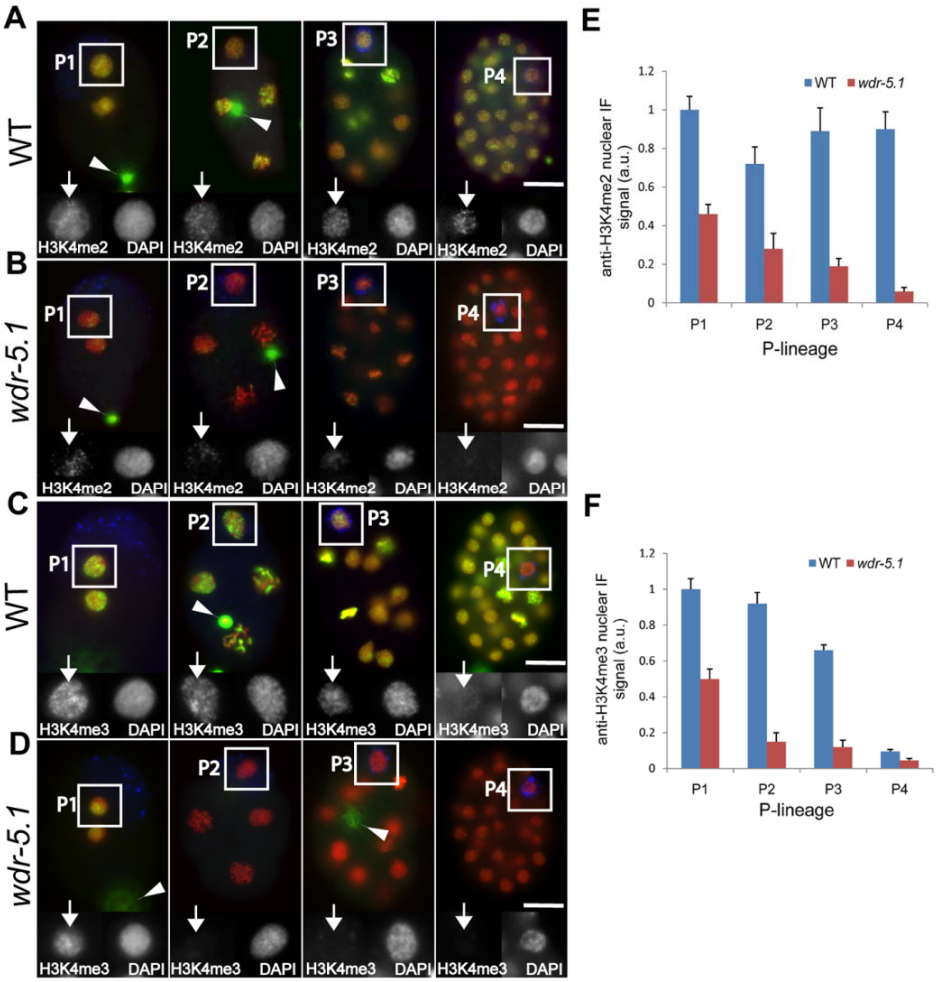
A
WT
P1
P2
P3
P4
H3K4me2
DAPI
B
wdr-5.1
C
WT
H3K4me3
D
wdr-5.1
E
WT
wdr-5.1
anti-H3K4me2 nuclear IF signal (a.u.)
P-lineage
F
anti-H3K4me3 nuclear IF signal (a.u.)

**Figure 2-7. RNAi knock-down of *ama-1* does not affect WDR-5.1-dependent H3K4 methylation in early embryos**

L4 larvae of WT and *wdr-5.1* animals were soaked in dsRNA targeting the large subunit of RNA Pol II (encoded by *ama-1*), or 1x soaking buffer in control samples as described in Materials and Methods, and their embryos were fixed and probed with either 8WG16 (AMA-1 protein) or mouse monoclonal antibodies against H3K4me2/3 as indicated. For each antibody staining, exposure times were determined by autoexposure of an interphase nucleus of control WT embryos and were used to take pictures for comparison. (A) Substantial AMA-1 depletion was achieved in all embryos, but H3K4me2/3 was not substantially affected in wild-type. (B) *ama-1(RNAi)*-resistant H3K4 methylation was absent in both control and *ama-1(RNAi)* treated *wdr-5.1(ok1417)* embryos. Bar=10um. (C) Quantitation of anti-AMA-1, H3K4me2 or me3 signals in the embryo nuclei. Individual interphase nuclei were chosen and the mean IF signal intensity of anti-H3K4me3 or H3K4me2 at mid-nucleus focal planes was measured. 5 nuclei from each of 3 embryos at similar stages were measured and analyzed as in Figure 2-6. Anti-AMA-1, H3K4me3 and H3K4me2 signals (arbitrary units ± SEM) were normalized to DAPI. Normalized signals were compared to those of wild type (RNAi control) which were arbitrarily set to 1. The graph represents results from 2 independent experiments.

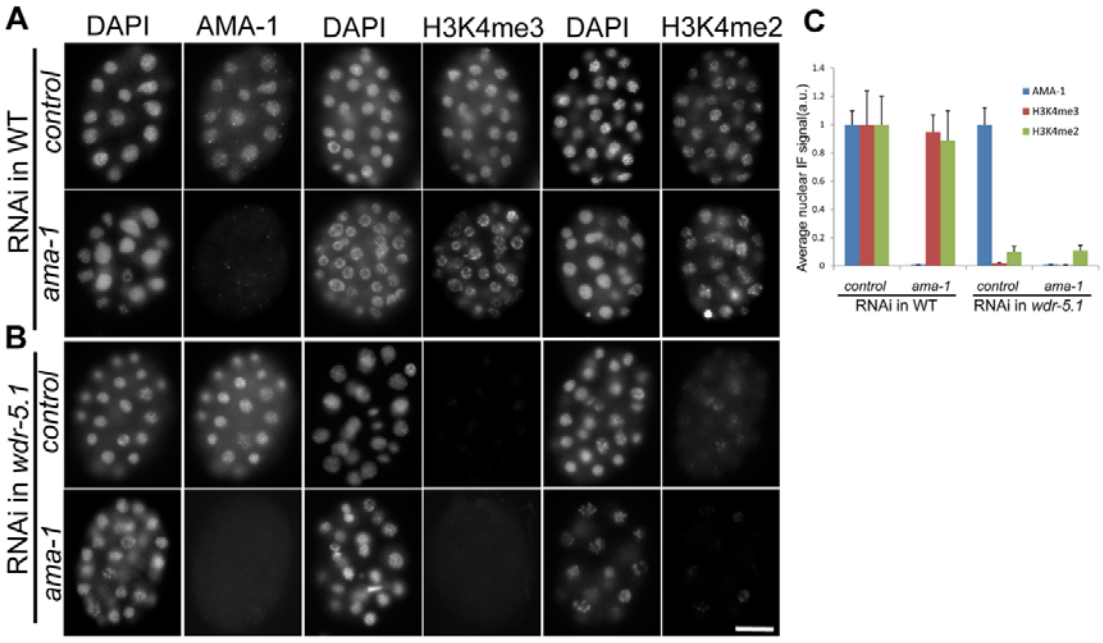
A
DAPI
AMA-1
DAPI
H3K4me3
DAPI
H3K4me2
RNAi in WT
control
ama-1
B
RNAi in wdr-5.1
control
ama-1
C
Average nuclear IF signal(a.u.)
AMA-1
H3K4me3
H3K4me2
control
ama-1
control
ama-1
RNAi in WT
RNAi in wdr-5.1

**Figure 2-8. *ama-1(RNAi)* depletion of Pol II phospho-Ser2 in embryos**

RNAi experiments targeting *ama-1* were done as in Figure 2-7. The embryos were fixed and stained with either monoclonal antibody (mAb) H5 for phospho-Ser2 epitope or mouse monoclonal antibodies against H3K4me3 as indicated. Exposure times were the same for each antibody for comparison. Bars=10um. (A) RNAi of *ama-1* depletes the mAb H5 signal to undetectable levels in both WT and *wdr-5.1*. (B) H3K4me3 dependent on *wdr-5.1* is not significantly affected by loss of *ama-1*/phospho-Ser2. (C) RNAi of *cdk-9* also depletes the mAb H5 signal to undetectable levels in WT. H3K4me3 is also not affected in these conditions.

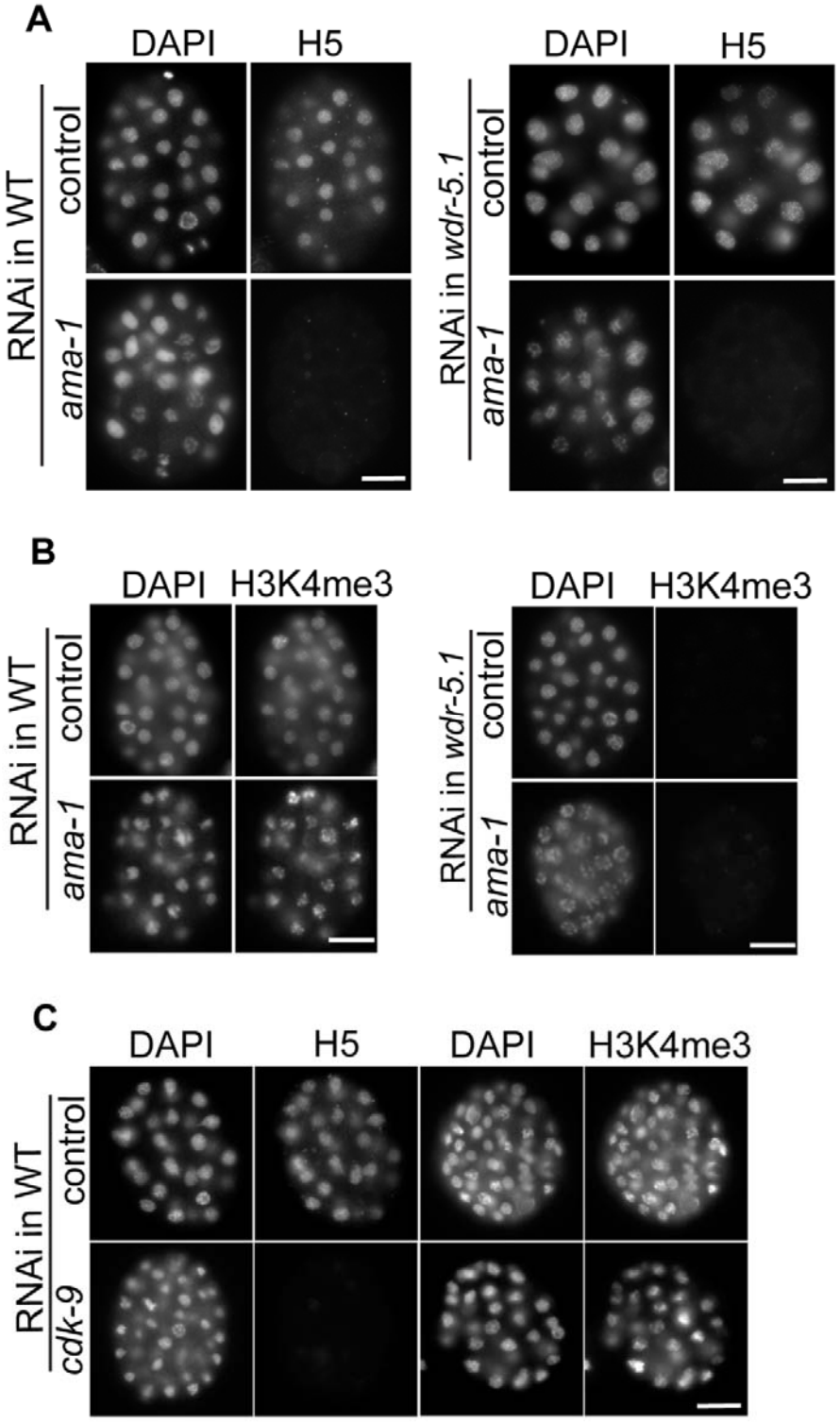
A
DAPI
H5
DAPI
H5
RNAi in WT
control
ama-1
RNAi in wdr-5.1
control
ama-1
B
DAPI
H3K4me3
DAPI
H3K4me3
RNAi in WT
control
ama-1
RNAi in wdr-5.1
control
ama-1
C
DAPI
H5
DAPI
H3K4me3
RNAi in WT
control
cdk-9

**Figure 2-9. H3K4me3 in adult germ cells is regulated by a subset of Set1/MLL complex components**

Dissected and fixed whole-mount adult gonads were probed with rabbit H3K4me3 antibodies and counter-stained with DAPI. Exposure times were the same for each condition. Gonads are displayed with the distal regions to the left; dashed lines in magnified views in A'-D' indicate where transition zone (transition from mitosis to meiosis) begins in each gonad. Images were taken with identical exposures for each probe and at the same magnification for comparison. Brackets highlight the region where nuclei were chosen for quantification (I). Scale bars represent 20um. (A-D) Wild-type (WT; N2) or indicated mutant strains; (E-H) *eri-1(mg366)* animals treated with control RNAi or RNAi targeting the indicated genes. H3K4me3 is present in the chromatin of all germ cell stages in wild-type animals, but is substantially decreased in nuclei of the distal mitotic germline stem cells (GSCs) in *set-2(tm1630), wdr-5.1(ok1417), and rbbp-5(tm3463)* mutants. In contrast, RNAi knockdown of *ash-2, dpy-30,* or *cfp-1* in *eri-1(mg366)* did not significantly affect H3K4me3 levels. (I) Quantitation of anti-H3K4me3 signals in distal nuclei randomly chosen from the region marked by brackets. The mean IF intensity in single nuclei was measured using Simple PCI software. 20-25 nuclei were measured from 3-5 gonads (4-5 nuclei/gonad) H3K4me3 signals (arbitrary units ± SEM) were normalized to DAPI. Normalized signals were compared to those of wild type or RNAi control which were arbitrarily set to 1. The graph represents results from 2 independent experiments.

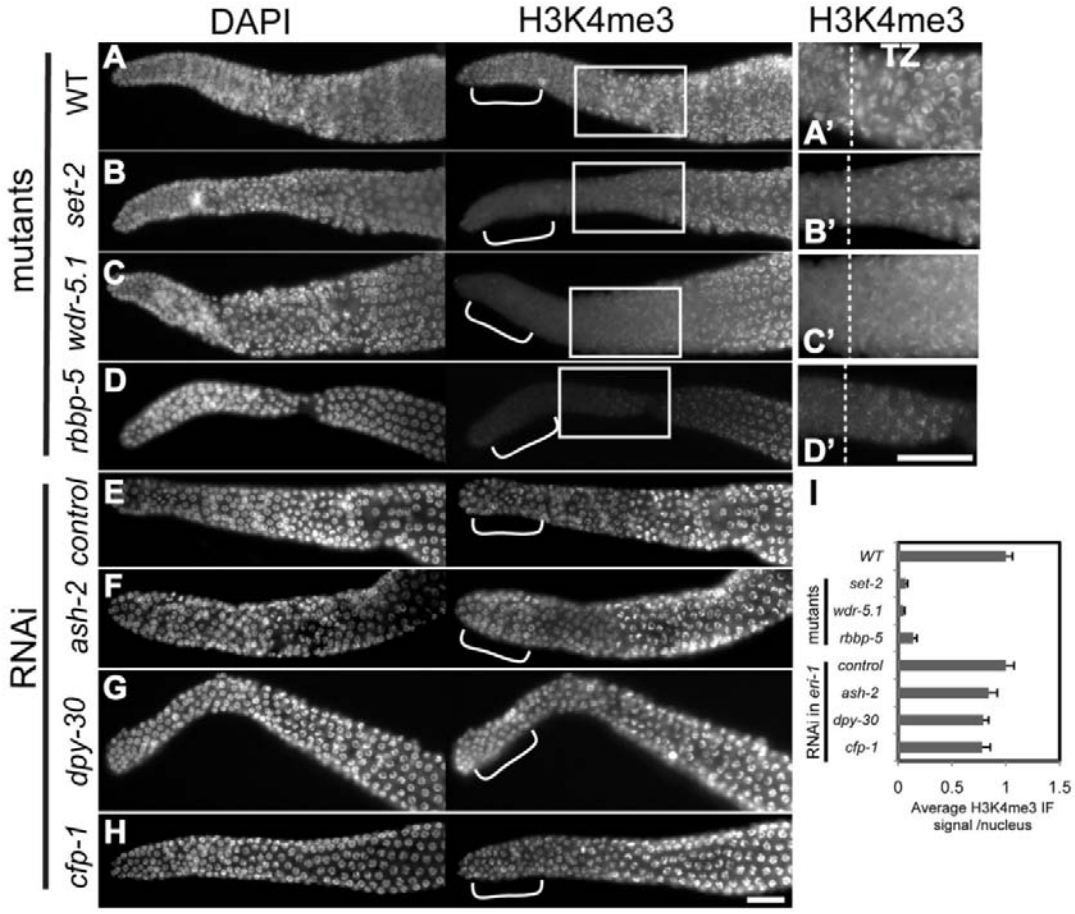
DAPI
H3K4me3
H3K4me3
TZ
mutants
WT
set-2
wdr-5.1
rbbp-5
RNAi
control
ash-2
dpy-30
cfp-1
A
A'
B
B'
C
C'
D
D'
E
F
G
H
I
WT
set-2
wdr-5.1
rbbp-5
mutants
control
ash-2
dpy-30
cfp-1
RNAi in eri-1
0
0.5
1
1.5
Average H3K4me3 IF signal /nucleus

**Figure 2-10. H3K4me2 in adult germ cells is also regulated by a subset of Set1/MLL complex components**

Experiments and data presented as in Figure 2-6. Samples were probed with mouse monoclonal antibody against H3K4me2 (CMA303). H3K4me2 is substantially reduced in *swd-3(ok1417)* and *rbbp-5(tm3463)* mutant germ cells within brackets (A-D), but appears unaffected in either *set-2(tm1630)* mutants, or *eri-1(mg366)* animals treated with RNAi as indicated (E-H). Bars represent 20um. (I) Quantitation of anti-H3K4me2 signals in distal nuclei randomly chosen from the region marked by brackets. The quantitation was done as in Figure 2-9. H3K4me2 signals (arbitrary units ± SEM) were normalized to wild-type germ cell nuclei. The graph represents results from 2 independent experiments.

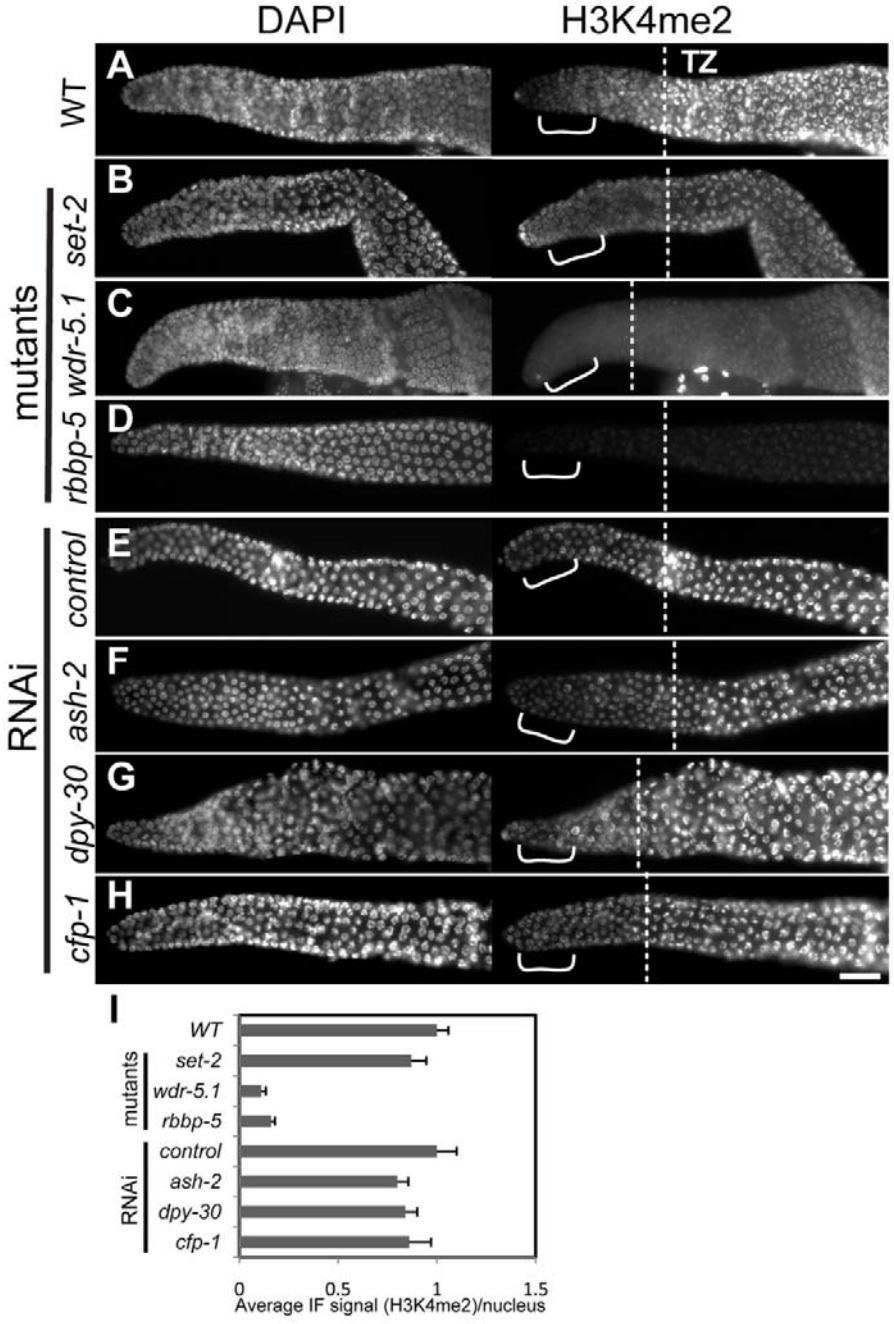
DAPI
H3K4me2
TZ
A
WT
B
set-2
C
wdr-5.1
D
rbbp-5
mutants
E
control
F
ash-2
G
dpy-30
H
cfp-1
RNAi
I
WT
set-2
wdr-5.1
rbbp-5
control
ash-2
dpy-30
cfp-1
mutants
RNAi
0
0.5
1
1.5
Average IF signal (H3K4me2)/nucleus

**Figure 2-11. H3K4me3 and H3K4me2 are decreased in *wdr-5.1 (ok1417)* male GSCs**

Experiments were performed as in Figure 2-9. (A) H3K4me3 is depleted from the distal region of gonad in *swd-3(ok1417)* mutant males. (B) H3K4me2 is substantially reduced in *swd-3(ok1417)* male germ cells. Bar= 20um.

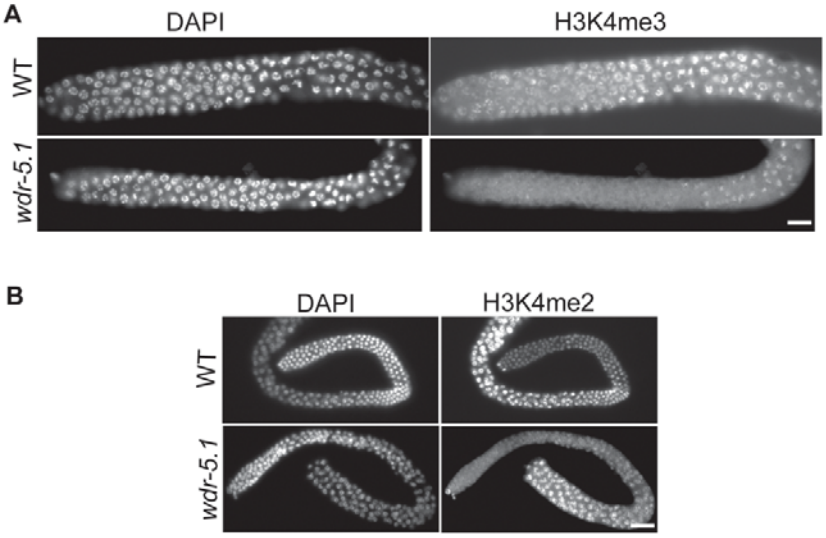
A
DAPI
H3K4me3
WT
wdr-5.1
B
DAPI
H3K4me2
WT
wdr-5.1

**Figure 2-12. Schematic of RNAi protocol used to target Set1/MLL complex component homologues**

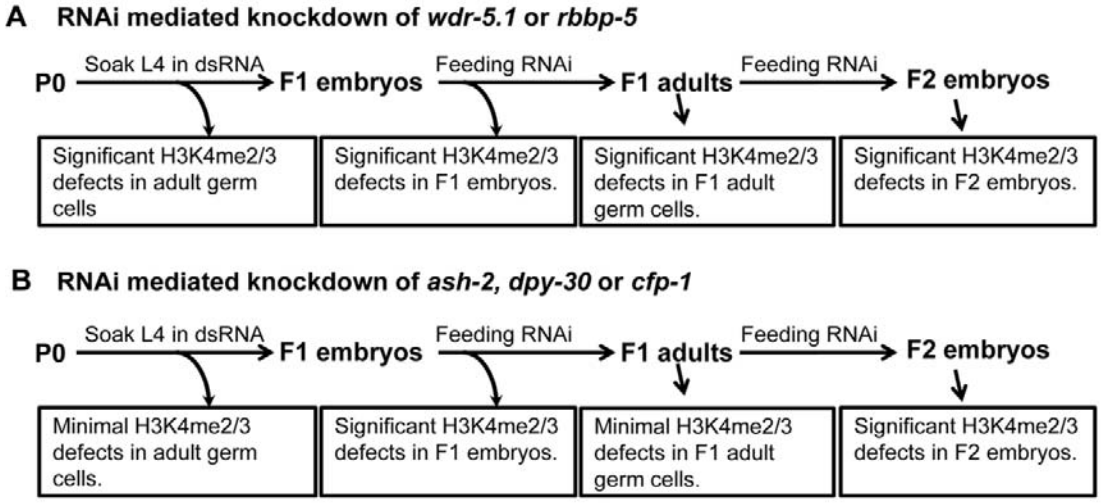

**Figure 2-13. H3K4me3 levels are reduced in all adult germ cell stages in *wdr-5.1* mutant gonad**

Dissected and whole-mount fixed gonads from wild-type (A, A') and *wdr-5.1(ok1417)* (B, B') adult hermaphrodites were probed with antibodies to H3K4me3 (A' and B') and counterstained with DAPI (A and B). Gonad arms are displayed with the distal regions to the left. Images were taken with identical exposure time for comparison. As in Figure 2-9, H3K4me3 is most strongly depleted from the chromatin of mitotic germ cells; however, significant decreases were also observed in more proximal pachytene and diakinesis regions. Bars=10 um. (C) Quantitation of anti-H3K4me3 IF signal in individual pachytene and diakinetic nuclei of wild-type and *wdr-5.1(ok1417)* nuclei. Mean IF signal of anti-H3K4me3 signal in single nuclei were measured and analyzed as in Figure 2-9. For qualification in pachytene, 20 nuclei from 4 gonads (5 nuclei/gonad) were measured and analyzed. For qualification of diakinetic nuclei, 12 nuclei from 4 gonads (3 nuclei/gonad) were measured and analyzed. Signals were compared to those in wild type nuclei which were arbitrarily set to 1. Error bars=SEM.

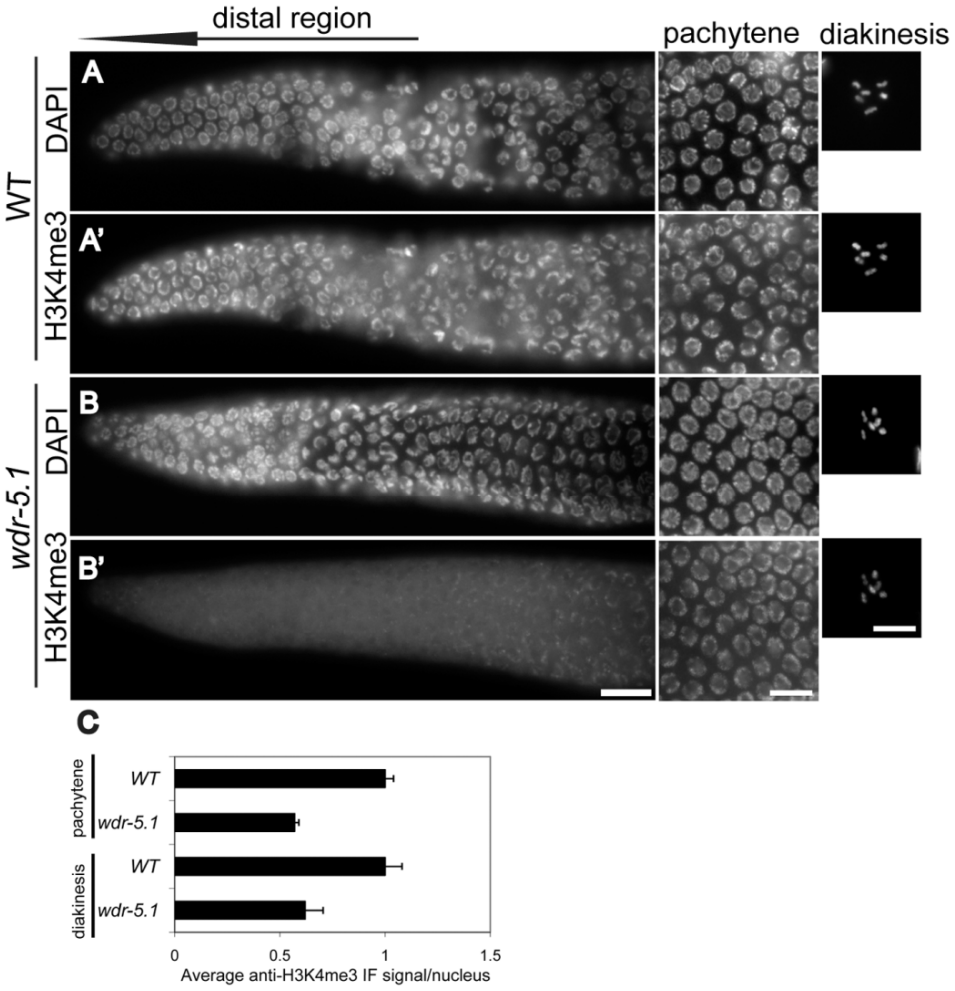
distal region
pachytene
diakinesis
WT
DAPI
A
H3K4me3
A'
wdr-5.1
DAPI
B
H3K4me3
B'
C
pachytene
WT
wdr-5.1
diakinesis
WT
wdr-5.1
0
0.5
1
1.5
Average anti-H3K4me3 IF signal/nucleus

**Figure 2-14. H3K4me2 levels are reduced in all adult germ cell stages in *wdr-5.1* mutant gonads**

The gonads of wild type and *wdr-5.1 (ok1417)* were probed with a mouse monoclonal antibody specific for H3K4me2 (mAb CMA303). The experiment was performed as in Figure 2-10. Images in (A) and (B) were taken with identical exposure time for each probe and at the same magnification for comparison. (A) H3K4me2 was present in all the nuclei of gonad in wild type. (B) H3K4me2 was significantly decreased, but not totally depleted in *wdr-5.1 (ok1417)* mutant. (C) The remaining, low level of H3K4me2 in the *wdr-5.1* GSCs exhibits a striking speckled pattern on the chromatin when observed with longer exposure times than that of the wild type image shown. Bars=10 um. (D) Quantitation of anti-H3K4me2 IF signal in individual pachytene and diakinetic nuclei of wild-type and *wdr-5.1(ok1417)* nuclei. Data was collected and analyzed as in Figure 2-13. For qualification in pachytene, 20 nuclei from 4 gonads (5 nuclei/gonad) were measured and analyzed. For qualification of diakinetic nuclei, 12 nuclei from 4 gonads (3 nuclei/gonad) were measured and analyzed. Signals were compared to those in wild type nuclei which were arbitrarily set to 1. Error bars=SEM.

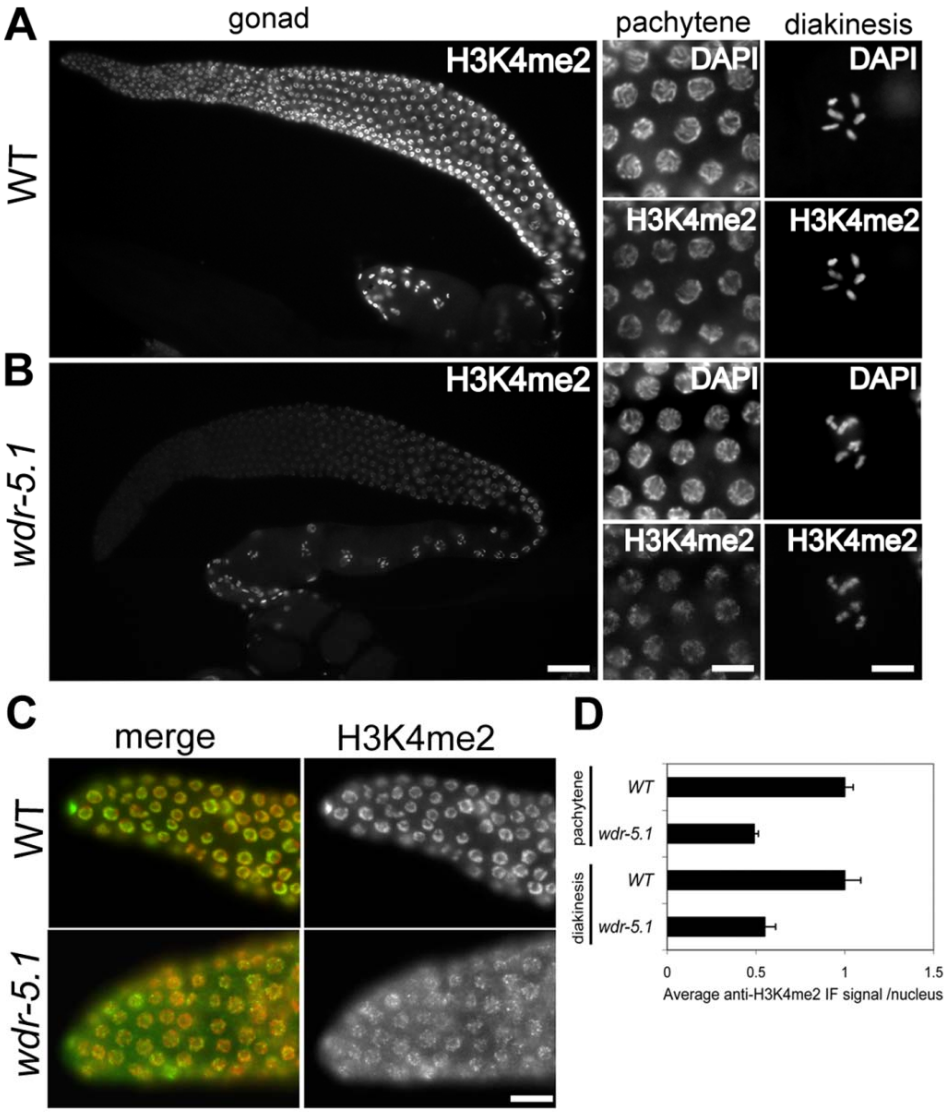
A
gonad
pachytene
diakinesis
WT
H3K4me2
DAPI
H3K4me2
DAPI
H3K4me2
B
wdr-5.1
H3K4me2
DAPI
H3K4me2
DAPI
H3K4me2
C
merge
H3K4me2
WT
wdr-5.1
D
pachytene
diakinesis
WT
wdr-5.1
WT
wdr-5.1
0
0.5
1
1.5
Average anti-H3K4me2 IF signal /nucleus

**Figure 2-15. WDR-5.1-dependent H3K4 methylation in adult GSCs is unaffected by RNAi mediated knockdown of *ama-1***

Wild-type (A) and *wdr-5.1(ok1417)* (B) animals were treated with control RNAi or *ama-1(RNAi)* as in Figure 2-7, The adult gonads from treated animals were dissected, fixed, and probed with anti- AMA-1(8WG16), or mouse monoclonal antibody against H3K4me2/3 as indicated. Exposure times were the same for each antibody for comparison. (A) AMA-1 is undetectable in the RNAi treated gonads from both WT and *wdr-5.1(ok1417)* animals except in more proximally-located cells (arrows) (b' and d'). (B) In parallel wild-type *ama-1(RNAi)* gonads, a broad band of nuclei that lacks both H3K4me3 and H3K4me2 is apparent (b', f' brackets). This band extends proximally from the transition/meiotic entry zone to the region where AMA-1 protein is still detectable in *ama-1(RNAi)* gonads. The band excludes the distal GSCs, where H3K4me2/3 are impervious to *ama-1(RNAi)*. In *wdr-5.1(ok1417); ama-1(RNAi)* gonads, all distal nuclei lack H3K4me2/3, including the GSCs (highlighted by brackets in B; d' and h'). Scale bars represent 20um. (C and D) Quantification of anti-H3K4me2 or me3 signals in the germ cell nuclei. Nuclei were randomly chosen from mitotic region, early pachytene (marked by brackets in b' and f') and late pachytene regions. Signals were measured and quantified as in Figure 2-9. For each stage, 12 nuclei from 3 gonads (4 nuclei/gonad) were qualified. Anti-H3K4me3 and H3K4me2 signals (arbitrary units ± SEM) were normalized to wild-type (RNAi control) mitotic nuclei. The graph represents results from 2 independent experiments.

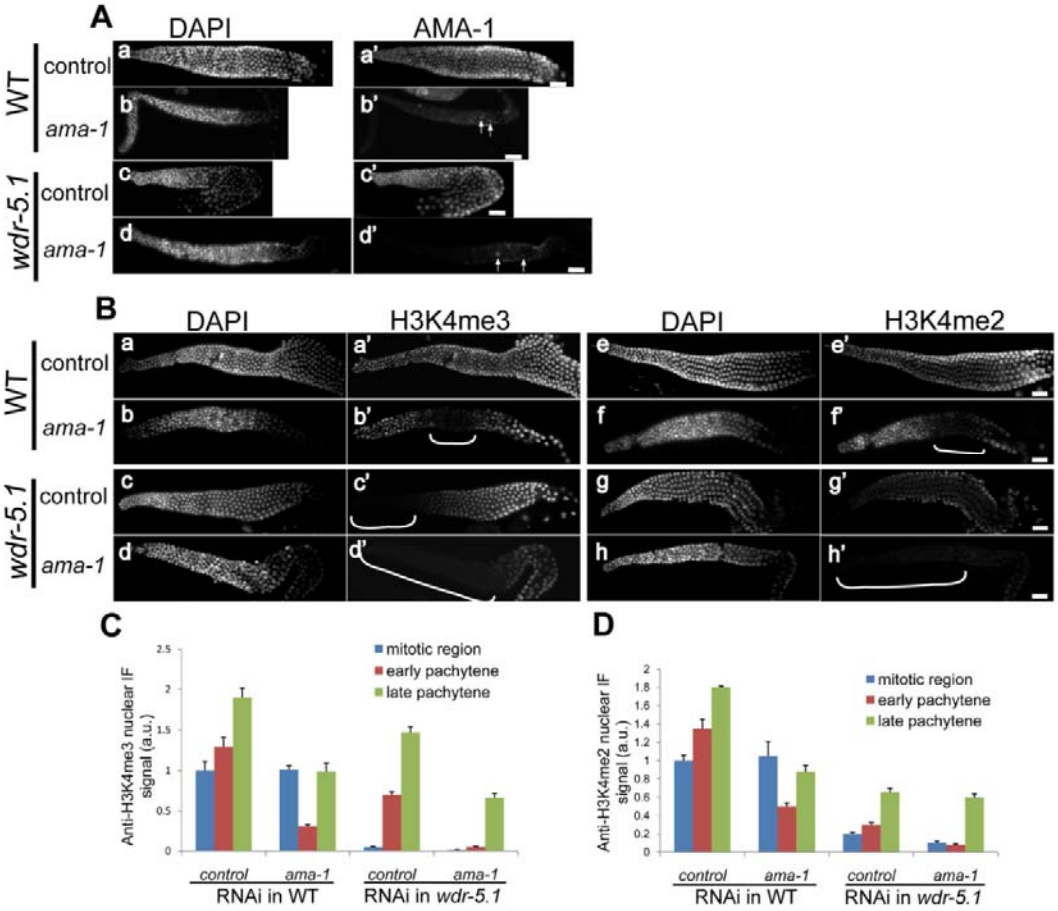
A
DAPI
AMA-1
WT
control
ama-1
wdr-5.1
control
ama-1
a
a'
b
b'
c
c'
d
d'
B
DAPI
H3K4me3
DAPI
H3K4me2
WT
control
ama-1
wdr-5.1
control
ama-1
e
e'
f
f'
g
g'
h
h'
C
Anti-H3K4me3 nuclear IF signal (a.u.)
mitotic region
early pachytene
late pachytene
control
ama-1
control
ama-1
RNAi in WT
RNAi in wdr-5.1
D
Anti-H3K4me2 nuclear IF signal (a.u.)
mitotic region
early pachytene
late pachytene
control
ama-1
control
ama-1
RNAi in WT
RNAi in wdr-5.1

**Figure 2-16. *ama-1(RNAi)* depletion of Pol II phospho-Ser2 in adult germ cells**

RNAi experiments were done as in Figure 2-7. Adult hermaphrodite gonads were dissected and fixed and probed with either mAb H5 for phosphor-Ser2 or mouse monoclonal antibodies against H3K4me3 as indicated. Exposure times were the same for each antibody for comparison. Bars=10um. (A and B) RNAi of *ama-1* depletes the mAb H5 signal to undetectable levels in both WT and *wdr-5.1* adult germ cells. (C and D) Similar H3K4me3 patterns as described for Figure 2-15 were observed.

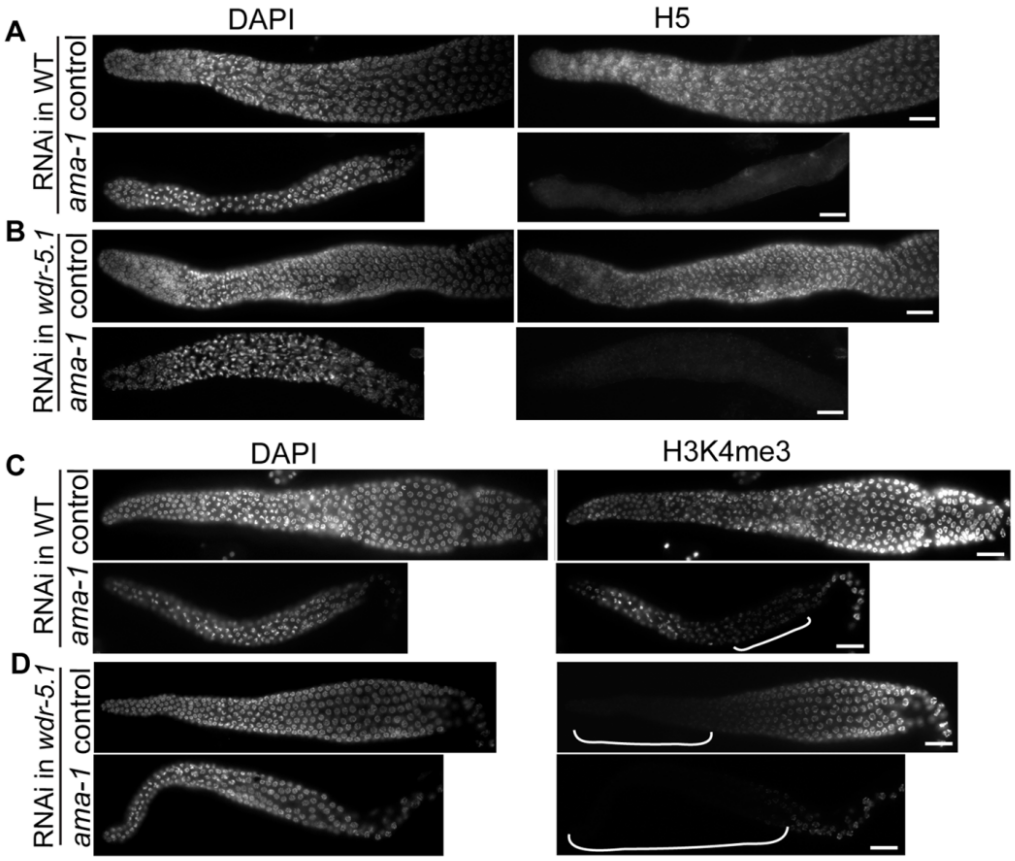
DAPI
H5
A
RNAi in WT
control
ama-1
B
RNAi in wdr-5.1
control
ama-1
DAPI
H3K4me3
C
RNAi in WT
control
ama-1
D
RNAi in wdr-5.1
control
ama-1

**Figure 2-17. H3K4me3 is transiently independent of WDR-5.1 activity in proliferating larval germ cells**

Two-fold stage embryos and larvae at L1, L2, and L3 stages were probed for H3K4me3 and PGL-1 to identify the germ cells, and counterstained with DAPI. Arrows and dashed lines highlight germ cells in embryos and larval gonad. The primordial germ cells (PGCs, marked by PGL-1 staining in blue), Z2 and Z3 (arrows), are boxed and enlarged in the embryo images. Red: DAPI; Green: H3K4me3; Blue: PGL-1. In the larval stage images, the full gonad is outlined at the indicated stages except in L3 larvae, in which just one gonad arm is illustrated and outlined. H3K4me3 is erased from PGC chromatin right after their birth ((Schaner et al., 2003) and A; embryos), but reappears after hatching in both WT (A; L1, arrows) and *wdr-5.1* (B; L1, arrows) larvae. In WT larvae, H3K4me3 persists through all larval germ cell stages (A; L1, L2, L3), but H3K4me3 is greatly reduced in *wdr-5.1* larval germ cells (B; L2 and L3). Thus only the initial appearance of H3K4me3 in post-embryonic germ cells is not dependent on WDR-5.1 function. Asterisks indicate distal end of gonad arms. Bars=10um.

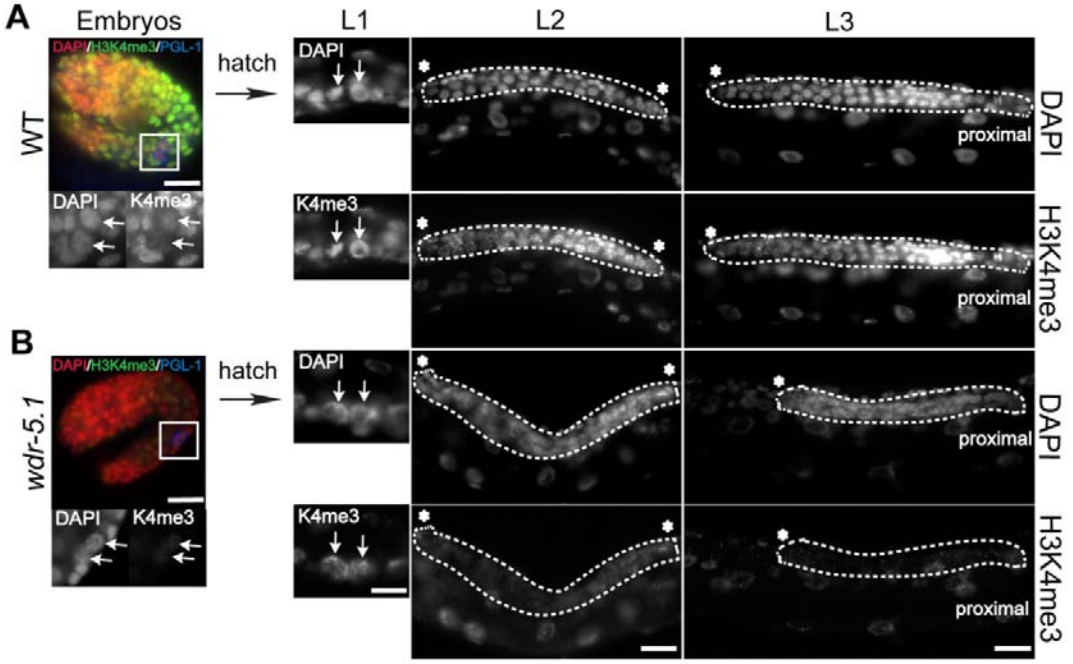
A
Embryos
L1
L2
L3
WT
DAPI/H3K4me3/PGL-1
hatch
DAPI
K4me3
proximal
DAPI
H3K4me3
B
wdr-5.1

**Figure 2-18. *wdr-5.1 and rbbp-5* mutants exhibit temperature sensitive germline stem cell defects**

L4 larvae were picked and shifted to 25°C for 24 hours. Gonads were dissected, fixed and probed with antibodies for SYP-1 protein, and counter stained with DAPI. The length of the germline stem cell compartment in each gonad was determined by counting the number of mitotic zone (MZ) nuclei from the distal tip to the beginning of the transition zone (TZ) of each gonad (dashed lines). (A-F) SYP-1 and DAPI stained gonads from wild-type (WT), *wdr-5.1(ok1417)*, and *rbbp-5(tm3463)* adult hermaphrodites; dashed lines indicate boundary between MZ and TZ. Arrows mark the crescent morphology of nuclei in TZ. Scale bars= 10um. (G) Box-plot showing distribution of MZ lengths observed from strains in (A); black line indicates median; top and bottom indicates maximum and minimum lengths observed for each strain. The number of gonads examined for each strain (n) is as follows: WT=32, *wdr-5.1(ok1417)*=43, *rbbp-5(tm3463)*=25.

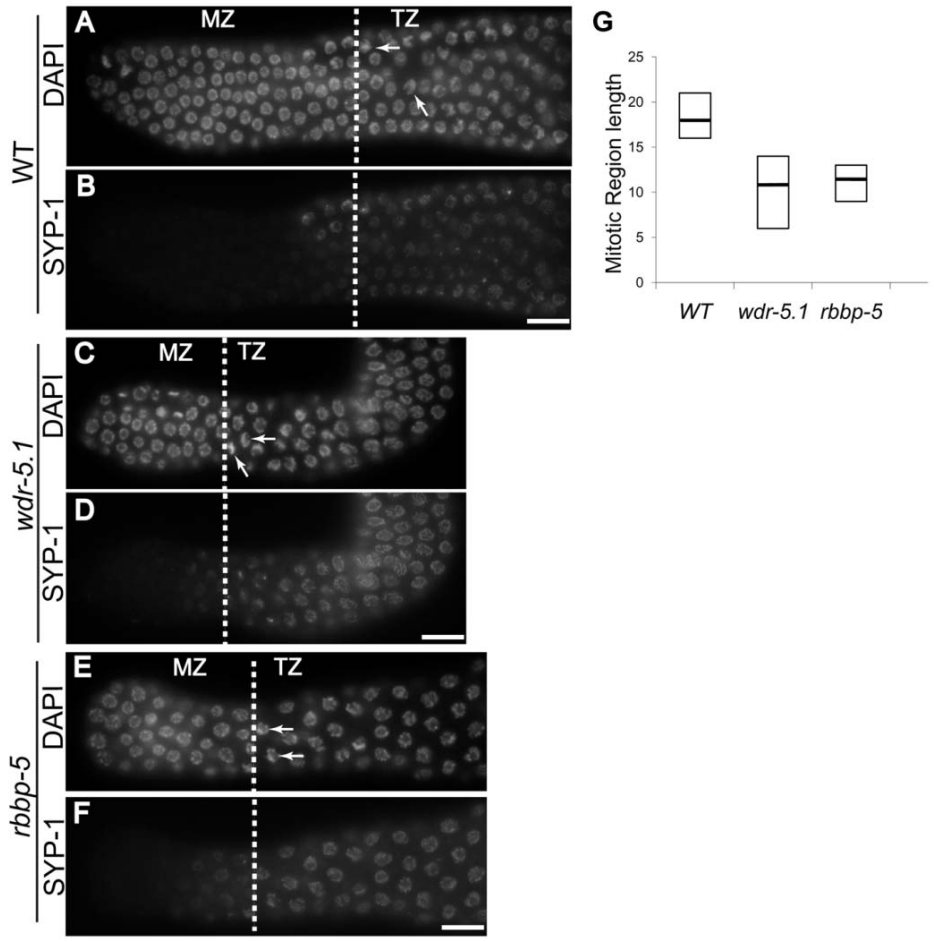
WT
DAPI
SYP-1
A
B
MZ
TZ
wdr-5.1
C
D
rbbp-5
E
F
G
Mitotic Region length
25
20
15
10
5
0
WT
wdr-5.1
rbbp-5

**Figure 2-19. Fertility and Germline mortality defects in *wdr-5.1(ok1417)* mutants**

(A) 10 WT or *wdr-5.1(ok1417)* hermaphrodites were grown continuously at 20°C, or were shifted to 25°C as L4 larvae and their F1 progeny were counted. (B) *wdr-5.1(ok1417)* L4 larvae were shifted to 25°C, and 100 F1 larvae were picked onto separate plates and scored for sterility. Fertile animals at each subsequent generation were further maintained at 25°C and the sterility of their offspring (F2-F6) was assessed.

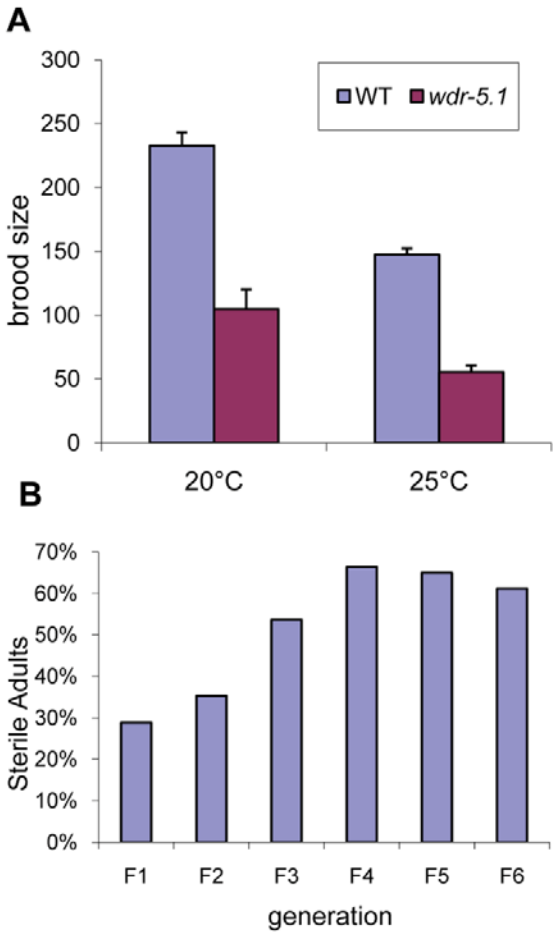
A
300
250
200
150
100
50
0
brood size
WT
wdr-5.1
20°C
25°C
B
70%
60%
50%
40%
30%
20%
10%
0%
Sterile Adults
F1
F2
F3
F4
F5
F6
generation

**Figure 2-20. Egl and Dpy phenotypes in *wdr-5.1(ok1417)* and *rbbp-5(tm3463)* mutants**

(A) DIC images of *wdr-5.1(ok1417)* and *rbbp-5(tm3463)* adults compared to wild type illustrating Egl defect; i.e., extensive accumulation of embryos *in utero*. Arrows mark late staged embryos not normally observed in wild type *utero*. (B) *rbbp-5(tm3463)* and wild type adult animals at same magnification, illustrating the Dpy phenotype observed in the *tm3463* strain.

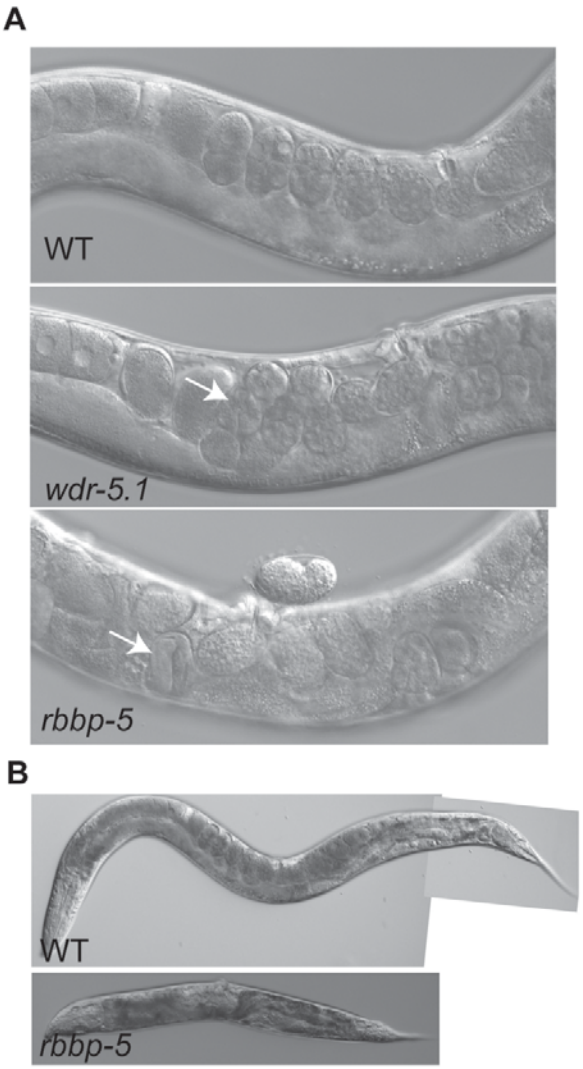
A
WT
wdr-5.1
rbbp-5
B
WT
rbbp-5

**Figure 2-21. Temperature-sensitive germ cell development defects in *wdr-5.1* and *rbbp-5* mutants**

L4 larvae were shifted to 25°C overnight and prepared as in Figure 2-18. (A) Wild-type hermaphrodite gonad showing normal germ cell development at 25°C from distal mitotic (upper left), and meiotic stages leading to proximal oocytes and sperm in spermatheca (lower right). (B) Examples and classification of defects observed in *wdr-5.1(ok1417)* 25°C mutants. Class I: Emo=endomitotic oocytes (oocytes that prematurely activate and undergo DNA endoreduplication); Class II: Mog=masculinization of germ line (fail to switch from spermatogenesis to oogenesis at L4/adult molt); Class III=gonads with severely defective DNA morphology at multiple germ cell stages. Arrows in lower image point to nuclei that appear polyploid or otherwise defective; arrowhead indicates what appear to be spermatid nuclei in mid-distal region of gonad. (C) Example of *rbbp-5(tm3463)* gonad exhibiting Emo phenotype; the arrow points to a megaploid oocyte. (D) Summary of types and frequency of each phenotype observed in indicated strains at 25°C. Scale bars= 20um.

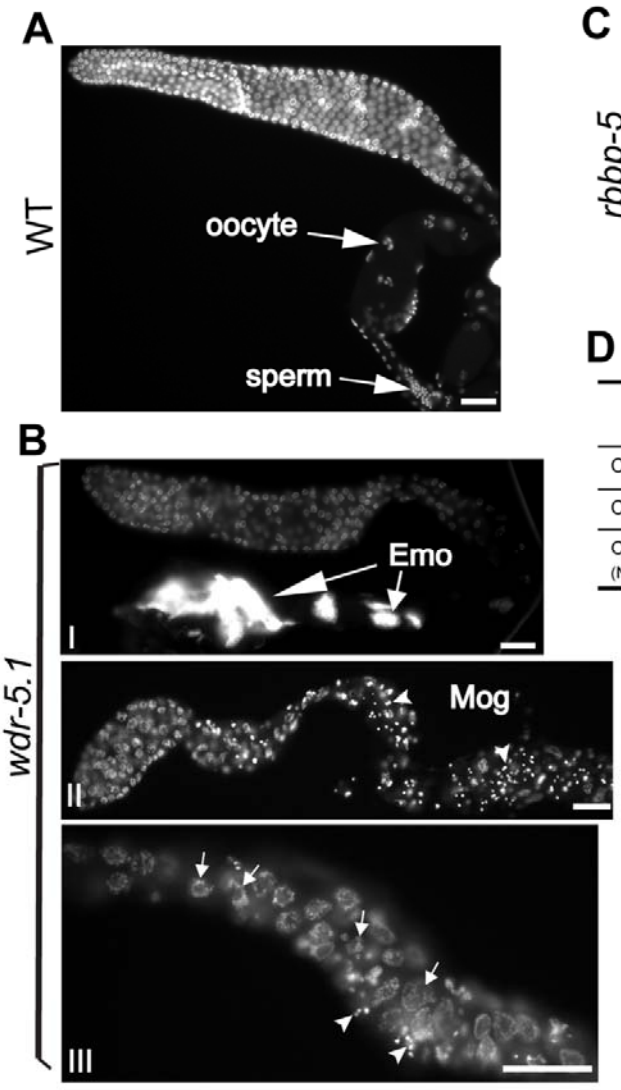


D

| | *wdr-5.1* (n=116) | *rbbp-5* (n=73) |
|---|---|---|
| Class I (Emo) | 75.9% | 100% |
| Class II (Mog) | 5.1% | 0 |
| Class III (Nuclear Morphology) | 19.0% | 0 |

**Figure 2-22. Summary of H3K4me3 and RNA Polymerase C-Terminal Domain phosphorylation dynamics during the *C. elegans* germline cycle**

Relative abundance of H3K4me3 in germ cell chromatin at different stages of germ cell development (indicated across the top of the graph) is plotted for wild type (WT; red solid line) and both *wdr-5.1* and *rbbp-5* mutants (blue dotted line). Superimposed on this is the dynamics we observe for the phosphorylation of Serine 2 of the C-terminal domain repeat of RNA Pol II (pSer2; green line; data from (Furuhashi et al., 2010)). Notice that pSer2 is absent in the P-cells, in which H3K4me3 is maintained, but the loss of H3K4me3 that occurs in the P-cell/PGC stage overlaps with appearance of pSer2.

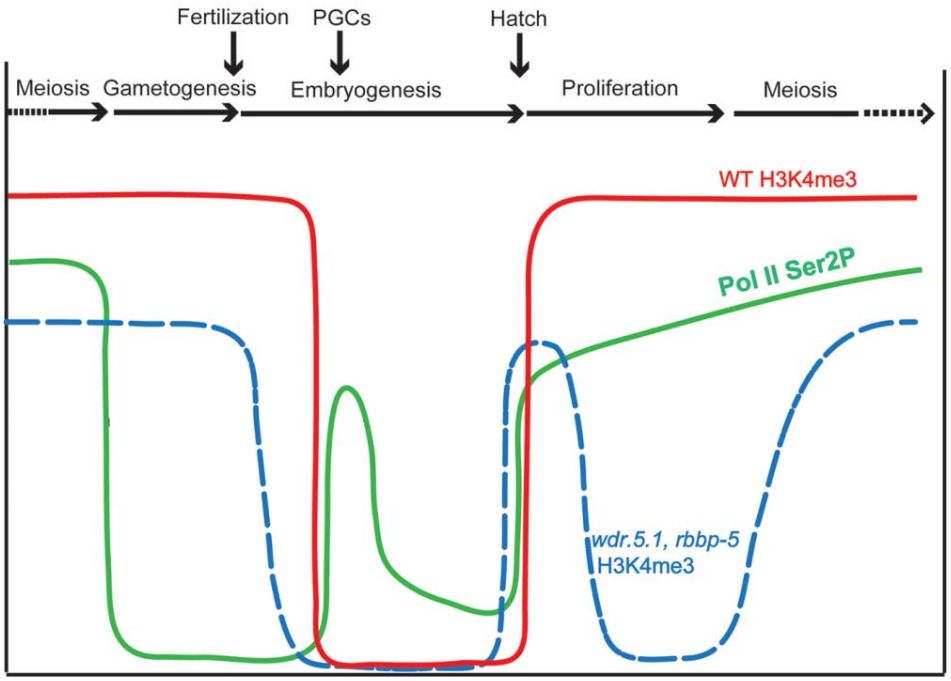
Fertilization
PGCs
Hatch
Meiosis
Gametogenesis
Embryogenesis
Proliferation
Meiosis
WT H3K4me3
Pol II Ser2P
wdr.5.1, rbbp-5
H3K4me3

# Chapter 3

## WDR-5 Is Involved in Regulation of Sex Determination of *Caenorhabditis elegans*

## Introduction

Sex determination in the nematode *Caenorhabditis elegans* is controlled genetically and regulated by cascades of regulatory proteins. The soil worm has two sexes: hermaphrodite and male. The hermaphrodite is somatically female, but the germ line produces both sperm and oocytes. In hermaphrodites, the first set of larval germ cells undergoing meiosis continue on through spermatogenesis for a short period of time during late larval stages. After the final larval molt, the germ cells permanently switch to oogenesis. The sex of the animal is determined by the ratio of X chromosomes to autosomes (X:A), with XX embryos (2X:2A) developing into hermaphrodites while XO animals (1X:2A) develop as males (Hubbard and Greenstein, 2000; Madl and Herman, 1979). The X:A ratio provides differing doses of several X- and autosome-linked regulatory factors that ultimately control the expression of the master regulator *xol-1*, which itself regulates a cascade of negative genetic interactions (Figure 3-5A). At the terminus of this cascade is TRA-1, a Zinc finger transcription factor, which plays an essential role in determining the sexual identity of both germ line and soma (Hodgkin, 1987). There are two known transcripts of *tra-1*: *tra-1A* and *tra-1B*. The TRA-1A protein is comprised of 1109 amino acids (Zarkower and Hodgkin, 1992, 1993). This protein contains five Zinc fingers and is closely related to *Drosophila Cubitus interruptus* (Ci) and mammalian Gli proteins. TRA-1B contains two Zinc fingers. It does not bind DNA and its function remains obscure (Zarkower and Hodgkin, 1992, 1993). Ci/Gli proteins play pivotal roles in development, stem cell maintenance, and tumorigenesis as transducers of Hedgehog signaling (Ingham and McMahon, 2001). There is no known Hedgehog-like signaling pathway in *C. elegans*. It has been suggested that TRA-1A

promotes female development by inhibiting genes that promote male differentiation (Hodgkin, 1987; Zarkower and Hodgkin, 1992). In germ cells, TRA-1A promotes oogenesis by inhibiting two genes required for spermatogenesis: *fog-1* and *fog-3* (discussed below). XX hermaphrodites with null mutations in *tra-1* develop as pseudomales and produce only sperm. In contrast, gain-of-function mutations in *tra-1* cause all germ cells to differentiate into oocytes (Hodgkin, 1987; Schedl et al., 1989). Further study reveals that TRA-1A binds to the promoter of *fog-3* and directly represses its expression (Chen and Ellis, 2000). In somatic tissues, two sexual developmental genes, *mab-3* and *egl-1,* have been identified as the direct targets of TRA-1A repression (Chen and Ellis, 2000; Conradt and Horvitz, 1998; Yi et al., 2000). Like Ci/Gli, TRA-1 undergoes proteolytical processing to generate multiple isoforms with molecular weights ranging from 90 to 110 kDa (Schvarzstein and Spence, 2006). Contributions to these isoforms may also result from phosphorylation of a 90KDa C-terminal truncated protein. Importantly, these isoforms have feminization activity and appear to be the active forms (Schvarzstein and Spence, 2006). Nevertheless, how *tra-1* regulates sex determination is not fully understood. Schvarzstein and Spence reported that the overall protein level of TRA-1 was higher in hermaphrodites, indicating that protein levels are important for TRA-1 regulation (Schvarzstein and Spence, 2006). In contrast, Segal and colleague found that TRA-1 protein levels were similar in both males and hermaphrodites. The difference was that more TRA-1A was localized in nuclei of hermaphrodites than in males, suggesting that the TRA-1 localization plays an important role in regulating sex determination (Segal et al., 2001).

Immediately upstream of *tra-1* in the sex determination pathway are *fem* genes (*fem-1, -2, -3*), which negatively regulate *tra-1*. Recently, it was reported that the FEM proteins (FEM-1,-2 and -3) were members of the CUL-2-based ubiquitin ligase complex, and that TRA-1 regulation involved CUL-2. This complex regulated TRA-1A levels through ubiquitin-directed proteasome degradation (Starostina et al., 2007). Downstream of *tra-1* are *fog-1* and *fog-3*, two genes that are terminal regulators in the sex determination pathway (Figure 3-5A). Both are required for spermatogenesis. FOG-3 is closely related to vertebrate Tob (Transducer of ErbB-2) family members (Chen and Ellis, 2000). Tob family proteins are associated with the deadenylase complex, which interacts with poly (A) binding protein to regulate translation (Kimble and Crittenden, 2007). FOG-3 is essential for germ cells to differentiate as sperm rather than oocytes. *fog-3* expression and activity seems to be restricted to the germline, and it has been suggested that sperm production requires continuous *fog-3* activity (Chen and Ellis, 2000). In hermaphrodites, *fog-3* is expressed during larval stages corresponding to spermatogenesis and is shut off coincident with the onset of oogenesis in adults (Chen and Ellis, 2000). The molecular function of *fog-3* remains unknown.

As discussed above, the regulation of *fog-1* and *fog-3* by *tra-1* seems to play decisive role in the sperm/oocyte decision. The other genes in the sex determination pathway ultimately function through their regulation of *tra-1* (Figure 3-5A). This network of regulation is tightly controlled, and imbalances can lead to sex determination defects. For example, loss of function mutation of *fem* genes results in feminization of the germline, i.e. the germ cells only produce oocytes. In contrast, worms with gain of function mutation of *fem-3* exhibit Mog (masculinization of germline) phenotype

(Ahringer and Kimble, 1991). These worms fail to switch to oogenesis and continuously produce sperm. In both cases, the hermaphrodites are self-sterile.

We previously showed that mutations in the conserved epigenetic modifier component, *wdr-5.1,* caused Mog phenotype with low penetrance in hermaphrodites (Chapter 1), suggesting that *wdr-5.1* might play a role in sex determination. WDR5 is a core subunit of MLL and Set1 Histone H3 Lysine 4 (H3K4) methyltransferase complexes (HMT), the so-called COMPASS (complex associated with Set1) (Shilatifard, 2008). H3K4 methylation is generally associated with transcription competency (Ruthenburg et al., 2007). WDR5 contains seven WD40 repeats and plays a central role in the regulation of the methyltransferase complex activity (Dou et al., 2006; Ruthenburg et al., 2007; Wysocka et al., 2005). Loss of WDR5 in 293 cells results in global decreases of H3K4 mono-, di-, and trimethylation (H3K4me1/2/3) to various degrees (Dou et al., 2006). WDR5 is required in the maintenance of H3K4me3 levels in HOXA9 and HOXC8 loci chromatin and is important for the expression of these two genes. Knockdown of WDR5 leads to reduction of mono- and tri-methylation levels and a variety of phenotypes, including somatic and gut defects, in *X. laevis* (Wysocka et al., 2005). Biochemical studies in yeast and mammalian cells demonstrate that WDR5, Ash2L and RbBP5 form a core complex that is essential for complex stability and enzymatic activity (Dou et al., 2006). Structure studies reveal that WDR5 recognizes the Ala1, Arg2 and Thr3 of H3, and can bind to H3 at the N-terminus regardless of the methylation status of Lys4 (Couture et al., 2006; Han et al., 2006; Ruthenburg et al., 2006; Schuetz et al., 2006).

A conserved WDR5-interacting (Win) motif located in the N-SET region of the histone methyltransferase Set1 was recently identified (Patel et al., 2008a). Strikingly,

the Win sequence in Set1 shares homology with the H3 N-terminus previously shown to interact with WDR5. This finding suggests that WDR5 and Set1 compete for the same substrate, and these interactions might be critical for the HMT activity. Curiously, this result also seems to rule out simultaneous interaction of WDR5 and Win motif-containing HMTs. Interestingly, it has been shown that WDR5 also functions within complexes without HMT activity. For example, Garapaty and colleagues reported that WDR5 was associated with the nuclear receptor complex interacting factor-1 (NIF-1) to promote the expression of target genes (Garapaty et al., 2009). WDR5 is also reported to be a subunit of CHD (Thompson et al., 2008)8 containing ATP-dependent chromatin remodeling complexes and the histone acetyltransferase complexes ATAC and MOF (Thompson et al., 2008). None of these complexes are known to contain Set1 or MLL related histone methyltransferases.

In *C. elegans*, conserved Set1/COMPASS complex components, including the worm ortholog of WDR5, WDR-5.1, are required to maintain H3K4 methylation in early embryos and in adult germline stem cells (Chaper 2). Interestingly, in both early embryos and germline stem cells, H3K4 methylation that is dependent on WDR-5.1 can occur in the absence of ongoing transcription. Mutation of *wdr-5.1* cause defects in germline stem cell maintenance and proper germline development (Chapter 2). In this chapter, we show that two of the three *C. elegans* WDR-5 homologs, *wdr-5.1* and *wdr-5.2*, are required redundantly for the switch from spermatogenesis to oogenesis to occur normally in hermaphrodites. Notably, this function of *wdr-5.1* appears to be independent of its role in H3K4 methylation. The absence of the two *C. elegans wdr-5* homologs causes ectopic expression of *fog-3* in adult germ cells, which results in germline masculinization. TRA-1,

the transcriptional repressor of *fog-3*, is depleted from the nuclei of the adult germ cells in *wdr-5.1;wdr-5.2* double mutants, indicating its stable association with chromatin is dependent on WDR-5 function. We conclude that TRA-1 mediated *fog-3* repression in adult germline is dependent on WDR-5.

## Results

### *wdr-5.1;wdr-5.2* double mutant shows fertility defects

We previously showed that *wdr-5.1*, a worm WDR5 ortholog, was required for the normal maintenance of H3K4me2/3 in early embryos and in the germline stem cell pool of the postembryonic germline. Mutation of *wdr-5.1* affected germline stem cell (GSC) population size and proper germ cell development (Chapter 1). The *C. elegans* genome contains three homologues of WDR5: *wdr-5.1, wdr-5.2*, and *wdr-5.3*. *wdr-5.1* shares 65% and 53% of homology with *wdr-5.2* and *wdr-5.3*, respectively. Interestingly, only *wdr-5.1* is essential for the normal maintenance of H3K4me2/3, indicating that of the three paralogs, only WDR-5.1 may be a component of an HMT complex (Chapter 1). Neither deletion of *wdr-5.2 (ok1444)*, nor knockdown of *wdr-5.3* by RNAi, caused obvious H3K4me2/3 defects in early embryos and adult germ cells by immunofluorescence (Figure 3-1 and data not shown). In addition, H3K4m2/3 was not significantly affected in mixed stage embryos of *wdr-5.2 (ok1444)* mutant by western analysis (Figure 2-2). *wdr-5.1*; *wdr-5.2* double mutant and triple mutant (RNAi knockdown of *wdr-5.3* in *wdr-5.1; wdr-5.2*) exhibited defects in H3K4 methylation identical to those of *wdr-5.1* single mutants (Figure 3-1 and data not shown). These data suggest that *wdr-5.1* plays an

essential role in regulating H3K4me2/3 in the distal region of gonads and embryos, whereas *wdr-5.2* and *wdr-5.3* are dispensable.

Surprisingly, we observed more severe phenotypes in *wdr-5.1;wdr-5.2* double mutants comparing to the individual mutants. *wdr-5.2 (ok1444)* did not exhibit obvious phenotypes at either 20°C or 25°C (Table 3-1). At 20°C, *wdr-5.1(ok1417)* showed 12% embryo lethality (Emb) and 2.5% sterility (Ste) (Table 2-1 and Table 3-1). However, *wdr-5.1;wdr-5.2* double mutants exhibited increases in both embryonic lethality and sterility (19% and 16%, respectively) at 20°C. At 25°C, embryonic lethality and sterility in *wdr-5.1(ok1417)* doubled to 36% and 29%, respectively. This strain also exhibited a temperature-sensitive mortal germline phenotype, in which the fraction of sterile animals rose with each successive generation raised at 25°C (Figure 2-19 and Table 3-1). Notably, if shifted to 25°C during the L4 stage, *wdr-5.1;wdr-5.2* double mutants developed into adults that were significantly defective in reproduction, with an average brood size of 35 compared to 145 in WT. 42% of the double mutant embryos that were produced died as embryos. The remainder hatched and developed into adults, but 100% of these animals were sterile (Table 3-1). Importantly, the loss of H3K4 methylation was fully penetrant at 20°C and was not noticeably worse at 25°C (Chapter 1 and not shown). These results suggest that *wdr-5.1* and *wdr-5.2* might have overlapping functions that are essential for normal fertility at elevated temperatures, and that these functions appear to be independent of WDR-5.1's role in H3K4 methylation.

Males could be generated in *wdr-5.1;wdr-5.2*. However, all these males had defective tail rays and were sterile at 20°C (Figure 3-2). 53% of *wdr-5.1* males were

sterile, indicating that *wdr-5.1* and *wdr-5.2* are both also required for normal male fertility.

**Sterile *wdr-5.1; wdr-5.2* mutant exhibits temperature sensitive sex determination defects**

To investigate the mechanism that underlies the sterility of *wdr-5.1; wdr-5.2* double mutants, we dissected the gonads from hermaphrodites and stained the DNA with DAPI. As shown in Figure 3-3A, at 20°C, the fertile *wdr-5.1; wdr-5.2* double mutant hermaphrodites have normal, well-developed and organized ovaries. Germ cells first undergo spermatogenesis and later switch to oogenesis within the same gonad, so both sperm and oocytes were present in the adult gonad. However, 88% of the gonads dissected from *wdr-5.1; wdr-5.2* worms grown at 25°C contained only sperm. This Mog phenotype (masculinization of germline) is indicative of a sex determination defect in which germ cells undergo spermatogenesis but fail to switch to oogenesis (Figures 3-3A and B). The germ cells in the remaining 11.8% gonads did exhibit signs of having switched to oogenesis, but the oocytes showed an endoreplication, or endomitotic (Emo) phenotype (Figure 3-3A). The sterility of the double mutant could be rescued by an integrated transgene expressing a WDR-5.1 and GFP fused protein (Figure 3-3C), suggesting the defect is at least partially dependent on *wdr-5.1*.

In contrast to the double mutant, the majority (75.9%) of the sterile animals observed in *wdr-5.1* single mutants raised at 25°C exhibited the Emo phenotype and only 5.1% were Mog (Chapter 1 and Figure 3-3B). The difference in the penetrance of the Mog and Emo phenotypes, depending on the presence or absence of WDR-5.2 is curious,

as neither phenotype is observed at any significant frequency in the *wdr-5.2* single mutant. The results suggest that WDR-5.2 can partially replace an essential function of WDR-5.1, but itself is insufficient for this role. The essential function is clearly related to sex determination (Mog phenotype), which may also influence normal gamete development (Emo phenotype). However, neither phenotype seems to be directly tied to the role of WDR-5.1 in H3K4 methylation. It's noteworthy that neither *set-2* nor *rbbp-5*, two other H3K4 HMT complex components, showed Mog phenotypes at either 20°C or 25°C (Chapter 1). Together these data indicate that both *wdr-5.1* and *wdr-5.2* are required for normal sex determination, and this role might be independent of the role of WDR5 in H3K4 methylation.

One interesting feature of the sterile phenotype of *wdr-5.1; wdr-5.2* is that it is temperature sensitive, even though these are null mutations. To determine the temperature-sensitive period (TSP), we shifted *wdr-5.1;wdr-5.2* hermaphrodites from 20°C to 25°C or *vice versa* at different developmental stages and scored the adults for sterility (Figure 3-3D). Up-shifting the worms during or before L2 resulted in sterility in 100% of the up-shifted animals. When the worms were up-shifted later, between late L3 and young adult stages, about 50% of them developed into sterile adults. On the other hand, downshifting *wdr-5.1;wdr-5.2* worms before the L3 stage restored fertility in most of the worms. More than 50% of the worms could not restore their fertility if downshifted at L4 or young adult stage. This data indicate that the TSP for *wdr-5.1; wdr-5.2* double mutant is between the L3 to young adult stages. During these stages the germ cells of hermaphrodite make sperm and then switch to oogenesis. Thus the TSP is consistent with the timing when sex determination occurs. Collectively, our data suggest that both *wdr-*

*5.1 and wdr-5.2* are partially redundantly required for proper sex determination regulation to occur at elevated temperatures.

### *wdr-5.1/wdr-5.2* function upstream of *fog-3* and downstream of *fem-3*

Germline sex determination in *C. elegans* is controlled by a pathway composed of a series of sequential activities that function as genetic switches (Figure 3-5A, for reviews, see (Ellis and Schedl, 2007)). Disruption of any gene in the pathway leads to sex determination problems or germline development defects. To understand where *wdr-5.1 and wdr-5.2's* roles in sex determination fit within this pathway, we conducted an epistatic analysis. *fog-1* and *fog-3* are at the end of the sex determination pathway and promote spermatogenesis. Hermaphrodites carrying *fog-3* null mutation only produce oocytes, a phenotype called Fog (feminization of germline), while gain of function mutation of *fog-3* exhibited Mog phenotype. To determine if *wdr-5.1/wdr-5.2* is upstream of *fog-3*, we knocked down *fog-3* in *wdr-5.1;wdr-5.2* by RNAi. L4 worms were soaked in *fog-3* dsRNA for 24 hours and were subsequently transferred to feeding plates. L1 worms of the *fog-3 (RNAi)* F1 generation were shifted to 25°C and grown to adulthood. The gonads were dissected from adults and stained with DAPI. As shown in Figures 3-4A and B, with control RNAi, 66.7% of the dissected gonads of *wdr-5.1;wdr-5.2* displayed the Mog phenotype. In striking contrast, 80% of the gonads of *wdr-5.1;wdr-5.2; fog-3(RNAi)* animals were feminized (Fog), producing only oocytes (Figure 3-4A and B). These data suggest that *wdr-5.1/wdr-5.2* act upstream of *fog-3* and normally play a negative role in *fog-3* function.

It has been shown that *fog-3* expression is negatively controlled by TRA-1, a transcription repressor. Disruption of *tra-1* causes upregulation of *fog-3* and promotes male differentiation (Chen and Ellis, 2000). Immediately upstream of *tra-1* are three *fem* genes: *fem-1, -2, -3* (Figure 3-5A). FEM-1, -2 and -3 are components of an ubiquitin ligase complex which targets TRA-1 for degradation (Starostina et al., 2007). Mutations in the *fem* genes lead to the feminization of the germline, resulting in a Fog phenotype. To determine the genetic position of *wdr-5.1/wdr-5.2* relative to *fem* genes, we knocked down *fem-3* in *wdr-5.1; wdr-5.2* by RNAi and analyzed the phenotypes of F1 adult worms grown at 25°C. In contrast to wild-type animals (N2) treated in parallel with *fem-3* RNAi, which exhibited high penetrance of the Fog phenotype, RNAi of *fem-3* activity could not reverse the *wdr-5.1/wdr-5.2* Mog phenotype (Figure 3-4C), indicating that *wdr-5.1/wdr-5.2* act downstream of *fem-3*. The difference is not due to a defect in RNAi sensitivity in the *wdr-5.1;wdr-5.2* strain, as this strain is fully sensitive to *fog-3(RNAi).* These experiments placed the function of the *wdr-5.1/.2* genes downstream of the *fem* genes and upstream of *fog-3.*

**_fog-3_ is ectopically expressed in _wdr-5.1; wdr-5.2_ germ cells**

The ability of the *fog-3 (RNAi)* to suppress the Mog phenotype of the *wdr-5.1;wdr-5.2* mutant indicated that the normal function of these genes was to suppress *fog-3* activity to promote the switch to oogenesis. One possible mechanism is that *wdr-5.1/wdr-5.2* promotes oogenesis by inhibiting *fog-3* expression either directly or indirectly in a temperature sensitive manner. To test this, we isolated gonads from both wild type and *wdr-5.1* single and double mutant adult animals grown at 20°C and 25°C and analyzed

the *fog-3* mRNA levels by qRT-PCR. At 20°C, *fog-3* mRNA was increased by 17.6-fold compared to that of wild type. Potentially associated with this, *wdr-5.1;wdr-5.2* double mutants show a low penetrance (16%) of sterility (Table 3-1). No changes were found in single *wdr-5.1 (OK1417*) or *set-2 (tm1630)* mutants (Figure 3-5B). At 25°C, *fog-3* mRNA was increased dramatically in both *wdr-5.1* single mutant and *wdr-5.1;wdr-5.2* double mutant by 48- and 77- fold, respectively (Figure 3-5B). Notably, *fog-3* mRNA levels appeared to be correlated with the penetrance of the sterile phenotype, as 42% of the single and 100% of the double mutant animals were sterile (Table 3-1 and Figure 3-5B). The correlation, however, did not extend to the detailed phenotype, since few of the single mutants were Mog (most were Emo; see Figure 3-3B), in contrast to the 88% Mog in the *wdr-5.1;wdr-5.2* double mutant (Figure 3-3B). Again, *fog-3* expression was unaffected in *set-2(tm1630)* at both 20°C and 25°C (Figure 3-5B). These data confirm that the sex determination defects we observe in *wdr-5.1;wdr-5.2* are linked to defects in repression of *fog-3* at the sperm/oocyte switch. Furthermore, the results also suggest that the Emo phenotype may represent an "intermediate" defect in sex determination caused by *fog-3* misregulation.

We also checked the mRNA levels of other genes in the sex determination pathway by qRT-PCR. These genes include: *fog-1, fog-2, gld-1, tra-2, fem-1/2/3, fbf-1/2, tra-1 and mog-1* (Figure 3-5A). The results revealed that the mRNA levels of all these genes were not significantly changed in *wdr-5.1;wdr-5.2* compared to those of wild type (data not shown). Notably, although *fog-1* is at the same genetic position as *fog-3* in the sex determination pathway (Figure 3-5A), *fog-1 mRNA* was not changed in *wdr-5.1;wdr-*

*5.2* mutant, nor could *fog-1* RNAi rescue the Mog phenotype of *wdr-5.1;wdr-5.2* (data not shown).

It has been suggested that *fog-3* expression is required for spermatogenesis in larvae and is repressed when oogenesis initiates in adult hermaphrodites (Chen and Ellis, 2000). Consistent with this, RT-PCR analysis revealed that *fog-3 mRNA* was present in both L4 and adult germ cells in *wdr-5.1;wdr-5.2* double mutants, whereas *fog-3* mRNA was not detectable in the adult germ cells of wild type (Figure 3-5C). To determine if this was due to defective transcriptional repression, we assayed for histone H3 tri-methylation at lysine 36 (H3K36me3) at the *fog-3* locus by chromatin immunoprecipitation/qPCR (ChIP-qPCR). H3K36me3 is normally associated with transcriptional elongation, thus actively transcribing genes have high levels of H3K36me3 in their gene bodies (Selth et al., 2010). As expected, in wild type gonads, H3K36me3 enrichment in *fog-3* was observed in L4 larvae, but decreased in the adult, consistent with a decline of *fog-3* transcription in adults. In *wdr-5.1; wdr-5.2* animals, however, H3K36me3 enrichment was detected at similar levels in both L4 and adult (Figure 3-5D), suggesting that *fog-3* is ectopically transcribed in adults in the absence of *wdr-5.1* and *wdr-5.2*. We conclude that *wdr-5.1* and *wdr-5.2* play a role in inhibiting *fog-3* transcription in adult germ cells of hermaphrodites.

### ***wdr-5.1/wdr-5.2* regulate *fog-3* expression independent of H3K4 methylation**

We previously showed that *wdr-5.1* and *rbbp-5*, two components of the potential Set-1/MLL related complex in worms, are essential for global maintenance of both H3K4me3 and H3K4me2 in early embryos and in germline stem cells (Chapter 1). SET-2 is an

H3K4 methyltransferase that appears to be specifically required for the generation of H3K4me3 in these stages. In contrast to the *wdr-5.*1 mutants, neither *set-2(tm1630)* nor *rbbp-5(e1834)* showed obvious sex determination defects. As mentioned previously, these data indicate that the roles of WDR-5.1/WDR-5.2 in *fog-3* regulation might be independent of the role of WDR-5.1 in H3K4 methylation. To more directly assess this, we next asked whether the regulation of *fog-3* by WDR-5.1/WDR-5.2 correlated with changes in H3K4 methylation. To address this, we performed a ChIP assay to analyze the level of H3K4me3 at the transcription start site of *fog-3* in both *set-2 (tm1630)* and *wdr-5.1; wdr-5.2*. As shown in Figure 3-6, H3K4me3 was reduced to similar levels in the two mutants; while *fog-3* expression is unchanged in *set-2* mutants but was upregulated in *wdr-5.1; wdr-5.2* double mutants (Figure 3-5B). These data strongly suggest that WDR-5.1/WDR-5.2 regulate *fog-3* in a mechanism that is independent of H3K4 methylation, and that defective H3K4 methylation does not correlate with defects in *fog-3* regulation.

**TRA-1 requires *wdr-5.1/wdr-5.2* to bind to chromatin in germ cells**

The only known direct transcriptional regulator of *fog-3* is TRA-1A. It has been shown that TRA-1A binds to the promoter of *fog-3* and represses its expression at the onset of oogenesis (Chen and Ellis, 2000). Intriguingly, *wdr-5.1/wdr-5.2* is also required for the inhibition of *fog-3* (Figure 3-5), and both *tra-1* and *wdr-5.1/wdr-5.2* are genetically at the same position in the sex determination pathway, as both are upstream of *fog-3* but downstream of the *fem* genes (Figure 3-4). Notably, qRT-PCR analysis revealed that *tra-1* mRNA levels were unchanged in the *wdr-5.1,wdr-5.2* mutant compared to wild type (data not shown), so it's unlikely that *wdr-5.1/wdr-5.2* inhibit *fog-3* by activating *tra-1*

expression. We then tested whether WDR-5.1/WDR-5.2 affected *fog-3* expression by regulating TRA-1 protein levels. We first probed for TRA-1 protein in adult germ cells using an antibody against TRA-1 (Schvarzstein and Spence, 2006). In the adult germline of WT hermaphrodite, TRA-1 was detected associated with chromatin in a banded pattern in the distal germ cells (Figure 3-7A and 3-8). The nuclear TRA-1 signal declined in germ cells as they progressed into early pachytene and become undetectable in later stages of meiosis (Figure 3-8). No TRA-1 staining was observed in the germ cells of a strain carrying the null allele of *tra-1(e1834),* (Figure 3-7A). Notably, TRA-1 nuclear staining was depleted in *wdr-5.1;5.2* double mutant germ cells, with increased cytoplasmic antibody signal evident, in animals raised at 25°C (Figure 3-7A). To determine if TRA-1 protein levels were affected, in addition to sub-cellular localization, gonads were isolated from WT and *wdr-5.1; wdr-5.2* double mutants grown at 25°C and lysates were analyzed by Western blot using the TRA-1 specific antibody. As shown in Figure 3-7B, TRA-1A was readily detectable in lysates from both wild type and *wdr-5.1; wdr-5.2* gonads, though there was a slight reduction in the mutant lysate relative to wild type. Importantly, the nuclear localization and association of TRA-1A with chromatin was restored in the double mutant by introduction of a transgene expressing *wdr-5.1* tagged with GDP (Figure 3-9B). This transgene was integrated in the original strain (Simonet et al., 2007) and was crossed to *wdr-5.1; wdr-5.2.* The homozygous state of both *wdr-5.1* and *wdr-5.2* mutations were verified by genotyping PCR. At 20°C, TRA-1 staining in *wdr-5.1; wdr-5.2* was similar to WT (Figure 3-8), indicating that the nuclear localization, like the Mog phenotype, was temperature-dependent. In agreement with this, when *wdr-5.1;wdr-5.2* animals were shifted to 25°C as young adults, TRA-1 nuclear

staining significantly decreased after 24 hours and declined to undetectable levels within 53 hours post upshift (data not shown). Taken together, our results suggest that the TRA-1 is unable to bind chromatin stably in the absence of WDR-5.1 and WDR-5.2 at 25°C. The depletion of TRA-1 from nuclei presumably directly leads to the ectopic expression of *fog-3* and the Mog phenotype.

**TRA-1 mediated *mab-3* and *egl-1* repression is *wdr-5.1/wdr-5.2* dependent**

In addition to *fog-3*, *mab-3* and *egl-1* are also known to be direct targets of TRA-1A repression (Conradt and Horvitz, 1998; Yi et al., 2000). The vitellogenin gene *vit-1* is expressed in intestinal cells only during female development. *vit-1* expression is repressed by MAB-3, and *vit-1* is thus indirectly dependent on TRA-1 since TRA-1 inhibits *mab-3* expression (Figure 3-10A). To address whether *wdr-5.1/wdr-5.2* participates in the regulation of these two genes, we performed qRT-PCR analysis using RNA purified from adult animals grown at 25°C. *mab-3* mRNA increased by 12-fold in *wdr-5.1;wdr-5.2* animals relative to wild type (Figure 3-10B). In agreement with this, *vit-1* mRNA levels were simultaneously reduced significantly in response to the elevated *mab-3* in the mutant (Figure 3-10C).

Another TRA-1 target, *egl-1,* is required for the male-specific apoptosis of HSNs (Hermaphrodite Specific Neurons), which are required for egg laying in hermaphrodites. TRA-1 promotes the survival of HSNs by inhibiting *egl-1* expression. In *wdr-5.1; wdr-5.2*, *egl-1* was upregulated compared to that of WT (Figure 3-10D). These data suggest that defective TRA-1 repression is a common characteristic of *wdr-5.1/wdr-5.2* mutants, and this defect is not restricted to *fog-3* regulation in the germline.

**Synthetic sterility between *wdr-5.1; wdr-5.2* and *set-9/set-26***

As previously discussed, WDR5 is a WD40 containing protein which has been shown to interact with SET domain proteins (Dou et al., 2006; Patel et al., 2008a). We tested several other SET-containing proteins for synthetic sterility by knocking down them by RNAi in the *wdr-5.1; wdr-5.2* double mutant. Two SET domain proteins: *set-9 (F15E6.1)* and *set-26 (Y51H4a.12)* were identified as exhibiting synthetic defects with the double mutant. Interestingly, *set-9* and *set-26* are paralogous, with 96% protein sequence identity. Both are predicted to produce proteins with both a SET domain and a PHD domain (plant homeodomain). The sequence identity is such that targeting either by RNAi is predicted to knock down the function of both. We did not observed obvious defects in wild type L4 animals treated with *set-9(RNAi)*, and *wdr-5.1; wdr-5.2* animals treated with *set-9* dsRNA developed into fertile adults. However, 100% of the offspring of the *wdr-5.1/5.2; set-9(RNAi)* animals were sterile at 20°C. DAPI staining of the dissected gonads showed 94.7% (n=19) exhibited the Mog phenotype (Figure 3-11A). Consistent with this, TRA-1 staining in the distal germ cell nuclei was significantly decreased in the mutant gonads at this temperature (Figure 3-11B), suggesting that *wdr-5.1/wdr-5.2* and *set-9/set-26* might work in parallel or in a complex to regulate TRA-1 localization. As no biochemical function has as yet been described for SET-9/SET-26, the role of these proteins in TRA-1-dependent regulation is undefined.

## Discussion

In this study, we provide evidence that *wdr-5.1* and *wdr-5.2* function redundantly as regulators of sex determination in *C. elegans*. Our data suggest that both WDR-5.1 and WDR-5.2 are required for TRA-1 to bind stably to chromatin at elevated temperatures. WDR-5.1, and with partial redundancy WDR-5.2, are thus required for TRA-1 to transcriptionally repress its sex-dependent targets, including *fog-3, mab-3,* and *egl-1*. The only partially redundant activity of WDR-5.2 indicates that it can probably compensate for the loss of WDR-5.1 in TRA-1 repression mechanisms, but it does so either poorly, or it is not expressed at sufficient levels in the right tissues. Interestingly, WDR-5.2 cannot compensate for loss of WDR-5.1 in the latter's role in H3K4 methylation (Chapter 1 and discussed below). This further indicates separate roles for WDR5 in the Set1/MLL like histone H3K4 methylation mechanisms and sex determination via TRA-1 mediated transcriptional repression. Intriguingly, two SET domain containing proteins, *set-9* and *set-26*, show synthetic fertility defects with *wdr-5.1/.2*, suggesting that they might operate in the same complex or in parallel pathways that both regulate sex determination.

### *wdr-5.1* and *wdr-5.2* are redundantly required for normal sex determination

Mammalian WDR5 is a WD40 repeat protein and an essential component of H3K4-specific HMTase complexes. WDR5 plays a central role in the assembly of the core complex and regulation of its HMT activity (Dou et al., 2006; Patel et al., 2008a; Ruthenburg et al., 2007). In *C. elegans*, there are 3 WDR5 homologues: *wdr5.1; wdr-5.2* and *wdr-5.3*. *wdr-5.1* is required for the normal maintenance of H3K4me3 and H3K4me2 in early embryos and the germline. Inactivation of *wdr-5.1* results in defects in a dramatic

loss of H3K4me2/3 from early embryonic and adult germline stem cell population, with defects in fertility (Chapter 2). In contrast, WDR-5.2 is dispensable for H3K4 methylation and deletion of *wdr-5.2* does not produce any obvious phenotypes on its own. Interestingly, WDR-5.1 and WDR-5.2 have partial, but not completely overlapping functions in the regulation of sex determination. Inactivation of both genes significantly increases the frequency of Mog, a sex determination defect with which the hermaphrodite germline fails to switch to oogenesis. *wdr-5.1/wdr-5.2* also contributes to the normal development of male tale sensory rays and male fertility (Figure 3-2). These activities appear to be independent of the role of WDR5 in H3K4 methylation. First, *wdr-5.1* and *rbbp-5* are both non-redundantly required for global H3K4me2/3 maintenance in early embryos and adult germline (Chapter 1, Figure 2, -1, -4 and -5). Disruption of either of them exhibits roughly the same H3K4me2/3 pattern defects, indicating that a complex that includes both proteins, as is the case in yeast and mammals, is probably involved (Dou et al., 2006; Miller et al., 2001; Ng et al., 2003; Roguev et al., 2001; Wysocka et al., 2005). However, the *rbbp-5* deletion mutant is not Mog at either 20°C or 25°C, whereas *wdr-5.1;wdr-5.2* show high frequency of Mog (Figure 3-3). These data strongly suggest that the function of *wdr-5* to regulate sex determination is independent of its role in H3K4 methylation. Second, *wdr-5* and *set-2* are both essential for the maintenance of H3K4me3 at the promoter of *fog-3* (Figure 3-6); while *set-2* mutation has no effects on *fog-3* expression (Figure 3-5). In contrast, inactivation of *wdr-5.1* and *wdr-5.2* causes a dramatic escalation of *fog-3* expression, indicating that *fog-3* repression is dependent on *wdr-5* but not H3K4 methylation.

WDR5 has been shown to operate in complexes without HMT activities in other systems. For example, it has been suggested that a WDR-5-Ash2L-RbBP5 tripartite complex interacts with NIF-1 (nuclear receptor co-regulator interacting factor 1) to promote the expression of nuclear hormone receptor responsive genes (Garapaty et al., 2009). WDR5 is also found in human CHD8-containing ATP-dependent chromatin-remodeling complex and ATAC complex (Thompson et al., 2008). However, none of these complexes exhibits MLL or Set1 based HMT activities. Our finding provides further evidence that WDR5 can play roles in transcriptional regulation, and that these roles function independent of H3K4 methylation.

**Regulation of TRA-1 by *wdr-5***

The nematode hermaphrodite germline first undergoes spermatogenesis during larval stages followed by a switch to oogenesis. This unique sperm/oocyte decision is tightly controlled by a genetic pathway composed a number of genes operating in a negative regulatory manner (Figure 3-5A). *tra-1* is the terminal transcription factor in this sex determination pathway. It has been shown that *tra-1* promotes female fate by repressing male-specific genes in all tissues. In the germ line, *tra-1* facilitates oogenesis by inhibiting the expression of *fog-1* and *fog-3*, which function as activators of spermatogenesis (Figure 3-5A). FOG-1 is a homolog of CREB (the cytoplasmic polyadenylation element binding protein), and FOG-3 is a member of the Tob family with an unknown molecular function. Both genes are required for initiation and maintenance of spermatogenesis (Chen and Ellis, 2000; Chen et al., 2000).

It has been shown that TRA-1A binds to the promoter of *fog-3* to repress its expression (Chen and Ellis, 2000). However, how the activity of TRA-1 is regulated remains unsolved. It is reported that the overall levels of TRA-1 is similar in both sexes whereas nuclear TRA-1 levels are higher in hermaphrodites that in males, suggesting that nuclear localization plays a role in the regulation of TRA-1 activity (Segal et al., 2001). However, the opposite conclusion was made in another study which found that TRA-1 was primarily localized in the nuclei in both sexes while the hermaphrodites have higher protein levels of TRA-1 (Schvarzstein and Spence, 2006).

We identified WDR-5.1 and WDR-5.2 as new regulators for normal sex determination in *C. elegans*. We demonstrated that WDR-5.1 and WDR-5.2 are partially redundantly required for normal sperm/oocyte switch at elevated temperature. Hermaphrodites lacking both *wdr-5.1* and *wdr-5.2* appear to be defective in either the initiation or the maintenance of oogenesis, and/or the repression of spermatogenesis and keep making sperm. We analyzed the mRNA levels for the major genes in the sex determination pathway including: *gld-1, fog-2, tra-2, mog-1, fbf-1/2, fem-1/2/3, tra-1,* and *fog-1/3* (Figure 3-5A). Among these genes, only *fog-3* was identified to be upregulated in the *wdr-5* double mutant. This upregulation appears to be controlled at the transcriptional level, which would implicate TRA-1 in the process. Notably, this function of *wdr-5.1* and *wdr-5.2* exhibits the maximal effect at 25°C. We detected low levels of *fog-3* expression in the adult germ cells in *wdr-5.1;wdr-5.2* at 20°C and these worms did not exhibit Mog. At 25°C, *fog-3* mRNA levels was dramatically increased in the germ cells of *wdr-5.1;wdr-5.2* and the animals showed high Mog frequency. Hence, it's possible that the dose of FOG-3 might play a critical role in sperm/oocyte decision.

Epistatic analysis reveals that *wdr-5.1/wdr-5.2* is upstream of *fog-3* and downstream of *fem-3* and thus is at the same position as *tra-1* (Figure 3-5A). TRA-1 can recognize the specific sequence in the promoter of *fog-3* and repress its expression (Chen and Ellis, 2000). Thus WDR-5.1/WDR-5.2 might execute their effect through regulating TRA-1 or in parallel with TRA-1. Given the fact that *wdr-5.1/wdr-5.2* has no effects on *tra-1* mRNA levels, they might regulate TRA-1 post-transcriptionally. Consistent with this idea, we found that TRA-1 was depleted from nuclei in the absence of *wdr-5.1* and *wdr-5.2*. This depletion might contribute to ectopic expression of *fog-3*, which then promotes spermatogenesis in adult germ cells. As a result, the animals exhibited Mog phenotype. Taken together, our data suggest that WDR-5 is required for the association of TRA-1 with chromatin to promote oogenesis by inhibiting *fog-3* expression. However, the molecular mechanisms underlying the interaction between WDR-5 and TRA-1 need further investigation.

**Synthetic effects with *set-9/set-16***

The worm SET-9 and SET-26 are 96% identical in protein sequence and are related to Set3 and Set4 in yeast and MLL5 in mammals. All these proteins contain a SET domain and a PHD finger close to the middle of the protein. The yeast Set3 has been shown to be a subunit of a complex including a WD40 repeat protein: Sif2 and two histone deacetylases: Hos2 and Hst1 (Pijnappel et al., 2001). This complex involves in the repression of sporulation genes during meiosis. No HMT activities are detected for Set3.

The mammalian MLL5 showed low similarity with Set1/MLL1-4 which contains HMT activities. This protein plays an important role in adult haematopoiesis (Zhang et al.,

2009). Recently it was reported that MLL5 operates in a complex containing retinoic acid receptor α (RARα). It has H3K4 mono- and di- methyltransferase activities that can be evoked by O-linked glycosylation at threonine 440 (T440) in the SET domain. This HMT activity then co-activates RARα dependent genes (Fujiki et al., 2009).

Worm *set-9* has been shown to regulate life span. RNAi of *set-9* was observed to extend life span in a manner that depends on the presence of DAF-16, a FoxO ortholog, while *set-26* had no obvious defects in their RNAi assay (Hamilton et al., 2005). RNAi inactivation of *set-9* is also reported to rescue some phenotypes of an *hpl-1* (heterochromatin protein-1 like) mutant, suggesting that *set-9* might antagonize *hpl-1* activities (Simonet et al., 2007). Whether SET-9 and SET-26 have any HMT activity is not known. In my hands, RNAi inactivation of both genes in the *eri-1(mg366)* genetic background, a hyper-sensitive RNAi strain, or RNAi knockdown of *set-26* in *set-9 (n4949)* showed neither fertility defects and nor affected global H3K4 methylation (data not shown). Interestingly, we observed a synthetic Mog effect between *wdr-5.1/wdr-5.2* and *set-9/set-26*. This effect was not temperature sensitive: *wdr-5.1;wdr-5.2* double mutant exhibits Mog phenotype at 25°C; RNAi inactivation of *set-9* and *set-26* in these animals leads to Mog at 20°C (Figure 3-11A). This indicates that SET-9/SET-26 are required for oogenesis in the absence of WDR-5.1/WDR-5.2 at 20°C. Furthermore, nuclear TRA-1 staining is significantly reduced in the adult germ cells of these animals; and TRA-1 staining can be restored by a transgene expressing only WDR-5.1::GFP. These data suggest that *wdr-5.1/wdr-5.2* and *set-9/set-26* may work in parallel pathways that converge at certain point to post-transcriptionally regulate TRA-1. Another possibility is that WDR-5.1/WDR-5.2 and SET-9/SET-26 are subunits of a yeast

Set3/Hos2-like repressive complex that contributes to the TRA-1 based repression. It has been suggested that TRA-1 operates in a complex composed of TRA-4, histone chaperone NASP and HDA-1/HDAC (Grote and Conradt, 2006). It's highly possible that WDR-5.1/WDR-5.2 and SET-9/SET-26 are subunits of this complex and function in a way similar as their yeast counterparts, Sif2 and Set3 respectively. Further studies are required to address this possibility.

## Materials and Methods

### Worm Strains:

*C. elegans* strains were maintained using standard conditions at 20°C unless otherwise noted. N2 (Bristol) was used as the wild-type *C. elegans* strain. The following mutant strains were used in this study: *set-2(tm1630)III, wdr-5.1(ok1417)III, wdr-5.2(ok1444)X, rbbp-5(tm3463)II, tra-1(e1834), set-9(n4949)*. Double mutant of *wdr-5.1;wdr-5.2* was generated by cross between *wdr-5.1(ok1417)III, wdr-5.2(ok1444)X*. The genotypes were confirmed with PCR. The *wdr-5.1::GFP* integrated transgenic strain was a generous gift from Dr. F.Palladino, Ecole Normale Superieure de lyon, France. The *wdr-5.1;wdr-5.2* strain carrying *wdr-5.1::GFP* was generated through crossing and conformed by genotyping PCR and the roller phenotype. Primers for genotyping were shown in Table 3-2.

### RNAi Analysis

Double stranded RNA (dsRNA) corresponding to *fog-3*, *fem-3, set-9 and set-16* were generated using the Ribomax Large Scale RNA production kit (Promega). L4 staged *wdr-5.1;wdr-5.2* animals were soaked in 1ug/ul of dsRNA for 24 hours at 20°C. The worms were then grown on feeding plates containing bacteria expressing dsRNA targeting the corresponding gene, or carrying the empty L4440 vector for control experiments. After the first 24 hours, the worms (P0) were transferred to a new set of feeding plates. F1 animals (24 hours post L4) were assessed for sterility and analyzed by immunofluorescence.

**Immunofluorescence**

Worms were dissected and fixed in paraformaldehyde/methanol for H3K4me2/3, TRA-1 and GFP staining. Rabbit anti-H3K4me3 (1:1000) was purchased from Abcam (ab8580). Mouse monoclonal antibody against H3K4me2 (CMA303; 1:20) were gifts from Dr. Hiroshi Kimura (Osaka University, Japan. Mouse monoclonal antibody against GFP (1:500) was purchased from Millipore. Rabbit anti-TRA-1 (1:100) antibodies were gifts from Drs. David Zarkower (University of Minnesoda) and Andrew Spence (University Torondo). DAPI (Sigma, 2ug/ul) was used to counter-stain DNA. All secondary antibodies were purchased from Molecular Probes and were used at 1:500 dilutions: goat anti-mouse IgG (Alexafluor 488); goat anti-rabbit IgG (Alexafluor 594), donkey anti-rabbitIgG (Alexafluor 488); donkey anti-mouse IgG (Alexafluor 594). Worms were mounted in anti-fade reagent (Prolong Gold, Molecular Probes). Images were collected using a Leica DMRXA fluorescence microscope and analyzed with Simple PCI software (Hamamatsu Photonics).

**Quantitative RT-PCR analysis**

About 80 gonads were dissected out in 30ul dissection buffer (0.5uM levamisole and 0.01% Tween 20 in 1X egg buffer) and transferred into a depressed glass well containing 200ul of wash buffer (0.01% Tween 20 in 1X egg buffer) using a mouth pipette. After washing, the gonads were transferred to Eppendorf tubes and centrifuged briefly to remove extra liquids. To purify RNA from whole worms, 100 L4 or adults were picked into 20ul of 1X PBS. 200ul Trizol reagent was added to the samples and frozen in liquid nitrogen. The samples were thawed, vortexed, and refrozen four times. After four cycles, the sample was extracted and precipitated with isopropanol, washed with 75% ethanol, and dissolved in RNase free water. The isolated RNA was reverse-transcribed by using the Invitrogen First Strand Synthesis System with Oligo(dT) 20 priming. The results were normalized to *actin-1* (act-1). The qPCR analyses were performed using a real-time PCR instrument (BIO-RAD CFX 96 real time system) with reaction mix (iQ SYBR Green Master Mix; Bio-Rad). The qPCR primers are shown in Table 3-2.

**Western Blot Analysis**

160 gonads were dissected and washed with PBS as described above. After removing extra PBS, SDS-PAGE sample buffer were added. To make whole worm lysate of *tra-1(e1834)*, 100 worms were picked into a tube contain 10ul of PBS. 10ul of 2XSDS-PAGE sample buffer were added to the samples and boiled for 5 min. The samples were loaded and run on an 8% SDS-PAGE gel and transferred to PVDF membrane. The

proteins were probed with a rabbit polyclonal antibody against TRA-1 at 1:1000 (a gift from Dr. Zarkowa, University of Minnesoda) or anti-ACTIN (Chemicon) at 1:1000.

**ChIP assay**

The H3K36me3 and H3K4me3 ChIP were done as described by Katz et al. (2009). Briefly, worms were collected in M9 buffer and bleached in 1N NaOH/20% bleach to collect embryos. The embryos were hatched overnight at 20°C and the synchronized L1 were transferred to NGM plates and grown at 25°C. L4 or adults were collected into 1X PBS containing proteinase inhibitor (Roche, Cat#: 11836170001) and frozen in liquid nitrogen. The worms were fixed in 1% formaldehyde and sonicated for 200 s (4 s on/10s off) at 20% in a Fisher Sonic Dismembrator 500. Rabbit anti-H3K4me3 (Abcam, ab 8580), anti-H3K36me3 (ab9050) and anti-H3 (ab1791) was used for immunoprecipitation. The primers (fog-3-F/R-promoter for H3K3me3 and fog-3-F2/R2 for H3K36me3) for QPCR are shown in Table 3-2.

**Table 3-1. Phenotypic analysis of *set-2* and *wdr-5* (*wdr-5.1 and wdr-5.2*) mutants** Adults of *swd3.1 (OK1417)* were picked and shifted to 25°C. 100 hermaphrodite adults of next generation (F1) were picked and checked for embryos. Animals containing no embryos were sterile.

| | Emb | | Sterility | |
|---|---|---|---|---|
| | 20°C | 25°C | 20°C | 25°C |
| WT | 0.6% (n=619) | 2.7% (n=1509) | 0 (n=114) | 0.75% (n=133) |
| *wdr-5.1 (ok1417)* | 12% (n=1201) | 36% (n=557) | 2.5% (n=119) | 29% (n=89) |
| *wdr-5.2 (ok1444)* | 0 (n=693) | 1.7% (n=1320) | 0 (n=101) | 0.9% (n=111) |
| *wdr-5.1; wdr-5.2* | 19% (n=616) | 42% (n=352) | 16% (n=141) | 100% (n=99) |

**Table 3-2. Primers used**

| | | |
|---|---|---|
| **qRT-PCR primers** | ***fog-3-F*** | **TTTATCGGAGAACGGAATCG** |
| | ***fog-3-R*** | **ACGTACTCGGGGACTGATTG** |
| | ***act-F*** | **TGCTGATCGTATGCAGAAGG** |
| | ***act-R*** | **TAGATCCTCCGATCCAGACG** |
| | ***mab-3-F*** | **CCCGAGATGGTAAAGAACCA** |
| | ***mab-3-R*** | **TGGACTTGCTGATGTTCCAA** |
| | ***egl-1-F*** | **CGATGACTTCGATGCTCAGA** |
| | ***egl-1-R*** | **GCGAAAAAGTCCAGAAGACG** |
| | ***vit-1-F*** | **CACAGTTCTGAAGCCAGACG** |
| | ***vit-1-R*** | **AATAAGCGACGCAAGCAACT** |
| **ChIP primers** | ***fog-3-F-promoter*** | **GAAGCTCGCACTTTCGTTTT** |
| | ***fog-3-R-promoter*** | **CGCGGACTTCGGTATACATT** |
| | ***fog-3-F2*** | **CAATGTATTCTCCATTGGCG** |
| | ***fog-3-R2*** | **TTTGAGCAGATGACGGCTTG** |
| **Genotype primers** | ***wdr-5.1-F*** | **ATTGTGTGTTCGCTGTGCAT** |
| | ***wdr-5.1-R*** | **TCTGGAGATTGGAGATGTAG** |
| | ***wdr-5.1-R2*** | **GAACGGATTCATCGAATGATCCGG** |
| | ***wdr-5.2-F*** | **TCTGGCAGTGTGCAAATGAT** |
| | ***wdr-5.2-R*** | **TCGAGTCGCTGCTCCATGAG** |
| | ***wdr-5.2-R2*** | **TGGAGCAACTTGAGCAAAGATATG** |

**Figure 3-1. *wdr-5.1* plays a primary role in the regulation of H3K4 methylation**

Gonads or embryos were dissected form WT, *wdr-5.1 (ok1417), wdr-5.2(ok1444), and wdr-5.1;wdr-5.2* double mutants and were probed with rabbit anti-H3K4me3 or mouse anti-H3K4me2 monoclonal antibodies; DNA was counterstained with DAPI. Exposure times were the same for each condition. Gonads were displayed with the distal region to the left. (A and B) *wdr-5.1*, but not *wdr-5.2*, were required for normal maintenance of H3K4me3 (panel A) and H3K4me2 (panel B) in the distal region of the gonads. Scale bars represent 20um. *wdr-5.1;wdr-5.2* double mutant exhibited similar defective pattern as that in *wdr-5.1*. (C) *wdr-5.1* played a primary role in the maintenance of H3K4me3 and H3K4me2 in embyos; while *wdr-5.2* is dispensable. Scale bar represents 10um.

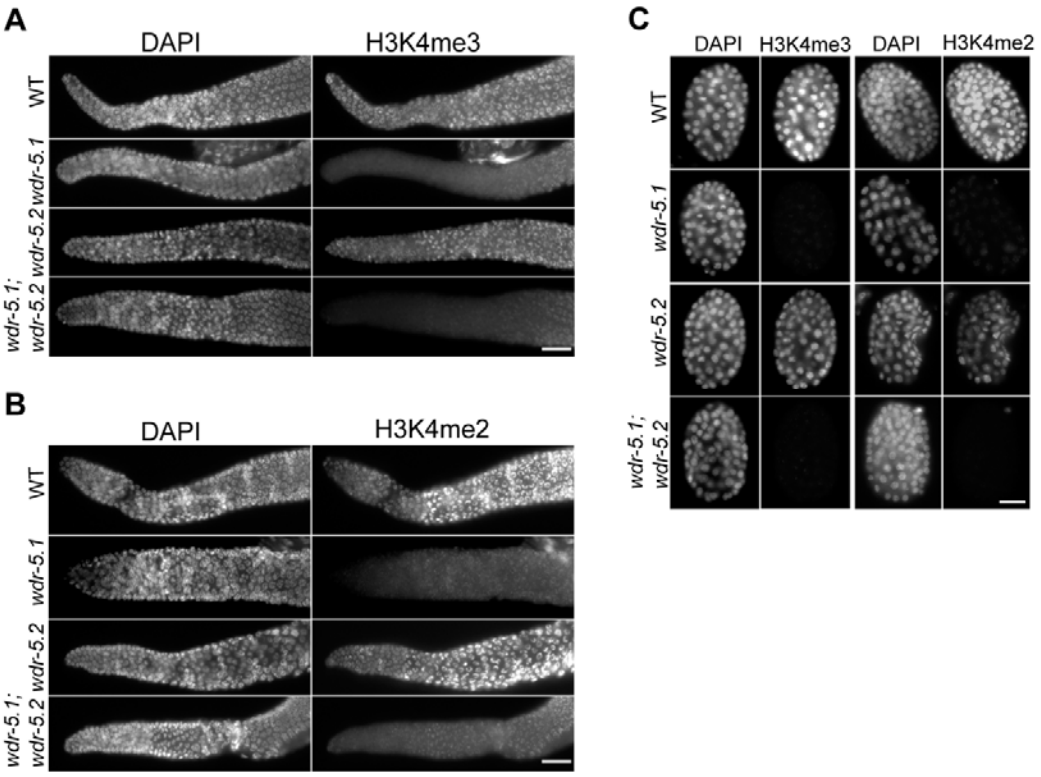
A
DAPI
H3K4me3
WT
wdr-5.1
wdr-5.2
wdr-5.1; wdr-5.2
B
DAPI
H3K4me2
WT
wdr-5.1
wdr-5.2
wdr-5.1; wdr-5.2
C
DAPI
H3K4me3
DAPI
H3K4me2
WT
wdr-5.1
wdr-5.2
wdr-5.1; wdr-5.2

**Figure 3-2. Male tail defects in *wdr-5.1;wdr-5.2***

Adult males (24 hours post L4) were mounted onto an agarose pad and images were taken using a Leica DMRXA fluorescence microscope.

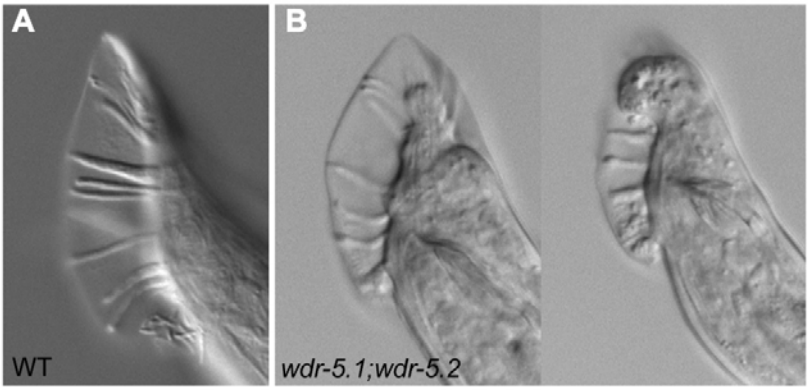
A
WT
B
wdr-5.1;wdr-5.2

**Figure 3-3. *wdr-5.1;wdr-5.2* double mutant exhibits temperature sensitive Mog phenotype**

Young adults of wild type and *wdr-5.1; wdr-5.2* were shifted to 25°C. Adults F1 animals (24 hours post L4) were picked and stained with DAPI. (A) DAPI staining of extruded gonads: Sterile *wdr-5.1; wdr-5.2* exhibited either Mog or Emo phenotypes at 25°C. Germ cells with Mog phenotype only produce sperm, while the gonads with Emo phenotype contain large nuclei composed of replicated DNA. (B) Summary of the frequency of Mog and Emo in *wdr-5.1(ok1417)* and *wdr-5.1;wdr-5.2*. (C) Differential interference contrast (DIC) micrographs of *wdr-5.1;wdr-5.2* and *wdr-5.1;wdr-5.2* carrying a transgene encoding WDR-5.1::GFP grown at 25°C. Arrow heads mark embryos. (D) *wdr-5.1; wdr-5.2* worms were upshifted from 20°C to 25°C or downshifted from 25°C to 20°C at different developmental stages. The animals were grown to adults and scored for sterility. The number of animals scored at each point was 100.

A

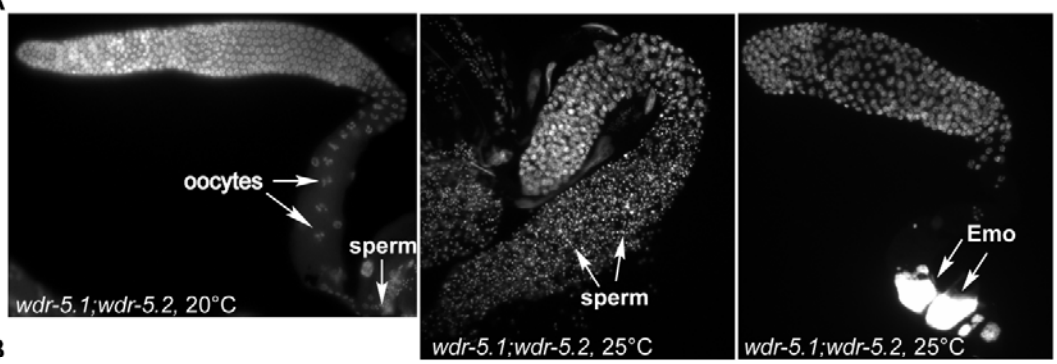


B

| | *wdr-5.1* (n=116) | *wdr-5.1; wdr-5.2* (n=237) |
|---|---|---|
| Emo | 75.9% | 11.8% |
| Mog | 5.1% | 88.2% |

C

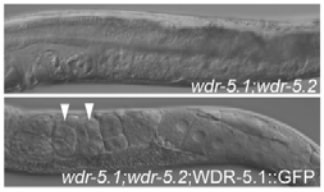


D

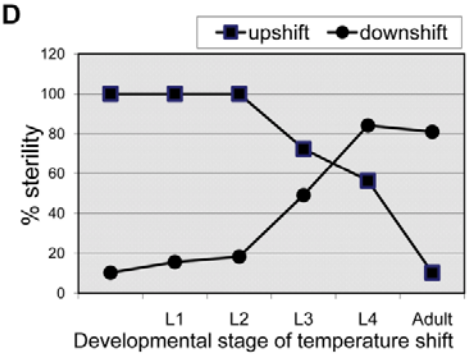

**Figure 3-4. Epistasis analysis of *wdr-5.1/wdr-5.2* in the sex determination pathway**

RNAi inactivation of *fog-3* or *fem-3* in *wdr-5.1; wdr-5.2* were done as described in materials and methods. 100 L1 larvae of F1 offspring were picked and grown at 25°C. The F1 Adults (24 hours post L4 at 25°C) were dissected and stained with DAPI. Pictures were taken and the phenotypes were analyzed. Gonads were displayed with the proximal region to the right. (A) RNAi inactivation of *fog-3* in *wdr-5.1; wdr-5.2* result in feminized germline. (B) Summary of the phenotypes of *fog-3* RNAi treated *wdr-5.1; wdr-5.2*. (C) Summary of the phenotypes of *fem-3* RNAi treated *wdr-5.1; wdr-5.2*. L4440 is vector-only control of RNAi. Knockdown of *fem-3* did not affect the Mog phenotype of *wdr-5.1; wdr-5.2*.

A

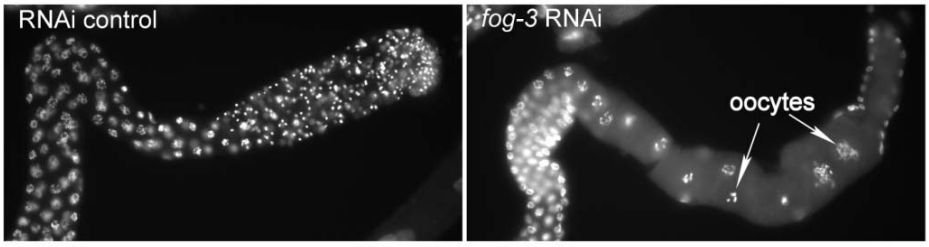


B

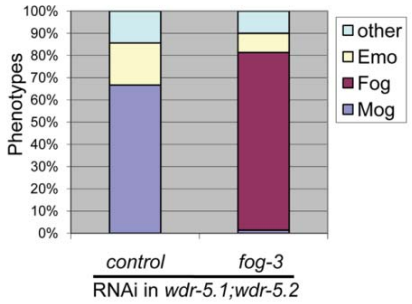


C

| | RNAi in *wdr-5.1; wdr-5.2* | |
|---|---|---|
| | L4440 (control) | *fem-3* |
| % of Mog | 60% (47/81) | 57.3% (39/68) |

**Figure 3-5. *wdr-5.1/wdr-5.2* negatively regulates the expression of *fog-3* in the germline**

(A) Genetic pathways of sex determination. Barred lines indicate negative regulations and arrows indicate positive regulations. (B) RNA was purified from dissected gonads and was converted to cDNA. qRT-PCR was performed using *fog-3* specific primers. *Actin-1* was used as an internal control. Signals were normalized to WT which was artificially set as 1. Error bars represent SEM based on 2 independent experiments. (C) RNA were purified from whole L4 or adult worms and converted to cDNA. RT-PCR was performed using *fog-3* specific primers. *Actin-1* was used as an internal control. The PCR products were analyzed on a 1.2% agrose gel. (D) ChIP assay of H3K36me3 of *fog-3*. H3K36me3 levels in the gen body of *fog-3* was reduced in WT adult compared to that of L4, while no significant changes were detected between L4 and adult in *wdr-5.1;wdr-5.2*. H3K36me3 were normalized to H3 levels at the same position. Error bars represent SEM based on 2 independent experiments.

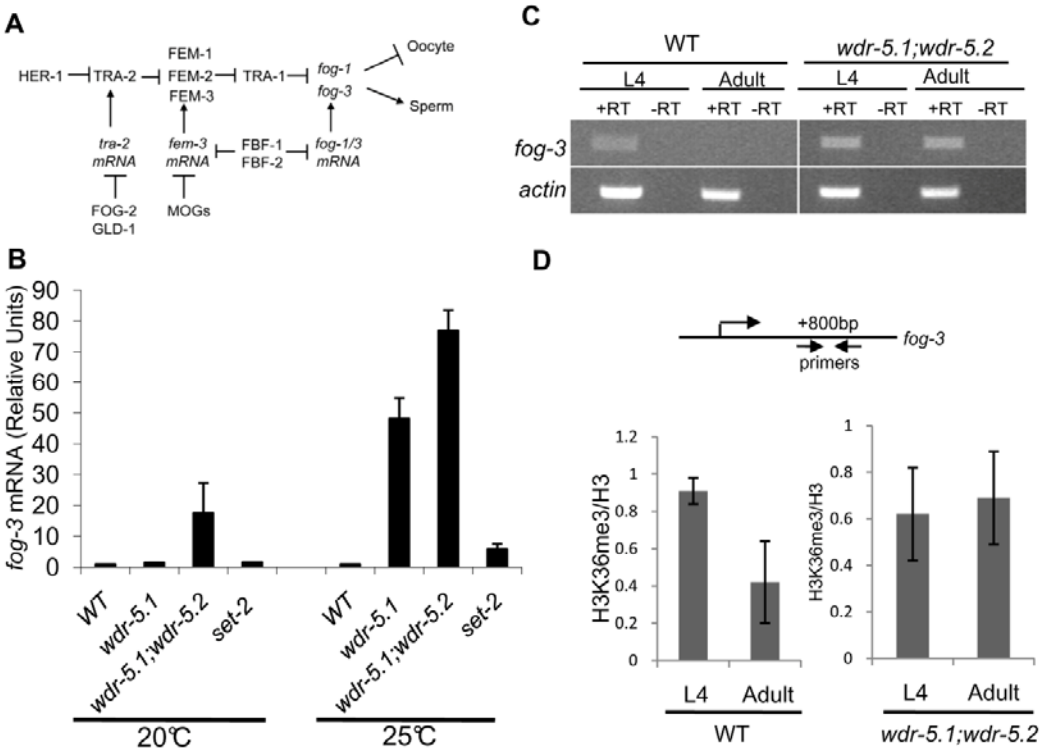
A
HER-1
TRA-2
FEM-1
FEM-2
FEM-3
TRA-1
fog-1
fog-3
Oocyte
Sperm
tra-2 mRNA
fem-3 mRNA
FBF-1
FBF-2
fog-1/3 mRNA
FOG-2
GLD-1
MOGs
B
fog-3 mRNA (Relative Units)
WT
wdr-5.1
wdr-5.1;wdr-5.2
set-2
20℃
25℃
C
WT
wdr-5.1;wdr-5.2
L4
Adult
+RT
-RT
fog-3
actin
D
+800bp
fog-3
primers
H3K36me3/H3
L4
Adult
WT
wdr-5.1;wdr-5.2

**Figure 3-6. *set-2* and *wdr-5* are required for normal H3K4me3 maintenance at *fog-3* promoter**

WT, *wdr-5.1;wdr-5.2* and *set-2* were grown at 25°C; adult worms were harvested for ChIP analysis. H3K4me3 levels at *fog-3* promoter were assayed by using anti-H3K4me3 and anti-H3 antibodies. H3K4me3 signals were normalized to H3.

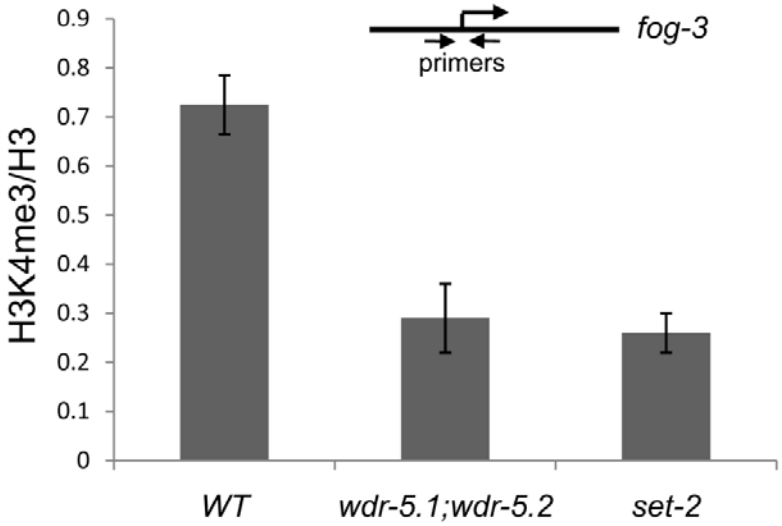
fog-3
primers
H3K4me3/H3
0.9
0.8
0.7
0.6
0.5
0.4
0.3
0.2
0.1
0
WT
wdr-5.1;wdr-5.2
set-2

**Figure 3-7. Both *wdr-5.1* and *wdr-5.2* are required for TRA-1 association with germline chromatin at 25°C**

(A) Dissected and fixed gonads was probed with rabbit anti-TRA-1 and counter stained with DAPI. The exposure time was equal for each condition. Gonads were displayed with the distal region to the left. TRA-1 staining was depleted from nuclei of *wdr-5.1;wdr-5.2*; while it remained largely unchanged in *wdr-5.1*. Bar=10um. (B) Gonads lysate from WT and *wdr-5.1;wdr-5.2* grown at 25°C and whole worm lysate of a *tra-1* null mutant *(e1834)* were analyzed by immunoblotting with a rabbit anti-TRA-1 antibody.

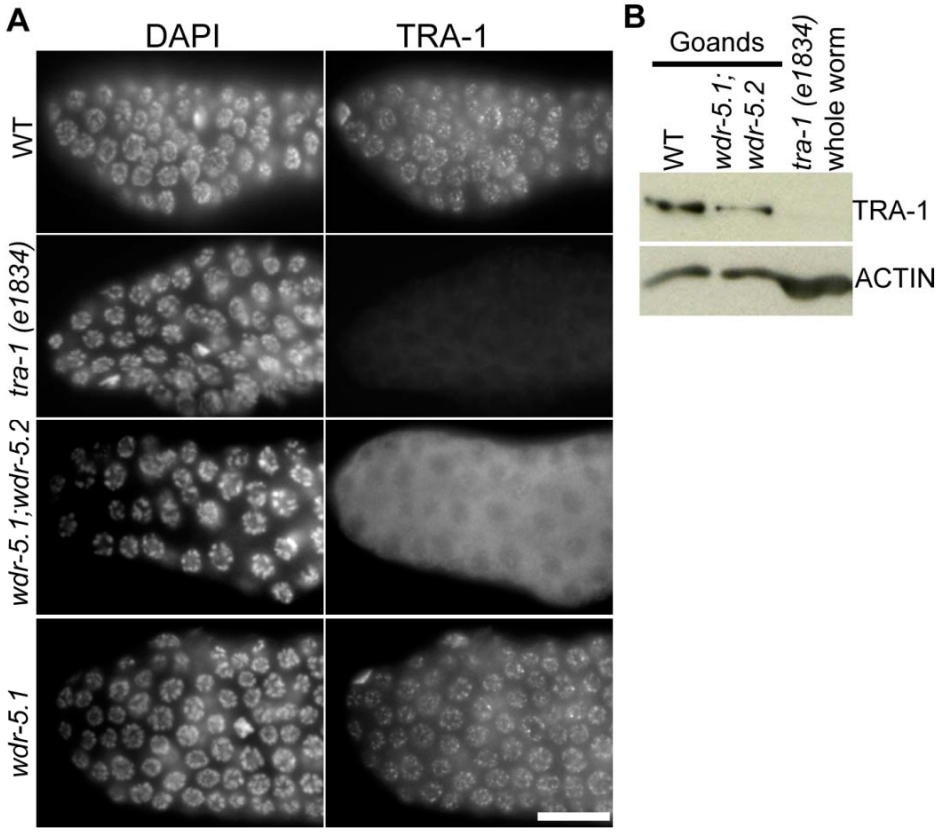
A
DAPI
TRA-1
WT
tra-1 (e1834)
wdr-5.1;wdr-5.2
wdr-5.1
B
Goands
WT
wdr-5.1; wdr-5.2
tra-1 (e1834)
whole worm
TRA-1
ACTIN

**Figure 3-8. TRA-1 staining pattern in the adult germ cells of WT and *wdr-5.1;wdr-5.2***

Adult animals were gown at 25°C; gonads were dissected and staining was performed as in Figure 4. DAPI was shown in red and TRA-1 in green. TRA-1 is associated with chromatin in distal germ cells in WT; *wdr-5.1;wdr-5.2* exhibited similar pattern.

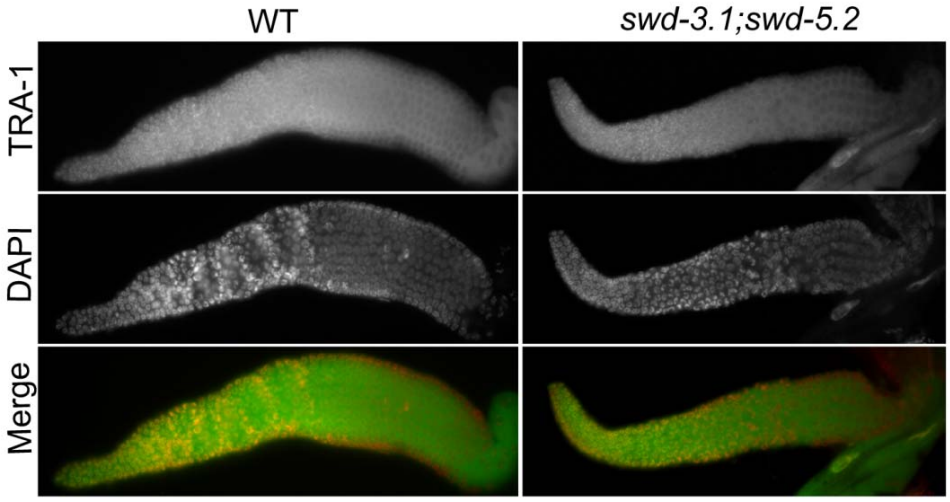
WT
swd-3.1;swd-5.2
TRA-1
DAPI
Merge

**Figure 3-9. A transgene expressing WDR-5.1::GFP restores the TRA-1 staining in the nuclei of *wdr-5.1;wdr-5.2***

Adult animals were gown at 25°C; gonads were dissected and staining was performed as in Figure 4. The transgenic WDR-5.1::GFP was expressed in adult germ cells (left panel) and TRA-1 staining were restored in the distal germ cells (middle panel). Bar=10um.

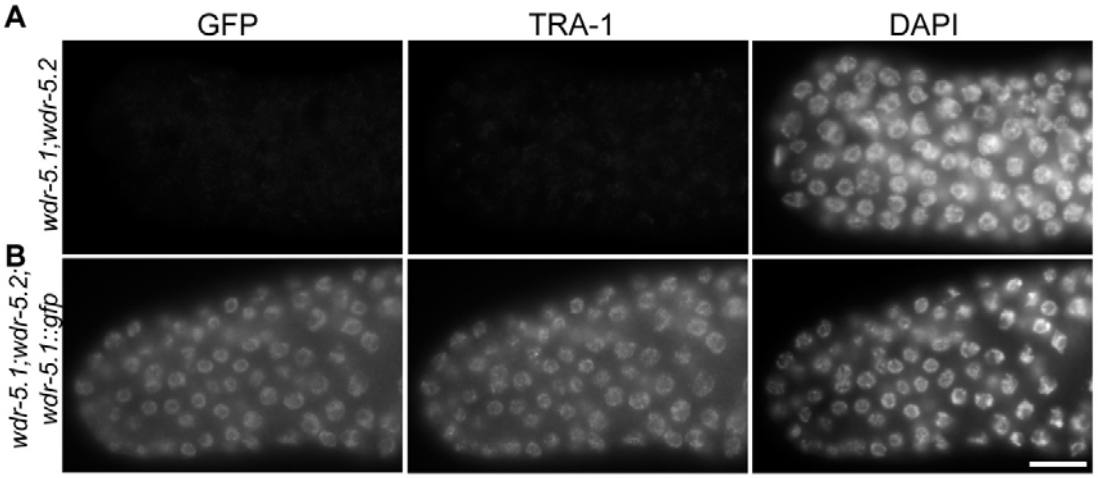
A
GFP
TRA-1
DAPI
wdr-5.1;wdr-5.2
B
wdr-5.1;wdr-5.2;
wdr-5.1::gfp

**Figure 3-10. *mab-3* and *egl-1* mRNA are upregulated in *wdr-5.1;wdr-5.2* mutant at 25°C**

100 worms of WT and *wdr-5.1;wdr-5.2* grown at 25°C were picked; RNA purification and qRT-PCR were performed as in Figure 3. *actin-1* was used as an internal control. Signals were normalized to WT which was artificially set as 1. Error bars represent SEM based on 2 independent experiments. (A) Genetic interactions controlling vitellogenin expression. Barred lines indicate negative regulations. (B) *mab-3* mRNA was upregulated in *wdr-5.1;wdr-5.2*. (C) *vit-1* mRNA was reduced in *wdr-5.1;wdr-5.2*. (D) *egl-1* mRNA was increased in both L4 larvae and adults in the absence of *wdr-5.1* and *wdr-5.2*.

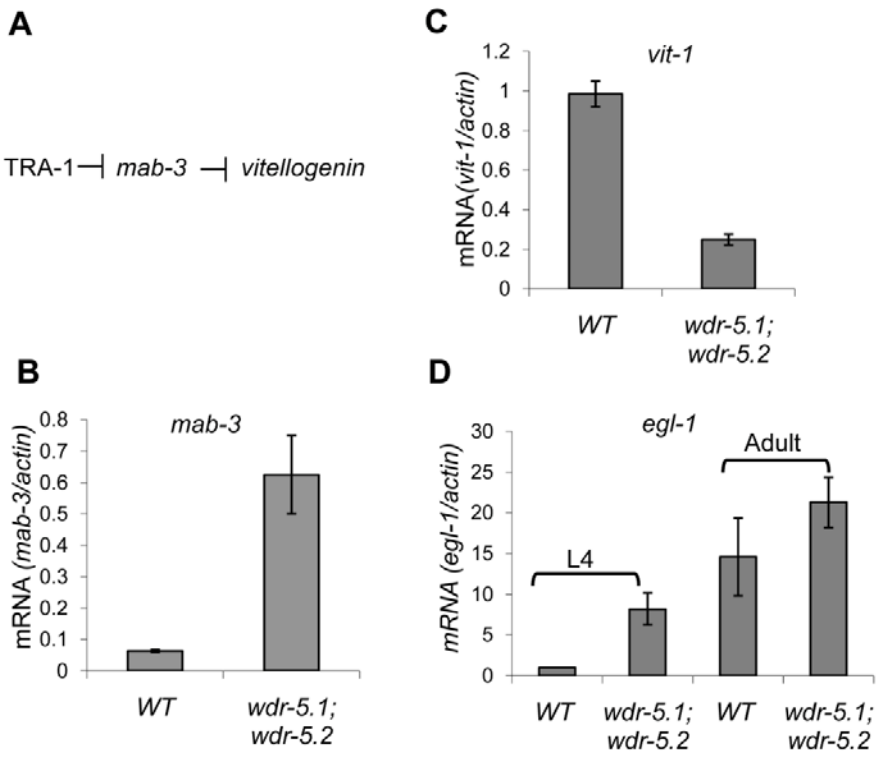
A
TRA-1 ⊣ mab-3 ⊣ vitellogenin
B
mab-3
mRNA (mab-3/actin)
0.8
0.7
0.6
0.5
0.4
0.3
0.2
0.1
0
WT
wdr-5.1; wdr-5.2
C
vit-1
mRNA(vit-1/actin)
1.2
1
0.8
0.6
0.4
0.2
0
WT
wdr-5.1; wdr-5.2
D
egl-1
mRNA (egl-1/actin)
30
25
20
15
10
5
0
L4
Adult
WT
wdr-5.1; wdr-5.2
WT
wdr-5.1; wdr-5.2

**Figure 3-11. Sythetic effects between *wdr-5.1/wdr-5.2* and *set-9/set-16* at 20°C**

RNAi treatment was performed for L4 larvae of *wdr-5.1;wdr-5.2* as described in materials and methods. All worms were grown at 20°C. Gonads of offspring (F1) were dissected and stained with DAPI or co-stained with TRA-1 and DAPI. Gonads were displayed with distal region to the left. (A) RNAi inactivation of *set-9/set-16* cause masculinization of germline in *wdr-5.1;wdr-5.2*. (B) TRA-1 staining was performed as in Figure 4. Knockdown of *set-9/set-16* in *wdr-5.1;wdr-5.2*.significantly reduce TRA-1 in the nuclei of the adult germ cells. Exposure times were the same for each condition. Bar=10um.

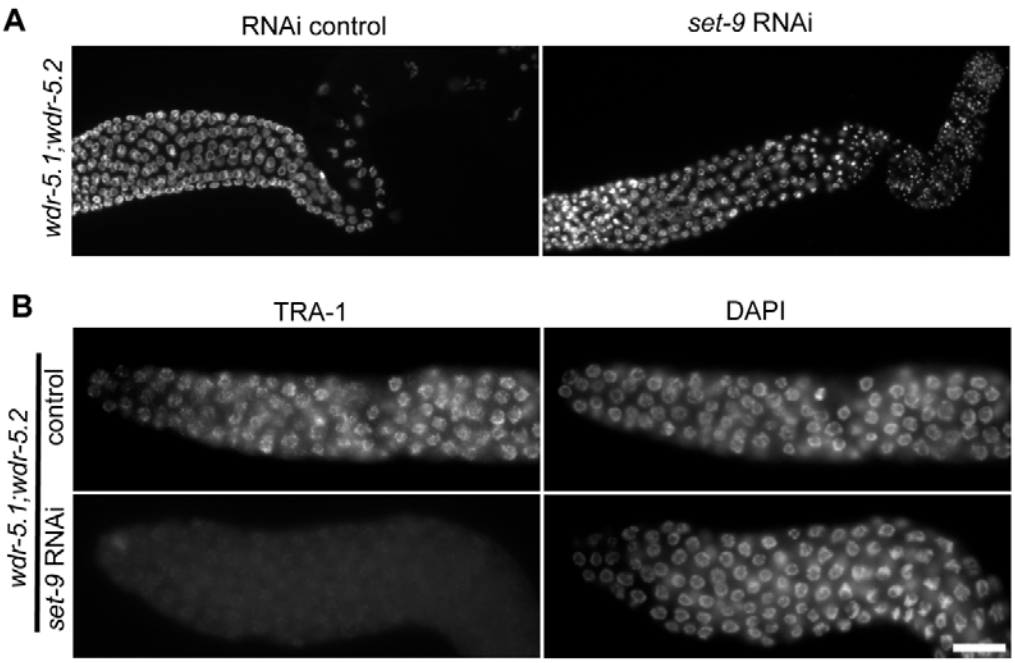
A
RNAi control
set-9 RNAi
wdr-5.1;wdr-5.2
B
TRA-1
DAPI
wdr-5.1;wdr-5.2
control
set-9 RNAi

# Chapter 4

## Discussion and Future Directions

The dynamics of histone modifications on chromatin is regulated in a number of ways. For example, they can be removed through histone variant incorporation which can occur independently of DNA replication. More commonly, the addition of a modification is catalyzed by histone modification enzyme activities. In *C. elegans*, the levels of methylation at lysine 4 of H3 (H3K4) change dramatically in the chromatin of germ cells at different developmental stages. These changes are thought to contribute to the specification and normal development of the germline (Schaner et al., 2003). The addition of methyl groups to H3K4 involves both transcription-dependent and transcription-independent mechanisms. The transcription independent mechanisms involve components that are homologues of the members of the yeast Set1/COMPASS complex (Chapter 2). These components include: WDR-5.1, RBBP-5, ASH-2, DPY-30 and CFP-1. They might create a platform that interacts with different HMTs to regulate H3K4 methylation. One component, WDR-5.1, can recognize the N-terminal tails of histone H3 and plays a central role in the regulation of HMT activities. Moreover, this WD40 repeat protein also plays a role in sex determination (Chapter 3). These findings have contributed to our knowledge regarding the regulation and the functions of H3K4 methylation and their regulators.

**Identification of components regulating H3K4 methylation in the germ cells of *C. elegans***

One of my goals was to identify HMTs that are responsible for the establishment and maintenance of the methylation patterns at H3K4 in germ cells. Since all known H3K4 specific HMTs share a SET domain (Martin and Zhang, 2007), we initially focused on

SET domain containing proteins. Blast searches with the SET domain sequence of yeast Set-1 identified 34 SET domain containing proteins in *C. elegans*. Homology analyses centering on the SET domain sequence, in addition to the presence and distribution of other motifs, revealed that worm SET-2 and SET-16 were most closely related to the mammalian Set-1A and MLLs, respectively (Figure 4-1). *set-2* and *set-16* have been indicated to be required for the maintenance of H3K4 methylation (Fisher et al., 2010; Simonet et al., 2007). However, their HMT activities in germ cells had not been described prior to my studies. In my hands, mutation of *set-2* only caused defects in H3K4me3 in the mitotic region of adult germ cells and in all cells in early embryos, but had no effect on H3K4me2 (Figure 2-2, 2-9 and 2-10). I also observed no increase in H3K4me2 in the *set-2* mutants, as might be expected from a defect in converting a di- to trimethyl state. Therefore, SET-2 activity may be completely processive; i.e., always converting from un- or mono- methylation to tri-methylation.

My data also indicates that separate HMT activities must be present to regulate H3K4me2. Surprisingly, although it is clear homolog to MLL, I observed no H3K4 methylation defects in the germ cells of *set-16* mutants. The lack of an obvious H3K4 methylation phenotype in the *set-16* mutant may be caused by two reasons: first, *set-16* may not be required for global maintenance and might function in a gene-specific manner, which we would not observe by immunofluorescence. Second, *set-16* may not be required in germ cells, which is the tissue I focused on—although I did not see obvious changes in somatic lineages. Interestingly, the *set-16(gk438)* mutation is lethal, which is the most severe phenotype I observed for any SET domain targets studied.

*set-9* and *set-2* have both been reported to play roles in antagonizing the effect of *hpl-2* (heterochromatin protein like-2) (Simonet et al., 2007), suggesting that *set-9*, like *set-2*, might have functions to promote H3K4 methylation. However, RNAi inactivation of *set-9* and its paralog, *set-26*, did not show defects in H3K4me2 and me3 in germ cells (data not shown). To identify additional HMTs, we tested a few other SET-domain containing proteins that might have HMT activities based on SET domain sequence and other motifs they contained (Figure 4-1). These genes include: *lin-59, set-12/K09F5.5, set-23/Y41H4a.12* and *set-25*. RNAi inactivation of each of these genes did not cause defects in H3K4me2/3 in germ cells. Future experiments might include combined RNAi to knock down two or more candidate genes to reduce the potential redundant effects between these genes. Alternatively, *in vitro* assays of purified SET domain polypeptides from these genes for HMT activities could be a powerful way to identify more HMTs and characterize their specificities.

The budding yeast Set-1 HMT operates in a complex called COMPASS composed of seven proteins (Dehe and Geli, 2006; Miller et al., 2001; Nagy et al., 2002; Roguev et al., 2001). *C. elegans* has orthologs for all the subunits except Shg1 (Table 2-1). All the worm components except *wdr-82* are non-redundantly required for both H3K4me2 and me3 in early embryos. Interestingly, only *wdr-5.1* and *rbbp-5* are required in the post embryonic germ cells. Therefore, WDR-5.1 and RBBP-5 might operate in a different complex with different components in post-embryonic germ cells. However, these different complexes presumably rely on common subunits, WDR-5.1 and RBBP-5, which are shared with the embryonic activity. In both tissues, the HMT required for H3K4me3 is SET-2; the HMT providing H3K4me2 is unknown, and is not among the

multiple SET domains our lab has tested. Interestingly, it was reported that a complex composed of WDR-5, RbBP5, Ash2L and Dpy30 was able to methylate unmodified H3 peptide at K4 (Patel et al. 2009). Recently another group report that the heterodimer of Ash2L and RbBP5 had intrinsic HMT activity (Cao et al., 2010). This raises the possibility that the H3K4me2 HMT activity shown in the WDR-5.1, Ash2L and RBBP-5 containing complexes comes from WDR-5.1, Ash2L or RBBP-5. It would be interesting to determine if a minimal complex of composed of these three worm proteins have HMT activity.

The yeast Set-1/COMPASS complex is recruited to chromatin by the transcription machinery and is thus strictly coupled to transcription (Krogan et al., 2003; Ng et al., 2003). Hence H3K4 methylation has been considered to be a direct consequence of transcription. In mammals, WDR5 and its associated complexes have been indicated in promoting transcription through methylating H3K4. Knockdown of WDR5 leads to downregulation of Hox genes (Wysocka et al., 2005). Surprisingly, the WDR-5 mediated H3K4 HMT activity can be uncoupled from ongoing transcription in *C. elegans*. For example, H3K4me2/3 is maintained in the chromatin in all nuclei, including the transcriptionally-inert P-lineage, in early embryos where there is little zygotic transcription, and clearly no genome-wide activation at these stages (Edgar et al., 1994; Seydoux and Dunn, 1997). Instead, these cells appear to be maintaining the H3K4me2 patterns that arrived within the gamete chromatin (J. Arico and WG Kelly, manuscript submitted). I have found that this global maintenance of gamete-derived H3K4me2 patterns is mediated by WDR-5 based mechanisms. It's highly possible that the embryonic cells at these stages are pluripotent and have properties resembling those of

mouse ES cells. It was reported that some regions of chromatin of ES cells are in a bivalent state which harbors both H3K4me3 and H3K27me3 (Bernstein et al., 2005; Bernstein et al., 2006). It would be very interesting to determine if such bivalent domains exist in worm chromatin in early embryos by using ChIP-chip or ChIP-Seq assays. It may be possible to determine the chromatin regions where H3K4 methylation is controlled by WDR-5 dependent mechanisms. These experiments might provide implications into the mechanisms responsible for the epigenetic signatures associated with pluripotency.

WDR-5.1 mediated HMT activities play a primary role in the population of mitotic germline stem cells located in the distal region of gonad. RNAi inactivation of *ama-1*, the large subunit of the RNA polymerase II, did not affect H3K4 methylation in these cells, although H3K4 methylation in the meiotic cells was decreased (Figure 2-16), suggesting that WDR-5.1 mediated HMT activities are independent of RNA polymerase II activities. Knockdown of *ama-1* in *wdr-5.1* abolished the H3K4 methylation in meiotic cells, too, indicating that H3K4 methylation in meiotic cells is regulated by two mechanisms: a transcription-dependent mechanism and transcription-independent HMT activities mediated by *wdr-5.1*. Furthermore, we observed *wdr-5.1*-independent HMT activities in late stages of embryogenesis and primordial germ cells in L1 and L2 larvae (Figure 2-18). A low level of H3K4me2, restricted to a banding pattern rather than the normal mostly even distribution, was also detected in the germline stem cells of *wdr-5.1* mutant (Figure 2-14). These HMT activities are presumably transcription-dependent, as they are affected by reduction in RNA Pol II. Further investigation is required to confirm this idea. Since embryos lacking AMA-1 cannot develop into late stages, a conditional *ama-1* knockout strain such as temperature sensitive mutation needs to be created. With

this strain, we would be able to study transcription-dependent H3K4 methylation and its functions. To identify transcription dependent HMTs, a pull down experiment with AMA-1 specific antibodies followed by mass spectrometry analysis may help to achieve this goal.

Taken together, the H3K4 methylation status seems to be controlled by two parallel mechanisms: one is transcription-dependent and the other is transcription-independent. However, it's possible that the two processes are linked in certain ways. We propose that transcription-dependent HMT activities contribute to the creation of H3K4 methylation patterns and WDR-5.1-dependent mechanisms can amplify the established H3K4 methylation in the absence of transcription. A H3K4 methylation ChIP assay on germ cells specific genes in *wdr-5.1* and *ama-1* conditional mutation strain might help elucidate the mechanisms coordinating the two processes.

Various phenotypes were observed in *wdr-5.1* and *rbbp-5* mutants. Emo and a reduced germline stem cell (GSC) population were prominent. The GSC population is regulated by the Notch signaling pathway and multiple other factors, including two RNA binding proteins: FBF-1 and FBF-2 (Lamont et al., 2004). The molecular mechanisms underlying Emo phenotypes are largely unknown. How *wdr-5.1/rbbp-5* regulates these processes is not understood. It's possible that the decrease of H3K4 methylation caused by the mutation of *wdr-5* or *rbbp-5* leads to down-regulation of a subset of genes which causes the phenotypes. Conversely, the absence of the H3K4me maintenance may cause a "memory defect" in which controlled meiotic differentiation may be poorly programmed. A gene expression profile analysis using microarray may lead to the identification of genes that are misregulated.

**Regulation of sex determination by WDR-5**

There are three homologs of WDR5 in the *C. elegnas* genome: *wdr-5.1, wdr-5.2* and *wdr-5.3*. *wdr-5.1* plays a primary role in the regulation of H3K4 methylation (Chapter 2). *wdr-5.2* and *wdr-5.3* seem to be dispensable for this mechanism. However, I found a synthetic phenotype between *wdr-5.1* and *wdr-5.2*: hermaphrodites carrying mutations in both genes exhibited 100% sterility at elevated temperature (Table 3-1). Further study revealed a germline sex determination defect in these animals (Figure 3-3). I found that *fog-3*, a terminal regulator promoting spermatogenesis, was ectopically expressed in adult germ cells of *wdr-5.1;wdr-5.2* (Figure 3-5). TRA-1, the transcriptional repressor of *fog-3*, was depleted from the nuclei of adult germ cells (Figure 3-7). Notably, this function of *wdr-5* appears to be independent of H3K4 methylation. We have also found that RNAi knockdown of *set-9/set-26* in *wdr-5.1;wdr-5.2* causes synthetic sterility and TRA-1 reduction in nuclei at normal temperature (20°C) (Figure 3-11). The molecular mechanism underlying the TRA-1 regulation remains unclear. What seems to be clear is that *set-9/set-16* and *wdr-5.1*/*wdr-5.2* play a partially redundant role in maintaining the stable association of TRA-1 with chromatin.

There are two hypotheses that might explain the mechanism. First, *set-9/set-16* and *wdr-5.1*/ *wdr-5.2* are subunits of a H3K4 specific HMT complex. This complex promotes the expression of an unidentified gene which mediates the interaction between TRA-1 and chromatin. We have analyzed the mRNA levels of the genes in the sex determination pathway (Figure 3-5). None of them except *fog-3* is changed in *wdr-5.1;wdr-5.2* at 25°C. A screen for temperature-dependent Mog phenotype may lead to

identification of the gene, but such screens have been performed to saturation in *C. elegans*, and we have ruled out all of these except *fog-3*. Second, SET-9/SET-26 and WDR-5.1/WDR-5.2 could be subunits of a repression complex associated with TRA-1 to stabilize the repressive state of target genes. WDR-5.1 is a WD40 repeat protein. Like its mammalian orthologs, it binds to chromatin through recognition of the N-terminal tails of H3 (Figure 2-5). SET-9 and SET-26 contain SET domains that have been shown to interact with WDR5 in mammals (Dou et al., 2006). Set3, the homolog of SET-9 and SET-26 in *S. cerevisiae*, is a component of a repressive complex. This complex contains two histone deacetylases (HDAC): Hst1 and Hos2, and a WD40 repeat protein Sif2 (Pijnappel et al., 2001). In fact, Ci and Gli proteins, the *Drosophila* and mammalian homologs of TRA-1, respectively, control transcription repression through interacting with corepressors and deacetylation of histones (Cheng and Bishop, 2002). Importantly, TRA-1 has been shown to interact with TRA-4/PLZF-like which is a component of a repression complex containing HDA-1/HDAC (Grote and Conradt, 2006). Based on these studies, I propose a model in which TRA-1 interacts with a yeast Set3/Sif2-like repressive complex to inhibit *fog-3* expression. This complex includes: HAD-1, SET-9/SET-26, WDR-5.1, WDR-5.2 and TRA-4. WDR-5.1 and WDR-5.2 may have partially redundant roles with SET-9/SET-26. TRA-1 cannot bind to chromatin at 25°C in the absence of WDR-5.1 and WDR-5.2. The complex is not stable at 20°C in worms lacking SET-9/SET-26, WDR-5.1 and WDR-5.2 (Figure 4-2). I am currently attempting co-immunoprecipitation to analyze the interactions between TRA-1, HDA-1 and WDR-5.1. We have introduced a transgene expressing GFP fused to WDR-5.1 into *wdr-5.1;wdr-5.2*. Future experiments may include a pulldown experiment using anti-GFP antibody

followed by a Mass spectrometry analysis. Ideally, we would be able to identify a complex containing TRA-1, SET-9/SET-26, HDA-1 and TRA-4. Lastly, it would be extremely interesting to check if mammalian WDR5 also plays a role in Gli protein mediated transcription regulation. This study will definitely contributes to our understanding of mechanisms through which Ci/Gli-like transcription factors control gene expression.

Taken together, I have identified a number of components that contribute to the maintenance of H3K4 methylation in germline using *C. elegans* as a model organism. My findings indicate that the histone modifying machinery is highly conserved among eukaryotes. My studies suggest that methylation of H3K4 relies on transcription-dependent and independent mechanisms. Furthermore, I have discovered a role of chromatin regulators in the regulation of sex determination. Considering the importance of epigenetic signatures to normal germ cell development, the chromatin regulators controlling these marks are likely involved in all aspects of the mechanisms that govern germ cell development. Therefore, my studies about the chromatin regulators and their effects on H3K4 methylation and germ cell development will shed light on some of the shady mechanisms underlying germ cell development.

**Figure 4-1. Phylogenetic tree of SET domain containing proteins**

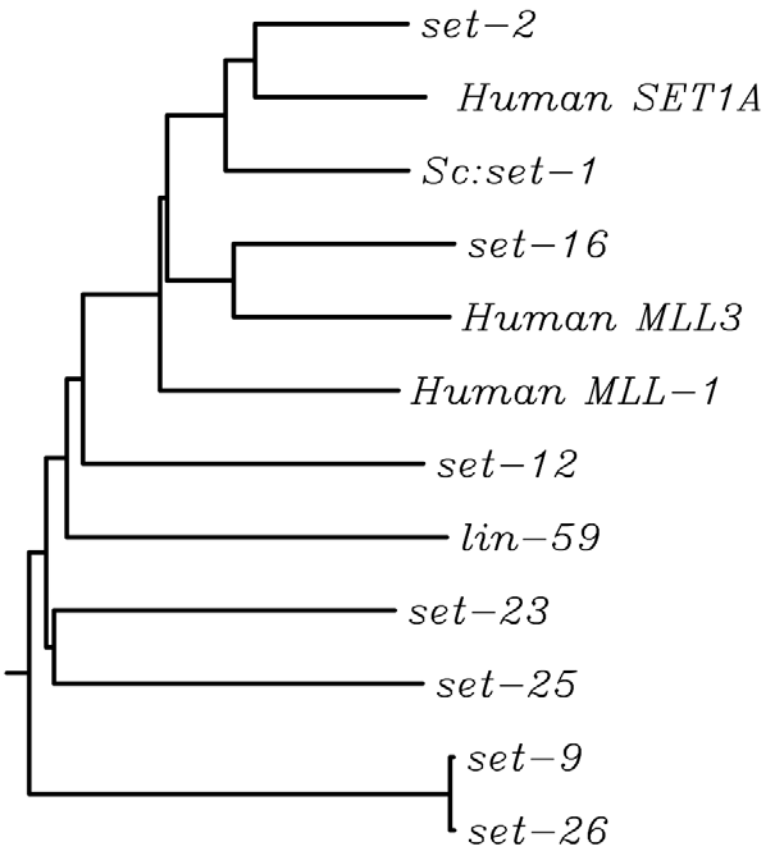

**Figure 4-2. Proposed model for the mechanism of *fog-3* repression**

A repressive complex composed of WDR-5.1, WDR-5.2, SET-9/SET-26, HAD-1, TRA-4 and TRA-1 plays a role in the inhibition of *fog-3* expression. In the absence of WDR-5.1 and WDR5.2, this complex cannot stably bind to *fog-3* promoter at 25°C. In the absence of WDR-5.1, WDR-5.2 and SET-9/SET26, TRA-1 cannot bind to *fog-3* promoter at 20°C and the repression is abolished.

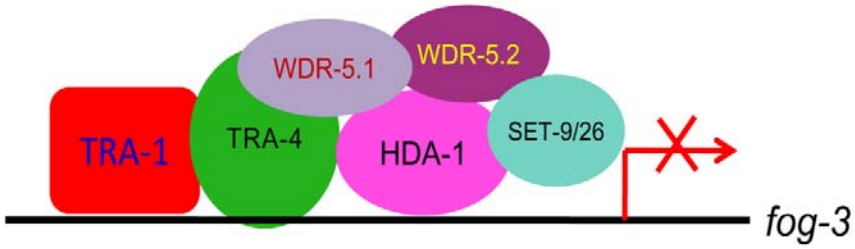
WDR-5.1
WDR-5.2
TRA-1
TRA-4
HDA-1
SET-9/26
fog-3

## References

Ahringer, J., and Kimble, J. (1991). Control of the sperm-oocyte switch in Caenorhabditis elegans hermaphrodites by the fem-3 3' untranslated region. Nature *349*, 346-348.

Akiyama, T., Nagata, M., and Aoki, F. (2006). Inadequate histone deacetylation during oocyte meiosis causes aneuploidy and embryo death in mice. Proceedings of the National Academy of Sciences of the United States of America *103*, 7339-7344.

Allegrucci, C., Thurston, A., Lucas, E., and Young, L. (2005). Epigenetics and the germline. Reproduction *129*, 137-149.

Ancelin, K., Lange, U.C., Hajkova, P., Schneider, R., Bannister, A.J., Kouzarides, T., and Surani, M.A. (2006). Blimp1 associates with Prmt5 and directs histone arginine methylation in mouse germ cells. Nature cell biology *8*, 623-630.

Austin, J., and Kimble, J. (1987). glp-1 is required in the germ line for regulation of the decision between mitosis and meiosis in C. elegans. Cell *51*, 589-599.

Azuara, V., Perry, P., Sauer, S., Spivakov, M., Jorgensen, H.F., John, R.M., Gouti, M., Casanova, M., Warnes, G., Merkenschlager, M., *et al.* (2006). Chromatin signatures of pluripotent cell lines. Nature cell biology *8*, 532-538.

Baugh, L.R., Hill, A.A., Slonim, D.K., Brown, E.L., and Hunter, C.P. (2003). Composition and dynamics of the Caenorhabditis elegans early embryonic transcriptome. Development *130*, 889-900.

Bean, C.J., Schaner, C.E., and Kelly, W.G. (2004). Meiotic pairing and imprinted X chromatin assembly in Caenorhabditis elegans. Nat Genet *36*, 100-105.

Bender, L.B., Suh, J., Carroll, C.R., Fong, Y., Fingerman, I.M., Briggs, S.D., Cao, R., Zhang, Y., Reinke, V., and Strome, S. (2006). MES-4: an autosome-associated histone methyltransferase that participates in silencing the X chromosomes in the C. elegans germ line. Development *133*, 3907-3917.

Bernstein, B.E., Kamal, M., Lindblad-Toh, K., Bekiranov, S., Bailey, D.K., Huebert, D.J., McMahon, S., Karlsson, E.K., Kulbokas, E.J., 3rd, Gingeras, T.R., *et al.* (2005). Genomic maps and comparative analysis of histone modifications in human and mouse. Cell *120*, 169-181.

Bernstein, B.E., Mikkelsen, T.S., Xie, X., Kamal, M., Huebert, D.J., Cuff, J., Fry, B., Meissner, A., Wernig, M., Plath, K., *et al.* (2006). A bivalent chromatin structure marks key developmental genes in embryonic stem cells. Cell *125*, 315-326.

Bird, A. (2002). DNA methylation patterns and epigenetic memory. Genes & development *16*, 6-21.

Bird, A.P. (1986). CpG-rich islands and the function of DNA methylation. Nature *321*, 209-213.

Blackwell, T.K. (2004). Germ cells: finding programs of mass repression. Curr Biol *14*, R229-230.

Briggs, S.D., Bryk, M., Strahl, B.D., Cheung, W.L., Davie, J.K., Dent, S.Y., Winston, F., and Allis, C.D. (2001). Histone H3 lysine 4 methylation is mediated by Set1 and required for cell growth and rDNA silencing in Saccharomyces cerevisiae. Genes & development *15*, 3286-3295.

Brykczynska, U., Hisano, M., Erkek, S., Ramos, L., Oakeley, E.J., Roloff, T.C., Beisel, C., Schubeler, D., Stadler, M.B., and Peters, A.H. (2010). Repressive and active histone

methylation mark distinct promoters in human and mouse spermatozoa. Nature structural & molecular biology *17*, 679-687.

Byrd, K.N., and Shearn, A. (2003). ASH1, a Drosophila trithorax group protein, is required for methylation of lysine 4 residues on histone H3. Proceedings of the National Academy of Sciences of the United States of America *100*, 11535-11540.

Cao, F., Chen, Y., Cierpicki, T., Liu, Y., Basrur, V., Lei, M., and Dou, Y. (2010). An Ash2L/RbBP5 heterodimer stimulates the MLL1 methyltransferase activity through coordinated substrate interactions with the MLL1 SET domain. PLoS One *5*, e14102.

Cao, R., and Zhang, Y. (2004). The functions of E(Z)/EZH2-mediated methylation of lysine 27 in histone H3. Curr Opin Genet Dev *14*, 155-164.

Checchi, P.M., and Kelly, W.G. (2006). emb-4 is a conserved gene required for efficient germline-specific chromatin remodeling during Caenorhabditis elegans embryogenesis. Genetics *174*, 1895-1906.

Chen, P., and Ellis, R.E. (2000). TRA-1A regulates transcription of fog-3, which controls germ cell fate in C. elegans. Development *127*, 3119-3129.

Chen, P.J., Singal, A., Kimble, J., and Ellis, R.E. (2000). A novel member of the tob family of proteins controls sexual fate in Caenorhabditis elegans germ cells. Developmental biology *217*, 77-90.

Cheng, S.Y., and Bishop, J.M. (2002). Suppressor of Fused represses Gli-mediated transcription by recruiting the SAP18-mSin3 corepressor complex. Proceedings of the National Academy of Sciences of the United States of America *99*, 5442-5447.

Cheng, X., Collins, Robert, and Zhang, Xing (2005). Structural and motifs of protein (histone) methylation enzymes. Annu Rev Biophysics BiomolStruct *34*, 267.

Cho, Y.W., Hong, T., Hong, S., Guo, H., Yu, H., Kim, D., Guszczynski, T., Dressler, G.R., Copeland, T.D., Kalkum, M., *et al.* (2007). PTIP associates with MLL3- and MLL4-containing histone H3 lysine 4 methyltransferase complex. The Journal of biological chemistry *282*, 20395-20406.

Clapier, C.R., and Cairns, B.R. (2009). The biology of chromatin remodeling complexes. Annual review of biochemistry *78*, 273-304.

Conradt, B., and Horvitz, H.R. (1998). The C. elegans protein EGL-1 is required for programmed cell death and interacts with the Bcl-2-like protein CED-9. Cell *93*, 519-529.

Cosgrove, M.S., and Patel, A. (2010). Mixed lineage leukemia: a structure-function perspective of the MLL1 protein. The FEBS journal *277*, 1832-1842.

Couture, J.F., Collazo, E., and Trievel, R.C. (2006). Molecular recognition of histone H3 by the WD40 protein WDR5. Nature structural & molecular biology *13*, 698-703.

Crawford, B.D., and Hess, J.L. (2006). MLL core components give the green light to histone methylation. ACS chemical biology *1*, 495-498.

Crittenden, S.L., Bernstein, D.S., Bachorik, J.L., Thompson, B.E., Gallegos, M., Petcherski, A.G., Moulder, G., Barstead, R., Wickens, M., and Kimble, J. (2002). A conserved RNA-binding protein controls germline stem cells in Caenorhabditis elegans. Nature *417*, 660-663.

Dehe, P.M., and Geli, V. (2006). The multiple faces of Set1. Biochemistry and cell biology = Biochimie et biologie cellulaire *84*, 536-548.

Dillon, S.C., Zhang, X., Trievel, R.C., and Cheng, X. (2005). The SET-domain protein superfamily: protein lysine methyltransferases. Genome biology *6*, 227.

Dolinoy, D.C., Weidman, J.R., and Jirtle, R.L. (2007). Epigenetic gene regulation: linking early developmental environment to adult disease. Reprod Toxicol *23*, 297-307.

Dou, Y., Milne, T.A., Ruthenburg, A.J., Lee, S., Lee, J.W., Verdine, G.L., Allis, C.D., and Roeder, R.G. (2006). Regulation of MLL1 H3K4 methyltransferase activity by its core components. Nature structural & molecular biology *13*, 713-719.

Dou, Y., Milne, T.A., Tackett, A.J., Smith, E.R., Fukuda, A., Wysocka, J., Allis, C.D., Chait, B.T., Hess, J.L., and Roeder, R.G. (2005). Physical association and coordinate function of the H3 K4 methyltransferase MLL1 and the H4 K16 acetyltransferase MOF. Cell *121*, 873-885.

Edgar, L.G., Wolf, N., and Wood, W.B. (1994). Early transcription in Caenorhabditis elegans embryos. Development *120*, 443-451.

Ellis, R., and Schedl, T. (2007). Sex determination in the germ line. WormBook, 1-13.

Fischle, W., Wang, Y., and Allis, C.D. (2003). Histone and chromatin cross-talk. Current opinion in cell biology *15*, 172-183.

Fisher, K., Southall, S.M., Wilson, J.R., and Poulin, G.B. (2010). Methylation and demethylation activities of a C. elegans MLL-like complex attenuate RAS signalling. Developmental biology *341*, 142-153.

Fong, Y., Bender, L., Wang, W., and Strome, S. (2002). Regulation of the different chromatin states of autosomes and X chromosomes in the germ line of C. elegans. Science *296*, 2235-2238.

Fujiki, R., Chikanishi, T., Hashiba, W., Ito, H., Takada, I., Roeder, R.G., Kitagawa, H., and Kato, S. (2009). GlcNAcylation of a histone methyltransferase in retinoic-acid-induced granulopoiesis. Nature *459*, 455-459.

Furuhashi, H., Takasaki, T., Rechtsteiner, A., Li, T., Kimura, H., Checchi, P.M., Strome, S., and Kelly, W.G. (2010). Trans-generational epigenetic regulation of C. elegans primordial germ cells. Epigenetics & chromatin *3*, 1-21.

Garapaty, S., Xu, C.F., Trojer, P., Mahajan, M.A., Neubert, T.A., and Samuels, H.H. (2009). Identification and characterization of a novel nuclear protein complex involved in nuclear hormone receptor-mediated gene regulation. The Journal of biological chemistry *284*, 7542-7552.

Glaser, S., Schaft, J., Lubitz, S., Vintersten, K., van der Hoeven, F., Tufteland, K.R., Aasland, R., Anastassiadis, K., Ang, S.L., and Stewart, A.F. (2006). Multiple epigenetic maintenance factors implicated by the loss of Mll2 in mouse development. Development *133*, 1423-1432.

Greer, E.L., Maures, T.J., Hauswirth, A.G., Green, E.M., Leeman, D.S., Maro, G.S., Han, S., Banko, M.R., Gozani, O., and Brunet, A. (2010). Members of the H3K4 trimethylation complex regulate lifespan in a germline-dependent manner in C. elegans. Nature *466*, 383-387.

Grote, P., and Conradt, B. (2006). The PLZF-like protein TRA-4 cooperates with the Gli-like transcription factor TRA-1 to promote female development in C. elegans. Developmental cell *11*, 561-573.

Guccione, E., Bassi, C., Casadio, F., Martinato, F., Cesaroni, M., Schuchlautz, H., Luscher, B., and Amati, B. (2007). Methylation of histone H3R2 by PRMT6 and H3K4 by an MLL complex are mutually exclusive. Nature *449*, 933-937.

Guenther, M.G., Jenner, R.G., Chevalier, B., Nakamura, T., Croce, C.M., Canaani, E., and Young, R.A. (2005). Global and Hox-specific roles for the MLL1 methyltransferase.

Proceedings of the National Academy of Sciences of the United States of America *102*, 8603-8608.

Hajkova, P., Ancelin, K., Waldmann, T., Lacoste, N., Lange, U.C., Cesari, F., Lee, C., Almouzni, G., Schneider, R., and Surani, M.A. (2008). Chromatin dynamics during epigenetic reprogramming in the mouse germ line. Nature *452*, 877-881.

Hamilton, B., Dong, Y., Shindo, M., Liu, W., Odell, I., Ruvkun, G., and Lee, S.S. (2005). A systematic RNAi screen for longevity genes in C. elegans. Genes & development *19*, 1544-1555.

Hammoud, S.S., Nix, D.A., Zhang, H., Purwar, J., Carrell, D.T., and Cairns, B.R. (2009). Distinctive chromatin in human sperm packages genes for embryo development. Nature *460*, 473-478.

Han, Z., Guo, L., Wang, H., Shen, Y., Deng, X.W., and Chai, J. (2006). Structural basis for the specific recognition of methylated histone H3 lysine 4 by the WD-40 protein WDR5. Mol Cell *22*, 137-144.

Hanyu-Nakamura, K., Sonobe-Nojima, H., Tanigawa, A., Lasko, P., and Nakamura, A. (2008). Drosophila Pgc protein inhibits P-TEFb recruitment to chromatin in primordial germ cells. Nature *451*, 730-733.

Harris, J.E., Govindan, J.A., Yamamoto, I., Schwartz, J., Kaverina, I., and Greenstein, D. (2006). Major sperm protein signaling promotes oocyte microtubule reorganization prior to fertilization in Caenorhabditis elegans. Developmental biology *299*, 105-121.

Hayashi, K., Yoshida, K., and Matsui, Y. (2005). A histone H3 methyltransferase controls epigenetic events required for meiotic prophase. Nature *438*, 374-378.

Hess, J.L. (2004). MLL: a histone methyltransferase disrupted in leukemia. Trends Mol Med *10*, 500-507.

Hodgkin, J. (1987). A genetic analysis of the sex-determining gene, tra-1, in the nematode Caenorhabditis elegans. Genes & development *1*, 731-745.

Hubbard, E.J., and Greenstein, D. (2000). The Caenorhabditis elegans gonad: a test tube for cell and developmental biology. Dev Dyn *218*, 2-22.

Hughes, C.M., Rozenblatt-Rosen, O., Milne, T.A., Copeland, T.D., Levine, S.S., Lee, J.C., Hayes, D.N., Shanmugam, K.S., Bhattacharjee, A., Biondi, C.A., *et al.* (2004). Menin associates with a trithorax family histone methyltransferase complex and with the hoxc8 locus. Mol Cell *13*, 587-597.

Hyllus, D., Stein, C., Schnabel, K., Schiltz, E., Imhof, A., Dou, Y., Hsieh, J., and Bauer, U.M. (2007). PRMT6-mediated methylation of R2 in histone H3 antagonizes H3 K4 trimethylation. Genes & development *21*, 3369-3380.

Ingham, P.W., and McMahon, A.P. (2001). Hedgehog signaling in animal development: paradigms and principles. Genes & development *15*, 3059-3087.

Jenuwein, T., and Allis, C.D. (2001). Translating the histone code. Science *293*, 1074-1080.

Jones, R.S., and Gelbart, W.M. (1993). The Drosophila Polycomb-group gene Enhancer of zeste contains a region with sequence similarity to trithorax. Molecular and cellular biology *13*, 6357-6366.

Kaletta, T., and Hengartner, M.O. (2006). Finding function in novel targets: C. elegans as a model organism. Nat Rev Drug Discov *5*, 387-398.

Katz, D.J., Edwards, T.M., Reinke, V., and Kelly, W.G. (2009). A C. elegans LSD1 demethylase contributes to germline immortality by reprogramming epigenetic memory. Cell *137*, 308-320.

Kelly, W.G., Schaner, C.E., Dernburg, A.F., Lee, M.H., Kim, S.K., Villeneuve, A.M., and Reinke, V. (2002). X-chromosome silencing in the germline of C. elegans. Development *129*, 479-492.

Kimble, J., and Crittenden, S.L. (2007). Controls of germline stem cells, entry into meiosis, and the sperm/oocyte decision in Caenorhabditis elegans. Annu Rev Cell Dev Biol *23*, 405-433.

Kimmins, S., and Sassone-Corsi, P. (2005). Chromatin remodelling and epigenetic features of germ cells. Nature *434*, 583-589.

Kimura, H., Hayashi-Takanaka, Y., Goto, Y., Takizawa, N., and Nozaki, N. (2008). The organization of histone H3 modifications as revealed by a panel of specific monoclonal antibodies. Cell structure and function *33*, 61-73.

Kirmizis, A., Santos-Rosa, H., Penkett, C.J., Singer, M.A., Vermeulen, M., Mann, M., Bahler, J., Green, R.D., and Kouzarides, T. (2007). Arginine methylation at histone H3R2 controls deposition of H3K4 trimethylation. Nature *449*, 928-932.

Kittler, R., Pelletier, L., Heninger, A.K., Slabicki, M., Theis, M., Miroslaw, L., Poser, I., Lawo, S., Grabner, H., Kozak, K.*, et al.* (2007). Genome-scale RNAi profiling of cell division in human tissue culture cells. Nature cell biology *9*, 1401-1412.

Kornberg, R.D., and Lorch, Y. (1999). Twenty-five years of the nucleosome, fundamental particle of the eukaryote chromosome. Cell *98*, 285-294.

Kouzarides, T. (2007). Chromatin modifications and their function. Cell *128*, 693-705.

Krogan, N.J., Dover, J., Khorrami, S., Greenblatt, J.F., Schneider, J., Johnston, M., and Shilatifard, A. (2002). COMPASS, a histone H3 (Lysine 4) methyltransferase required for telomeric silencing of gene expression. The Journal of biological chemistry *277*, 10753-10755.

Krogan, N.J., Dover, J., Wood, A., Schneider, J., Heidt, J., Boateng, M.A., Dean, K., Ryan, O.W., Golshani, A., Johnston, M., *et al.* (2003). The Paf1 complex is required for histone H3 methylation by COMPASS and Dot1p: linking transcriptional elongation to histone methylation. Mol Cell *11*, 721-729.

Lamont, L.B., Crittenden, S.L., Bernstein, D., Wickens, M., and Kimble, J. (2004). FBF-1 and FBF-2 regulate the size of the mitotic region in the C. elegans germline. Developmental cell *7*, 697-707.

Lee, J.H., and Skalnik, D.G. (2005). CpG-binding protein (CXXC finger protein 1) is a component of the mammalian Set1 histone H3-Lys4 methyltransferase complex, the analogue of the yeast Set1/COMPASS complex. The Journal of biological chemistry *280*, 41725-41731.

Lee, S., Lee, D.K., Dou, Y., Lee, J., Lee, B., Kwak, E., Kong, Y.Y., Lee, S.K., Roeder, R.G., and Lee, J.W. (2006). Coactivator as a target gene specificity determinant for histone H3 lysine 4 methyltransferases. Proceedings of the National Academy of Sciences of the United States of America *103*, 15392-15397.

Li, B., Carey, M., and Workman, J.L. (2007). The role of chromatin during transcription. Cell *128*, 707-719.

Li, E., Bestor, T.H., and Jaenisch, R. (1992). Targeted mutation of the DNA methyltransferase gene results in embryonic lethality. Cell *69*, 915-926.

Luger, K., Mader, A.W., Richmond, R.K., Sargent, D.F., and Richmond, T.J. (1997). Crystal structure of the nucleosome core particle at 2.8 A resolution. Nature *389*, 251-260.

MacQueen, A.J., Colaiacovo, M.P., McDonald, K., and Villeneuve, A.M. (2002). Synapsis-dependent and -independent mechanisms stabilize homolog pairing during meiotic prophase in C. elegans. Genes & development *16*, 2428-2442.

Madl, J.E., and Herman, R.K. (1979). Polyploids and sex determination in Caenorhabditis elegans. Genetics *93*, 393-402.

Malik, H.S., and Henikoff, S. (2003). Phylogenomics of the nucleosome. Nat Struct Biol *10*, 882-891.

Martens, J.A., and Winston, F. (2003). Recent advances in understanding chromatin remodeling by Swi/Snf complexes. Curr Opin Genet Dev *13*, 136-142.

Martin, C., and Zhang, Y. (2007). Mechanisms of epigenetic inheritance. Current opinion in cell biology *19*, 266-272.

Mello, C.C., Schubert, C., Draper, B., Zhang, W., Lobel, R., and Priess, J.R. (1996). The PIE-1 protein and germline specification in C. elegans embryos. Nature *382*, 710-712.

Mikkelsen, T.S., Ku, M., Jaffe, D.B., Issac, B., Lieberman, E., Giannoukos, G., Alvarez, P., Brockman, W., Kim, T.K., Koche, R.P.*, et al.* (2007). Genome-wide maps of chromatin state in pluripotent and lineage-committed cells. Nature *448*, 553-560.

Miller, T., Krogan, N.J., Dover, J., Erdjument-Bromage, H., Tempst, P., Johnston, M., Greenblatt, J.F., and Shilatifard, A. (2001). COMPASS: a complex of proteins associated with a trithorax-related SET domain protein. Proceedings of the National Academy of Sciences of the United States of America *98*, 12902-12907.

Milne, T.A., Dou, Y., Martin, M.E., Brock, H.W., Roeder, R.G., and Hess, J.L. (2005). MLL associates specifically with a subset of transcriptionally active target genes. Proceedings of the National Academy of Sciences of the United States of America *102*, 14765-14770.

Mizuguchi, G., Shen, X., Landry, J., Wu, W.H., Sen, S., and Wu, C. (2004). ATP-driven exchange of histone H2AZ variant catalyzed by SWR1 chromatin remodeling complex. Science *303*, 343-348.

Mohan, M., Lin, C., Guest, E., and Shilatifard, A. (2010). Licensed to elongate: a molecular mechanism for MLL-based leukaemogenesis. Nat Rev Cancer *10*, 721-728.

Morgan, H.D., Santos, F., Green, K., Dean, W., and Reik, W. (2005). Epigenetic reprogramming in mammals. Hum Mol Genet *14 Spec No 1*, R47-58.

Muramoto, T., Muller, I., Thomas, G., Melvin, A., and Chubb, J.R. (2010). Methylation of H3K4 Is required for inheritance of active transcriptional states. Curr Biol *20*, 397-406.

Nagy, P.L., Griesenbeck, J., Kornberg, R.D., and Cleary, M.L. (2002). A trithorax-group complex purified from Saccharomyces cerevisiae is required for methylation of histone H3. Proceedings of the National Academy of Sciences of the United States of America *99*, 90-94.

Ng, H.H., Robert, F., Young, R.A., and Struhl, K. (2003). Targeted recruitment of Set1 histone methylase by elongating Pol II provides a localized mark and memory of recent transcriptional activity. Mol Cell *11*, 709-719.

Ng, R.K., and Gurdon, J.B. (2008). Epigenetic memory of an active gene state depends on histone H3.3 incorporation into chromatin in the absence of transcription. Nature cell biology *10*, 102-109.

Ohinata, Y., Payer, B., O'Carroll, D., Ancelin, K., Ono, Y., Sano, M., Barton, S.C., Obukhanych, T., Nussenzweig, M., Tarakhovsky, A.*, et al.* (2005). Blimp1 is a critical determinant of the germ cell lineage in mice. Nature *436*, 207-213.

Okano, M., Bell, D.W., Haber, D.A., and Li, E. (1999). DNA methyltransferases Dnmt3a and Dnmt3b are essential for de novo methylation and mammalian development. Cell *99*, 247-257.

Patel, A., Dharmarajan, V., and Cosgrove, M.S. (2008a). Structure of WDR5 bound to mixed lineage leukemia protein-1 peptide. The Journal of biological chemistry *283*, 32158-32161.

Patel, A., Dharmarajan, V., Vought, V.E., and Cosgrove, M.S. (2009). On the mechanism of multiple lysine methylation by the human mixed lineage leukemia protein-1 (MLL1) core complex. The Journal of biological chemistry *284*, 24242-24256.

Patel, A., Vought, V.E., Dharmarajan, V., and Cosgrove, M.S. (2008b). A conserved arginine-containing motif crucial for the assembly and enzymatic activity of the mixed lineage leukemia protein-1 core complex. The Journal of biological chemistry *283*, 32162-32175.

Peters, A.H., Kubicek, S., Mechtler, K., O'Sullivan, R.J., Derijck, A.A., Perez-Burgos, L., Kohlmaier, A., Opravil, S., Tachibana, M., Shinkai, Y.*, et al.* (2003). Partitioning and plasticity of repressive histone methylation states in mammalian chromatin. Mol Cell *12*, 1577-1589.

Peters, A.H., O'Carroll, D., Scherthan, H., Mechtler, K., Sauer, S., Schofer, C., Weipoltshammer, K., Pagani, M., Lachner, M., Kohlmaier, A.*, et al.* (2001). Loss of the

Suv39h histone methyltransferases impairs mammalian heterochromatin and genome stability. Cell *107*, 323-337.

Petruk, S., Sedkov, Y., Smith, S., Tillib, S., Kraevski, V., Nakamura, T., Canaani, E., Croce, C.M., and Mazo, A. (2001). Trithorax and dCBP acting in a complex to maintain expression of a homeotic gene. Science *294*, 1331-1334.

Pijnappel, W.W., Schaft, D., Roguev, A., Shevchenko, A., Tekotte, H., Wilm, M., Rigaut, G., Seraphin, B., Aasland, R., and Stewart, A.F. (2001). The S. cerevisiae SET3 complex includes two histone deacetylases, Hos2 and Hst1, and is a meiotic-specific repressor of the sporulation gene program. Genes & development *15*, 2991-3004.

Pokholok, D.K., Harbison, C.T., Levine, S., Cole, M., Hannett, N.M., Lee, T.I., Bell, G.W., Walker, K., Rolfe, P.A., Herbolsheimer, E.*, et al.* (2005). Genome-wide map of nucleosome acetylation and methylation in yeast. Cell *122*, 517-527.

Rechtsteiner, A., Ercan, S., Takasaki, T., Phippen, T.M., Egelhofer, T.A., Wang, W., Kimura, H., Lieb, J.D., and Strome, S. (2010). The histone H3K36 methyltransferase MES-4 acts epigenetically to transmit the memory of germline gene expression to progeny. PLoS genetics *6*, 1-15.

Regnier, V., Vagnarelli, P., Fukagawa, T., Zerjal, T., Burns, E., Trouche, D., Earnshaw, W., and Brown, W. (2005). CENP-A is required for accurate chromosome segregation and sustained kinetochore association of BubR1. Molecular and cellular biology *25*, 3967-3981.

Reik, W., and Walter, J. (2001). Genomic imprinting: parental influence on the genome. Nature reviews *2*, 21-32.

Ringrose, L., and Paro, R. (2004). Epigenetic regulation of cellular memory by the Polycomb and Trithorax group proteins. Annual review of genetics *38*, 413-443.

Rodenhiser, D., and Mann, M. (2006). Epigenetics and human disease: translating basic biology into clinical applications. CMAJ *174*, 341-348.

Roguev, A., Schaft, D., Shevchenko, A., Aasland, R., Shevchenko, A., and Stewart, A.F. (2003). High conservation of the Set1/Rad6 axis of histone 3 lysine 4 methylation in budding and fission yeasts. The Journal of biological chemistry *278*, 8487-8493.

Roguev, A., Schaft, D., Shevchenko, A., Pijnappel, W.W., Wilm, M., Aasland, R., and Stewart, A.F. (2001). The Saccharomyces cerevisiae Set1 complex includes an Ash2 homologue and methylates histone 3 lysine 4. The EMBO journal *20*, 7137-7148.

Rowley, J.D. (1998). The critical role of chromosome translocations in human leukemias. Annual review of genetics *32*, 495-519.

Ruthenburg, A.J., Allis, C.D., and Wysocka, J. (2007). Methylation of lysine 4 on histone H3: intricacy of writing and reading a single epigenetic mark. Mol Cell *25*, 15-30.

Ruthenburg, A.J., Wang, W., Graybosch, D.M., Li, H., Allis, C.D., Patel, D.J., and Verdine, G.L. (2006). Histone H3 recognition and presentation by the WDR5 module of the MLL1 complex. Nature structural & molecular biology *13*, 704-712.

Saffman, E.E., and Lasko, P. (1999). Germline development in vertebrates and invertebrates. Cell Mol Life Sci *55*, 1141-1163.

Saha, A., Wittmeyer, J., and Cairns, B.R. (2006). Chromatin remodelling: the industrial revolution of DNA around histones. Nat Rev Mol Cell Biol *7*, 437-447.

Santos-Rosa, H., Schneider, R., Bannister, A.J., Sherriff, J., Bernstein, B.E., Emre, N.C., Schreiber, S.L., Mellor, J., and Kouzarides, T. (2002). Active genes are tri-methylated at K4 of histone H3. Nature *419*, 407-411.

Sasaki, H., and Matsui, Y. (2008). Epigenetic events in mammalian germ-cell development: reprogramming and beyond. Nature reviews *9*, 129-140.

Schaner, C., Deshpande, G., Schedl, P., and Kelly, W. (2003). A conserved chromatin architecture marks and maintains the restricted germ cell lineage in worms and flies. Developmental cell *5*, 747-757.

Schaner, C., and Kelly, W. (2006). Germline Chromatin. Wormbook, ed The *Celegnas* Research Community, 1-14.

Schedl, T., Graham, P.L., Barton, M.K., and Kimble, J. (1989). Analysis of the role of tra-1 in germline sex determination in the nematode Caenorhabditis elegans. Genetics *123*, 755-769.

Schneider, J., Wood, A., Lee, J.S., Schuster, R., Dueker, J., Maguire, C., Swanson, S.K., Florens, L., Washburn, M.P., and Shilatifard, A. (2005). Molecular regulation of histone H3 trimethylation by COMPASS and the regulation of gene expression. Mol Cell *19*, 849-856.

Schneider, R., Bannister, A.J., Myers, F.A., Thorne, A.W., Crane-Robinson, C., and Kouzarides, T. (2004). Histone H3 lysine 4 methylation patterns in higher eukaryotic genes. Nature cell biology *6*, 73-77.

Schotta, G., Lachner, M., Sarma, K., Ebert, A., Sengupta, R., Reuter, G., Reinberg, D., and Jenuwein, T. (2004). A silencing pathway to induce H3-K9 and H4-K20 trimethylation at constitutive heterochromatin. Genes & development *18*, 1251-1262.

Schuetz, A., Allali-Hassani, A., Martin, F., Loppnau, P., Vedadi, M., Bochkarev, A., Plotnikov, A.N., Arrowsmith, C.H., and Min, J. (2006). Structural basis for molecular recognition and presentation of histone H3 by WDR5. The EMBO journal *25*, 4245-4252.

Schvarzstein, M., and Spence, A.M. (2006). The C. elegans sex-determining GLI protein TRA-1A is regulated by sex-specific proteolysis. Developmental cell *11*, 733-740.

Segal, S.P., Graves, L.E., Verheyden, J., and Goodwin, E.B. (2001). RNA-Regulated TRA-1 nuclear export controls sexual fate. Developmental cell *1*, 539-551.

Seki, Y., Yamaji, M., Yabuta, Y., Sano, M., Shigeta, M., Matsui, Y., Saga, Y., Tachibana, M., Shinkai, Y., and Saitou, M. (2007). Cellular dynamics associated with the genome-wide epigenetic reprogramming in migrating primordial germ cells in mice. Development *134*, 2627-2638.

Seligson, D.B., Horvath, S., Shi, T., Yu, H., Tze, S., Grunstein, M., and Kurdistani, S.K. (2005). Global histone modification patterns predict risk of prostate cancer recurrence. Nature *435*, 1262-1266.

Selth, L.A., Sigurdsson, S., and Svejstrup, J.Q. (2010). Transcript Elongation by RNA Polymerase II. Annual review of biochemistry *79*, 271-293.

Seydoux, G., and Braun, R.E. (2006). Pathway to totipotency: lessons from germ cells. Cell *127*, 891-904.

Seydoux, G., and Dunn, M.A. (1997). Transcriptionally repressed germ cells lack a subpopulation of phosphorylated RNA polymerase II in early embryos of Caenorhabditis elegans and Drosophila melanogaster. Development *124*, 2191-2201.

Seydoux, G., and Fire, A. (1994). Soma-germline asymmetry in the distributions of embryonic RNAs in Caenorhabditis elegans. Development *120*, 2823-2834.

Shi, X., Hong, T., Walter, K.L., Ewalt, M., Michishita, E., Hung, T., Carney, D., Pena, P., Lan, F., Kaadige, M.R., *et al.* (2006). ING2 PHD domain links histone H3 lysine 4 methylation to active gene repression. Nature *442*, 96-99.

Shilatifard, A. (2006). Chromatin modifications by methylation and ubiquitination: implications in the regulation of gene expression. Annual review of biochemistry *75*, 243-269.

Shilatifard, A. (2008). Molecular implementation and physiological roles for histone H3 lysine 4 (H3K4) methylation. Current opinion in cell biology *20*, 341-348.

Simonet, T., Dulermo, R., Schott, S., and Palladino, F. (2007). Antagonistic functions of SET-2/SET1 and HPL/HP1 proteins in C. elegans development. Developmental biology.

Sims, R.J., 3rd, and Reinberg, D. (2006). Histone H3 Lys 4 methylation: caught in a bind? Genes & development *20*, 2779-2786.

Smith, S., and Stillman, B. (1991). Stepwise assembly of chromatin during DNA replication in vitro. The EMBO journal *10*, 971-980.

Song, J.J., and Kingston, R.E. (2008). WDR5 interacts with mixed lineage leukemia (MLL) protein via the histone H3-binding pocket. The Journal of biological chemistry *283*, 35258-35264.

Starck, J., and Brun, J. (1977). Autoradiographic localization of RNA synthesis in vitro during oogenesis in Parascaris equorum. Comptes rendus hebdomadaires des seances de l'Academie des sciences *284*, 1341-1344.

Starostina, N.G., Lim, J.M., Schvarzstein, M., Wells, L., Spence, A.M., and Kipreos, E.T. (2007). A CUL-2 ubiquitin ligase containing three FEM proteins degrades TRA-1 to regulate C. elegans sex determination. Developmental cell *13*, 127-139.

Steward, M.M., Lee, J.S., O'Donovan, A., Wyatt, M., Bernstein, B.E., and Shilatifard, A. (2006). Molecular regulation of H3K4 trimethylation by ASH2L, a shared subunit of MLL complexes. Nature structural & molecular biology *13*, 852-854.

Strahl, B.D., and Allis, C.D. (2000). The language of covalent histone modifications. Nature *403*, 41-45.

Strome, S. (2005). Specification of the germ line. WormBook, 1-10.

Strome, S., and Wood, W.B. (1983). Generation of asymmetry and segregation of germ-line granules in early C. elegans embryos. Cell *35*, 15-25.

Sun, Z.W., and Allis, C.D. (2002). Ubiquitination of histone H2B regulates H3 methylation and gene silencing in yeast. Nature *418*, 104-108.

Surani, M.A., Hayashi, K., and Hajkova, P. (2007). Genetic and epigenetic regulators of pluripotency. Cell *128*, 747-762.

Thompson, B.A., Tremblay, V., Lin, G., and Bochar, D.A. (2008). CHD8 is an ATP-dependent chromatin remodeling factor that regulates beta-catenin target genes. Molecular and cellular biology *28*, 3894-3904.

Thomson, J.P., Skene, P.J., Selfridge, J., Clouaire, T., Guy, J., Webb, S., Kerr, A.R., Deaton, A., Andrews, R., James, K.D., *et al.* (2010). CpG islands influence chromatin structure via the CpG-binding protein Cfp1. Nature *464*, 1082-1086.

Tschiersch, B., Hofmann, A., Krauss, V., Dorn, R., Korge, G., and Reuter, G. (1994). The protein encoded by the Drosophila position-effect variegation suppressor gene Su(var)3-9 combines domains of antagonistic regulators of homeotic gene complexes. The EMBO journal *13*, 3822-3831.

Turner, B.M. (2000). Histone acetylation and an epigenetic code. Bioessays *22*, 836-845.

Tweedie, S., Charlton, J., Clark, V., and Bird, A. (1997). Methylation of genomes and genes at the invertebrate-vertebrate boundary. Molecular and cellular biology *17*, 1469-1475.

Vakoc, C.R., Mandat, S.A., Olenchock, B.A., and Blobel, G.A. (2005). Histone H3 lysine 9 methylation and HP1gamma are associated with transcription elongation through mammalian chromatin. Mol Cell *19*, 381-391.

Valls, E., Sanchez-Molina, S., and Martinez-Balbas, M.A. (2005). Role of histone modifications in marking and activating genes through mitosis. The Journal of biological chemistry *280*, 42592-42600.

Vastenhouw, N.L., Zhang, Y., Woods, I.G., Imam, F., Regev, A., Liu, X.S., Rinn, J., and Schier, A.F. (2010). Chromatin signature of embryonic pluripotency is established during genome activation. Nature *464*, 922-926.

Wang, Z., Zang, C., Rosenfeld, J.A., Schones, D.E., Barski, A., Cuddapah, S., Cui, K., Roh, T.Y., Peng, W., Zhang, M.Q., *et al.* (2008). Combinatorial patterns of histone acetylations and methylations in the human genome. Nat Genet *40*, 897-903.

Wood, A., Schneider, J., Dover, J., Johnston, M., and Shilatifard, A. (2003). The Paf1 complex is essential for histone monoubiquitination by the Rad6-Bre1 complex, which signals for histone methylation by COMPASS and Dot1p. The Journal of biological chemistry *278*, 34739-34742.

Workman, J.L. (2006). Nucleosome displacement in transcription. Genes & development *20*, 2009-2017.

Wu, M., Wang, P.F., Lee, J.S., Martin-Brown, S., Florens, L., Washburn, M., and Shilatifard, A. (2008). Molecular regulation of H3K4 trimethylation by Wdr82, a component of human Set1/COMPASS. Molecular and cellular biology *28*, 7337-7344.

Wysocka, J. (2006). Identifying novel proteins recognizing histone modifications using peptide pull-down assay. Methods (San Diego, Calif *40*, 339-343.

Wysocka, J., Myers, M.P., Laherty, C.D., Eisenman, R.N., and Herr, W. (2003). Human Sin3 deacetylase and trithorax-related Set1/Ash2 histone H3-K4 methyltransferase are tethered together selectively by the cell-proliferation factor HCF-1. Genes & development *17*, 896-911.

Wysocka, J., Swigut, T., Milne, T.A., Dou, Y., Zhang, X., Burlingame, A.L., Roeder, R.G., Brivanlou, A.H., and Allis, C.D. (2005). WDR5 associates with histone H3 methylated at K4 and is essential for H3 K4 methylation and vertebrate development. Cell *121*, 859-872.

Yi, W., Ross, J.M., and Zarkower, D. (2000). Mab-3 is a direct tra-1 target gene regulating diverse aspects of C. elegans male sexual development and behavior. Development *127*, 4469-4480.

Ying, Y., Qi, X., and Zhao, G.Q. (2001). Induction of primordial germ cells from murine epiblasts by synergistic action of BMP4 and BMP8B signaling pathways. Proceedings of the National Academy of Sciences of the United States of America *98*, 7858-7862.

Ying, Y., and Zhao, G.Q. (2001). Cooperation of endoderm-derived BMP2 and extraembryonic ectoderm-derived BMP4 in primordial germ cell generation in the mouse. Developmental biology *232*, 484-492.

Yokoyama, A., Wang, Z., Wysocka, J., Sanyal, M., Aufiero, D.J., Kitabayashi, I., Herr, W., and Cleary, M.L. (2004). Leukemia proto-oncoprotein MLL forms a SET1-like histone methyltransferase complex with menin to regulate Hox gene expression. Molecular and cellular biology *24*, 5639-5649.

Yu, B.D., Hess, J.L., Horning, S.E., Brown, G.A., and Korsmeyer, S.J. (1995). Altered Hox expression and segmental identity in Mll-mutant mice. Nature *378*, 505-508.

Zarkower, D., and Hodgkin, J. (1992). Molecular analysis of the C. elegans sex-determining gene tra-1: a gene encoding two zinc finger proteins. Cell *70*, 237-249.

Zarkower, D., and Hodgkin, J. (1993). Zinc fingers in sex determination: only one of the two C. elegans Tra-1 proteins binds DNA in vitro. Nucleic acids research *21*, 3691-3698.

Zhang, F., Barboric, M., Blackwell, T.K., and Peterlin, B.M. (2003a). A model of repression: CTD analogs and PIE-1 inhibit transcriptional elongation by P-TEFb. Genes & development *17*, 748-758.

Zhang, L., Eugeni, E.E., Parthun, M.R., and Freitas, M.A. (2003b). Identification of novel histone post-translational modifications by peptide mass fingerprinting. Chromosoma *112*, 77-86.

Zhang, Y., Wong, J., Klinger, M., Tran, M.T., Shannon, K.M., and Killeen, N. (2009). MLL5 contributes to hematopoietic stem cell fitness and homeostasis. Blood *113*, 1455-1463.